2023

ASSESSING THE TREATMENT EFFICIENCY OF EXPANDED SHALE AS A FILTER MEDIUM IN A BIOSWALE

Ashish Bhurtyal

ASSESSING THE TREATMENT EFFICIENCY OF EXPANDED SHALE AS A FILTER MEDIUM IN A BIOSWALE

By

Ashish Bhurtyal

Presented to the Faculty of the Graduate School of
The University of Texas at Arlington in Partial Fulfillment of the
Requirements for the Degree of

MASTER OF SCIENCE IN CIVIL ENGINEERING

The University of Texas at Arlington

August 2023

Supervising Committee:

Habib Ahmari, Supervising Professor

Michelle Hummel

Srinivas Prabakar

ABSTRACT

This thesis presents a laboratory investigation focusing on the use of expanded shale as a filter media in bioswales. Bioswales are known for their effectiveness in improving water quality by removing pollutants such as total suspended solids (TSS) and turbidity. While conventional filter media with rocks, sand, and mulches have been utilized in bioswales to enhance infiltration capacity, the potential of expanded shale as an engineered media has not been thoroughly assessed and documented.

The study conducted a series of thirty experiments involving three different flow conditions to mimic typical Best Management Practices (BMP) applications. The primary focus was on investigating the efficiency of the swale constructed with expanded shale in removing TSS and turbidity, which are key indicators of stormwater pollutants.

The experiments were carried out in a rectangular flume measuring 15 feet in length and 4 feet wide, filled with expanded shale media with thicknesses of 6 inches and 4 inches. The study presented the performance of two different types of expanded shale with varying gradations, fine and coarse sizes. Additionally, the impact of influent concentration on the expanded shale media's effectiveness was examined, and two scenarios representing bioswales with and without an underdrain system were studied.

The results demonstrated that expanded shale was highly effective in removing both TSS and turbidity under all tested conditions. The mean weighted average removal efficiency of TSS was found to be 42%, 43%, and 68% for the middle section of the channel, overflow, and infiltered flow, respectively, with a range of 20% to 75%, 19% to 75%, and 55% to 82%. Similarly, mean weighted turbidity removal was 17%, 15%, and 40% for the middle section, overflow, and infiltered flow, respectively, with a range of -4% to 43%, -7% to 49%, and 22% to 61%.

Approximately 42% of TSS and 17% of turbidity removal occurred within the first half of the flow length.

Due to the sedimentation process, coarser particles were observed to settle along the flow length of the flume. However, the particle gradation of the suspended sediment remained constant with time at a specific sampling location.

Overall, the results indicated that greater filter media thickness, coarser expanded shale materials, and lower inflow rates consistently resulted in higher removal efficiency. Moreover, the influent concentration did not significantly impact the treatment efficiency of the expanded shale media.

This study highlights the promising potential of expanded shale as an effective filter media in bioswales for enhancing water quality by removing pollutants such as TSS and turbidity.

ACKNOWLEDGEMENT

I extend my heartfelt gratitude and appreciation to all those who have helped me throughout my journey to completing this thesis at the University of Texas at Arlington. This milestone would not have been possible without the guidance and help of numerous individuals.

First and foremost, I would like to express my deepest gratitude to my esteemed advisor, Dr. Habib Ahmari, for his unwavering support and mentorship. His expertise and feedback were invaluable for shaping the direction of this research and have been a constant source of inspiration. Also, I would like to thank NCTCOG for providing funding for this study.

Besides my advisor, I would like to express my sincere gratitude to my thesis committee members, Dr. Srinivas Prabakar and Dr. Michelle Hummel, for their insightful comments. I want to thank Mr. Qays Mohammed, technical staff at UTA's Department of Civil Engineering for his technical support throughout the study. I thank Dr. Hu Qinhong and Tao Zhang of UTA Shimadzu Laboratory for giving me access to the lab equipment. Similarly, Giang Tran and Ryan Hurley, undergraduate students who always supported me throughout the study period and did their best to manage time and helped me during the experiments. Likewise, help from my peers Qazi Ashique E Mowla, Nabila Rashid Khandaker, Niloofar Ahmari, Hassan Aslaud, Mohammad Moradi, and Dipesh Dahal were always there whenever needed; I am genuinely grateful for them.

My special appreciation goes out to my parents (Sthaneshwor Bhurtyal and Namuna Bhurtyal), my brother (Anish Bhurtyal), and my wife (Tara Budhathoki). My parents have been my continuous source of love, support, and motivation. My brother has always been a constant source of strength. My wife, who has always been with me throughout my challenging academic endeavor, kept always supporting me.

TABLE OF CONTENTS

LISTS OF FIGURES

LISTS OF TABLES

Table 2.1: Various treatment mechanisms in BMPs (Ekka and Hunt 2020) 14
Table 2.2: Summary of various BMPs and their treatment phenomena (NCDOT 2014)..... 15
Table 2.3: Summary of the effectiveness of different BMPs in reducing major pollutants 20
Table 2.4: General properties of expanded shale (ESCS) vs. Typical Granular Filter Media..... 32

CHAPTER 1
INTRODUCTION

1.1 Background and Motivation

Water quality is a critical issue for both human health and the environment. Runoff from urban areas can carry pollutants such as sediment, nutrients, and bacteria into waterways, where they can degrade water quality and harm aquatic life. Bioswales are Best Management Practices (BMPs) that can intercept and filter the runoff before it reaches waterways through filtration, adsorption, and plant uptake. They are a cost-effective and sustainable way to improve water quality and provide other benefits, such as stormwater management.

The infiltration rate of a bioswale is the rate at which water can move through the provided soil media. The infiltration rate is vital in designing infiltration BMPs because it determines how much pollutants can be removed by the infiltration process. The soil media in a bioswale can affect the infiltration rate in several ways. The soil type, the amount of organic matter in the soil, its gradation, and the moisture content of the soil can all affect the infiltration rate.

Bioswales are a promising tool for improving water quality. Laboratory experiments on bioswales can help us better understand how they work and how they can be used to achieve the best results. Several factors, such as soil properties, flow rate, filter media thickness, and influent concentration, affect the performance of bioswale. By understanding the factors that affect the pollutant removal efficiency of bioswales, we can design bioswales that are more effective at filtering stormwater runoff and improving water quality.

Also, bioswales' practice has limitations, such as area requirements and depth restrictions for the water quality flow. Even though expanded shale has not been exclusively used for its effectiveness in improving water quality in bioswales, it has been used as an amendment to promote drainage properties of soil (Mechleb et al. 2014) and aeration to plant roots (Sloan et al. 2010), and as a filler in filtering medium for enhancing efficiency for phosphorus removal (Forbes et al. 2004). Hence, this study focused on evaluating a hypothesis that the expanded shale, as a soil media in bioswales, would promote infiltration. The improved infiltration rate and the expanded shale adsorbing capacity will contribute to higher pollutant removal efficiency.

1.2 Research Objective

The research objective of this thesis is to:

a) Evaluate the effectiveness of expanded shale as the filter media of bioswales in removing sediment from stormwater runoff.
b) Evaluate the effect of the thickness of soil media on removal efficiency.
c) Investigate the effect of inflow rate on removing TSS and turbidity from stormwater runoff.
d) Investigate the influent sediment concentration effects on the TSS and turbidity removal efficiency of expanded shale media.
e) Investigate the effect of underdrain systems on the TSS and turbidity removal.
f) Compare the obtained efficiencies with other bioswales practices.

1.3 Thesis Organization

The thesis is organized into several chapters to comprehensively explore the research topic. The structure of the thesis is outlined as follows:

Chapter 1: Introduction

In this chapter, the research topic is introduced, along with its motivation and objectives. The significance of the research and the rationale for utilizing expanded shale in bioswales are discussed, providing a clear context for the study.

Chapter 2: Literature Review

This chapter conducts an in-depth review of the existing literature on various aspects related to the research, including stormwater pollutants, best management practices, bioswales, and expanded shale. It specifically presents the properties and past applications of expanded shale, serving as a foundation for the subsequent chapters.

Chapter 3: Experimental Setup and Procedures

This chapter presents a comprehensive description of the experiment setup and the specific procedures employed in the research. It provides detailed information on the materials and scenarios utilized, as well as the standards adhered to in conducting various tests.

Chapter 4: Results and Analysis

The core of the thesis is presented in this chapter, where the study's findings are depicted, interpreted, evaluated, and analyzed. The results of the experiments are thoroughly discussed, allowing for a comprehensive understanding of the outcomes.

Chapter 5: Conclusion and Future Research

The final chapter serves as a summary of the research undertaken, emphasizing the key findings and their implications. Additionally, this chapter provides suggestions for future research endeavors, thereby inspiring further exploration in the field.

CHAPTER 2
LITERATURE REVIEW

2.1 Introduction

This chapter provides an overview of literature on stormwater control measures and associated best management practices. It discusses different stormwater pollutants and their implication in receiving waterbodies. The review focuses on introducing expanded shale, its performance, and the need for utilizing expanded shale in stormwater management practices.

2.2 Urban Landscape

With highly populated areas and paved ground surfaces, artificial flow paths and streambeds in the urban landscape have been altering the natural hydrologic systems (Sun et al. 2019). Urbanization has changed the natural hydrology of large to small watersheds by introducing new hydrological, ecological, and environmental-related mechanisms that affect water quality (Yang et al. 2021). McGrane (2016) showed that urban surfaces have accelerated the mobilization of pollutants due to increased surface runoff and hydraulic efficiency of artificial channels. An increased runoff will cause more pollutants accumulation in receiving water during storm events due to rainfall and snowfall.

2.3 Problems in Urban Landscape

With the increase in urbanization, hydrologic modifications like dam construction, river channelization, and flow diversion cause environmental problems from eutrophication to flooding. Problems involving sediments, nutrients, and pathogens are not only issues associated with urbanization but also involves hydrologic time shifts in terms of hydrologic perspective (Pringle

2000). Stormwater quantity and quality are both concerns associated with problems caused by urbanization (Akan and Houghtalen 2003).

Similarly, source interaction phenomena such as vehicles releasing pollutants into the atmosphere may later deposit on the paved surface, and this may involve the same pollutant to be considered in two diverse sources of pollutants, such as brake-induced dust particles and tire dust. Both sources contain heavy metals and sediment. Hence, it is not easy to identify the source of pollutants. Further, this source identification of pollutants is complicated by phenomena such as suspension and re-suspension (Thorpe and Harrison 2008). These are the various associated phenomena that make it challenging to study the effect of urbanization and disentangle the pollutant sources (EPA 2017a).

Due to the increased industrial activities, natural gases and particles move into the atmosphere by pollen, microorganisms, and wind-blown debris are later combined or sometimes converted into complex urban pollutants such as aerosols and trace gasses. Similarly, heavy metals generated from vehicle abrasion, oil spillage, construction site debris, and acid rain-induced corrosion are familiar sources of pollutants in urban catchments when washed or carried by rainwater (Brinkmann 1985). Water quality parameters such as total suspended solids (TSS), chemical oxygen demand (COD), pH, heavy metals, nitrates, and phosphate are found to be considered for urban stormwater runoff quality assessment (Björklund et al. 2018; Lee et al. 2007; Zhang et al. 2021).

2.4 First-Flush

The first-flush refers to the runoff initially generated from a surface during precipitation. The number of pollutants present in the initial runoff, or "first-flush" is influenced by the interval between rainfall events, with longer dry intervals leading to higher pollutant levels (Wang et al.

2022). A comprehensive study on first-flush in urban catchments found that a significant portion of pollutant mass was present in the initial portion of runoff volume (Dang et al. 2023); however, the characteristics of first-flush, including flow and concentration, varied widely across different sites and climates (Maniquiz-Redillas et al. 2022). Water quality parameters, namely suspended solids, COD, total phosphorus, heavy metals, and total nitrogen were mainly considered to study the first-flush in stormwater runoff (Lee et al. 2002; Maniquiz-Redillas et al. 2022; Zhang et al. 2021). These studies found that the stormwater treatment targeted for first-flush could trap many pollutants.

The US Department of Agriculture (USDA 2020) also indicated that the initial runoff from a site tends to be the most contaminated, and treatment of the initial runoff, i.e., first-flush, is sufficient to address the water quality issues. If the runoff contains harmful substances, extra treatment methods might be required, and it is equally important to acknowledge the impact of peak flow and volume.

2.5 Pollutants Origin and Indicator Pollutants

Urban areas, due to reduced perviousness, have been a source of non-point source pollutants. Pollutants of natural origin and anthropogenic sources are often found to be the major contributors to urban water. Often pollutant in stormwater comes in various forms primarily due to various sources (Akan and Houghtalen 2003).

Solids generally originate from washing off sediment deposited from construction or agricultural sites over impervious layers. Nutrients such as phosphorus and nitrogen cause unwanted algae growth and increase the demand for dissolved oxygen in receiving water streams. Organic carbon sources such as litter, debris, and animal waste are also additional sources for depleting the

dissolved oxygen of receiving water bodies. Also, hydrocarbons and trace metals are toxic pollutants from oil spillage and automobiles (EPA 2017b)

A solid form of pollutant refers to all sorts of solid particulate matter that may be freely floating, suspended, or dissolved solids. Solid particles that included dissolved and suspended solids were solely found to account for 72% of pollutants in stormwater runoff (Xiao and McPherson 2011). In many cases, solids act as a medium to carry other pollutants, such as metals, gases, and microorganisms, which may be attached to the solid particles. They are generally soil particles from construction sites, debris, floating particles, and sometimes trash that comes along the way of flowing water. Suspended solids limit light penetration and function as a carrier for other pollutants that harm aquatic ecosystems (iSWM 2014 a). Hence, suspended sediment is a primary indicator pollutant of stormwater runoff (Akan and Houghtalen 2003, iSWM 2014 a).

2.6 History of Stormwater Management Practices

Before the early 70s, stormwater management practices were only considered in terms of conveyance (Bertrand-Krajewski 2021). Conventional stormwater infrastructure or gray infrastructure management is quickly bypassing the stormwater away from urban areas (EPA 2023a). These practices did not consider the treatment aspect of runoff. The concept of disconnecting the imperviousness of the land uses, retaining, detaining, and infiltrating stormwater was realized over time to achieve the natural water balance best (Bertrand-Krajewski 2021; Fletcher et al. 2015).

In 1998, D'Arcy developed the concept of a sustainable urban drainage system (SUDS). The SUDS triangle comprises three corners of the integrated approach: water quality, water quantity, and underlying habitat. This concept has been used since then, particularly in European countries

(Fletcher et al. 2015). Similarly, in the U.S., the BMP (best management practice) term is used for pollution-preventing mechanisms for stormwater under Pollution Prevention Act.

2.7 Best Management Practices (BMPs)

Stormwater runoff is water flowing overland or over impervious surfaces such as highways or parking lots because of limited infiltration into the groundwater. Due to snow and rainfall events, runoff from various municipal sewer systems and highway pavements is eventually discharged to local waterbodies (Akan and Houghtalen 2003; EPA 2023b). The nature of this runoff may be a mixture of complex organic and inorganic compounds and usually acts as a source of suspended and dissolved solids, heavy metals, and various microorganisms (USGS 2023). The introduction of such sediments into receiving waters leads to siltation, which causes a negative impact on the aquatic ecosystem (EPA 1999a).

Stormwater management can be recognized as a necessary measure to curtail the potential effects of runoff generated from urbanized areas. Stormwater quantity and quality have significant impacts on the environment as they are interlinked with urbanization (Akan and Houghtalen 2003; Walsh et al. 2005). Due to the increase in imperviousness, hydrological changes that limit the baseflow and groundwater recharge from the urban streams and stream flooding events becoming more frequent and peak flow intensity fluctuating at an unprecedented rate after the storm event. Hence, to address the adverse consequence of such impacts of stormwater on the urban environment; riverbank erosion control, flow control, and flood mitigation are the goals of BMPs such as vegetated swales and infiltration trenches (Bertrand-Krajewski 2021).

Stormwater best management practices began in the United States in the early 1990s, prompted by the legal obligation to address the need for stormwater quality control. Nowadays, safeguarding the habitats, mitigating floods, enhancing water quality in receiving water systems, preserving

water resources, and protecting public health can be the positive outcomes that one could expect from effective management of stormwater runoff (EPA 2014). BMPs are broadly classified practices for representing physical, chemical, structural, or managerial measures or all that may incorporate more than one practice. They are practices employed to reduce or prevent stormwater pollution by controlling the volume, timing, and quality of stormwater runoff (EPA 2014). Hence, BMPs are found to be implemented to decrease peak flow or peak volume based on their implication.

2.8 Need of BMPs

The conventional sewer network that was constructed solely for hydraulic control is now being supplemented by additional local requirements and diversified objectives. These objectives commonly incorporate flooding mitigation, urban ecology, public health, water quality, etc., (Bertrand-Krajewski 2021). Conventional stormwater control methods based on flow control, i.e., collect peak flow, provide local drainage and convey the flow safely to receiving water. Also, they are only capable of reducing peak timing and runoff rate but not reducing stormwater volume. So, in addition to the conventional control, reducing the stormwater volume is needed. In practice, BMPs incorporating on-site infiltration are required and they can be constructed in smaller footprints than conventional treatment systems like detention ponds (Brander et al. 2004). Flow control measures such as bioretention, constructed wetlands, flow separators, vegetative swales, and porous pavement are most practiced. These practices alter the flow characteristics and treat water by the combined phenomenon of sedimentation, infiltration, adsorption, plant uptake, etc. (Caltrans 2012; EPA 1999a).

2.9 Application of BMPs

The EPA (1999a) recognized stormwater pollution as a contributing factor to the poor water quality of the nation's waterbodies. After the recognition by EPA, BMPs have been included and regulated in design manuals for practicing engineers across the U.S. The effectiveness of any BMP's implementation should be based on holistic management approaches such as costs and its effectiveness in an overall system rather than individual BMPs applications only (EPA 2022). For example, flood control is an objective that the BMPs could be considered while they are designed for pollution reduction (Caltrans 2012). In some cases, BMPs are also used to decrease the adverse impacts of post-construction runoff (Osouli et al. 2017).

If the specific site requirement is to promote natural movement and enhance infiltration while maintaining the aesthetic aspect in addition to the primary goal of improving water quality, infiltration BMP techniques could be implemented (EPA 2022). Likewise, when there is limited infiltration in case of a low infiltration rate of native soils and high groundwater table, bioretention-based BMPs are feasible (Riverside County 2020). Such bioretention techniques rely on evaporation for flow reduction and prolonged infiltration for flow reduction.

Barret et al. (1998) showed that an effective treatment system was required to meet design standards, which typically require first-flush to be considered for stormwater runoff treatment; however, for highway runoff, the study suggested considering constant pollutant concentration for a single storm event. Several studies also suggested that BMPs, which often target to treat the first-flush are subject to an opportunity to treat the high concentrations of different pollutants such as total suspended solids (TSS), chemical oxygen demand (COD), biological oxygen demand (BOD), turbidity, heavy metals, and nutrients (Lee et al. 2002; Maniquiz-Redillas et al. 2022; Zhang et al. 2021).

2.10 Types of BMPs

The BMPs are classified based on geometric properties and on the goal of practice. These classifications are discussed in the following sections.

2.10.1 Geometric Properties

BMPs can be classified according to their physical characteristics and design elements. These properties are mainly related to the specific structural features of the practice. As per EPA (2014), BMPs are classified into point, linear, and area BMPs.

Point BMPs:

Practices that collect and treat upstream water at a specific location by the combination of detention, infiltration, sedimentation, and conversion of pollutants across the infrastructure are point BMPs. Constructed wetlands, infiltration basins, etc., are examples of point BMPs.

Linear BMPs:

Streams or channels that allow pollutants to filtrate across the channel, infiltrate through porous media, be consumed by vegetation, and preserve the aesthetic value of the location are linear BMPs. Grass swale, wet swale, and vegetated filter strips are such examples.

Area BMPs:

Practices involving land management measures to meet the water quality and quantity criteria by altering the perviousness of the existing surface and involving pollutant controls are area BMPs. Green roofs and permeable pavements are common area BMPs in practice.

2.10.2 Goal of BMPs

BMP practices can be designed based on the goal for which it is intended. There are three different classifications, including flow control, pollutant source control, and treatment control BMPs (Riverside County 2020, EPA 1999a).

Flow Control BMPs:

The increased stormwater runoff because of urbanization will collect a higher portion of sediments and hence, attach nutrients and metals along with it. Similarly, due to increased flow, the chances of eroding banks and beds of streams due to higher velocity also threaten the receiving water. To address these concerns, flow control BMPs are designed to effectively control the runoff volume and peak timing of the stormwater runoff. Hence, to reduce the chances of collecting pollutants and eroding banks, they can limit the stormwater runoff generated by enhancing the infiltration and providing some storage for incoming water on-site. Detention basins, rain barrels, vegetated filter strips, and infiltration wells are typical examples of such BMPs, which can be designed based on the flow control principle.

Pollutant Source Control BMPs:

Pollutant source control BMPs target pollutant removal before they are washed by stormwater runoff. They are standard practices that aim to reduce runoff pollutants, specifically by nonstructural measures. They involve public participation and awareness by limiting and controlling the extent of current practices such as chemical usage, identification, and regulating sanitary behaviors within the vicinity affecting urban runoff. Sweeping impervious surfaces, limiting the use of pesticides and herbicides, proper disposal of waste, and public awareness falls under the pollutant-source control BMPs.

Treatment Control BMPs:

BMPs that treat/capture the contaminants to address the detrimental effect of stormwater runoff over receiving waterbodies by the combined action of physical process, chemical process, and biological processes are treatment control BMPs. Normally, for such BMPs there is a target concentration or amount of pollutants that is considered safe to dispose into the natural water streams. They may incorporate one or many pollutant removal mechanisms to achieve the goal, such as sedimentation, flotation, filtration, infiltration, adsorption, plant uptake, and chemical reaction.

2.10.3 Low Impact Developments BMPs

Low Impact Developments (LID) or green infrastructure (GI) are practices that intend to reduce the runoff volume of stormwater and restore it or construct natural processes for controlling water quality and the surrounding habitat/ecosystem within the watershed or ecosystem (EPA 2012; Eckart et al. 2017; Riverside County 2020). LID BMPs are only those that are effective in on-site treating stormwater through natural processes such as infiltration, biological retention, and evapotranspiration. LID features are the natural or engineered media used to reduce runoff promoting infiltration under Water Quality Management Plan (WQMP). WQMP includes the on-site retention of runoff volume, pollutant reduction based on their types, and specific BMPs that could address the relevant pollutants (Riverside County 2020).

Stormwater treatment methods such as bioretention, biofiltration, and rain gardens are the most desired water treatments that incorporate both infiltration and biofiltration LID BMPs.

2.11 Selection of BMPs

When the rainfall falls over the ground, it may collect sediments, chemicals, nutrients such as pesticides and fertilizers, oils, and various human and animal waste that falls on its route. Hence, the selection of the BMPs is governed by the nature of the pollutants in the flowing water. Based on the nature of the pollutants, several BMPs have their significance depending on sediment sizes, pollutant types, incoming pollutant concentrations, and end goal (Ekka et al. 2021).

Broadly, based on the site constraints, the selection of treatment BMPs can also be influenced by the space availability and site conditions. For example, for limited space, bioretention systems are preferred over grassed channels for urban sites. Similarly, site conditions such as groundwater level, native soil properties, topography, and working head also influence the selection of BMPs (Clar et al. 2004).

2.12 Treatment Phenomena in BMPs

Various phenomena such as sedimentation, flotation, filtration, infiltration, sorption, nutrient uptake, biological conversion, and degradation of chemical compounds can be the governing mechanisms for determining the efficiency of pollutant control BMP (Caltrans 2012). They are summarized in Table 2.1.

Table 2.1: *Various treatment mechanisms in BMPs (Ekka and Hunt 2020)*

Phenomenon	**Descriptions**
Sedimentation	Settlement of the particles at the bottom of the channel due to gravity
Infiltration	Movement of water percolating through the soil media promoting recharge and flow reduction
Sorption	The combined chemical process of absorption and adsorption. Absorption is caused due to sediment trapped in the porous surface of soil media; similarly, adsorption is due to physical-chemical interactions. They may include dissolved or particulate matter. Ion exchange and interlocking of particles are common
Filtration	They are gross filtration which is caused due to trapping of particles by vegetation blocking the particle flow direction.
Biological interaction	They may be phenomena such as nitrification, denitrification, plant uptake, or any chemical reaction involving ion exchange

Flow control BMPs such as bioswales, infiltration wells, and vegetated filter strips also function as treatment control BMPs. Various BMPs with their treatment phenomena are summarized in Table 2.2, illustrating the basic description of underlying phenomena for pollutant reduction.

Table 2.2: *Summary of various BMPs and their treatment phenomena (NCDOT 2014)*

BMPs	Descriptions	Treatment Phenomena
Biofiltration Systems	Consists of sand or mulches as a filter media, provided with underdrain without soil amendment to drain once infiltrated	Filtration, Adsorption, nutrient uptake, assimilation
Enhanced biofiltration system with underdrain	Biofiltration basins with impervious base/ with amended soil, drained once infiltrated, under-drain provided	Filtration, Adsorption, nutrient uptake, Assimilation, Ponding-induced settlement
Filter strips*	Sloped vegetated land with/without amended soils	Infiltration, Sedimentation, Adsorption, Filtration
Dry detention basins/Retention basins	Shallow depressions typically with dual outlet, i.e., orifice and weir outlets, permanent pool of water	Ponding-induced settling, infiltration, Biological uptake, Chemical reaction
Wet detention basins	Captures and temporarily stores runoff volume, permanent pool of water	Ponding-induced settling, Sedimentation, Biological uptake, Filtration
Infiltration systems	Captures the runoff and infiltrates the water gradually, no under-drain system	Natural Filtration, Sedimentation, Adsorption, Biological uptake, Dilution
Wet swales	Depression with vegetated strip over natural soil, no under-drain provided, near or at water-table level, the soil may be amended	Vegetation uptake, Adsorption, Sedimentation, Infiltration
Dry swales/ Bioswales	Vegetated channels may or may not be with check dams and under-drains	Infiltration, Vegetation uptake, Sorption, Sedimentation

** Cannot meet 80% TSS reduction performance goal (iSWMM 2006, iSWM 2015)*

2.13 Biofiltration Swales/Bioswales

Bioswales are primarily wide, open channels of shallow depth and are constructed using native soils/engineered media to convey runoff generated during storm events. Bioswales can be used as an alternative or as a supplemental treatment method for traditional stormwater management systems. Bioswales collect water from impervious surfaces like paved parking lots, highways, and rooftops and partially absorb and carry runoff directly to sewer conveyance infrastructure (NRCS 2005).

Likewise, biofiltration swales are designed to infiltrate the water into the surrounding soils and can be constructed over the native soils/amended media. The required media properties can be determined using the gradation curve of the soil. If the existing soil has a particle size of $d_{10} > 0.02$ mm and $d_{20} > 0.06$ mm, it indicates slow filtration rates and require soil amendment (Caltrans 2020). Filtration and infiltration are the main contributors to pollutant removal in bioswales. They can be employed for water quality flow, flood control, or both (Caltrans 2012).

Several measures can be implemented in bioswales to handle the designed discharge to be released from the system. Such measures may include amending the infiltration rates of soil, altering the flow path length, providing underdrain for enhanced infiltration, or implementing all these measure together. Depending on their function, there are two categories of bioswales: wet swales and dry swales (Ekka and Hunt 2020). Schematics of these bioswales are presented in Figure 2.1 and Figure 2.2.

Wet swales function as a wetland with shallow groundwater level and native vegetation. The groundwater level in wet swales is near/at the swale level, so vegetation requires no or less irrigation frequency. Filtration within thick vegetation, sedimentation due to flatter slopes, and nutrient uptake mass due to biomass are the governing processes in wet swales for water treatment (NPDES 2021). Because of the large area requirements and mosquito breeding possibilities, wet swales are not suitable for urban landscapes (EPA 2021; Nuamah et al. 2020).

On the other hand, dry swales, also be referred to as grassed swales, typically have vegetation over engineered/soil media that promote capturing of pollutants by slowing down flow and increasing the chances of settlement and adsorption (Mustaffa et al. 2016). Dry swales typically have an underdrain that facilitates draining such that the ponding time is at most 48 hours. Dry swales are designed to keep the bottom of the channel at least 2 ft above the groundwater level (EPA 2021).

Thus, it can also be designed additionally as a structure that acts as a groundwater recharge facility. Another advantage of dry swales over wet swales is that dry swales can handle hotspot runoff from point sources, preventing groundwater contamination (EPA 2021). Underdrains and check dams can be added as per inflow quantity and downstream peak flow desired.

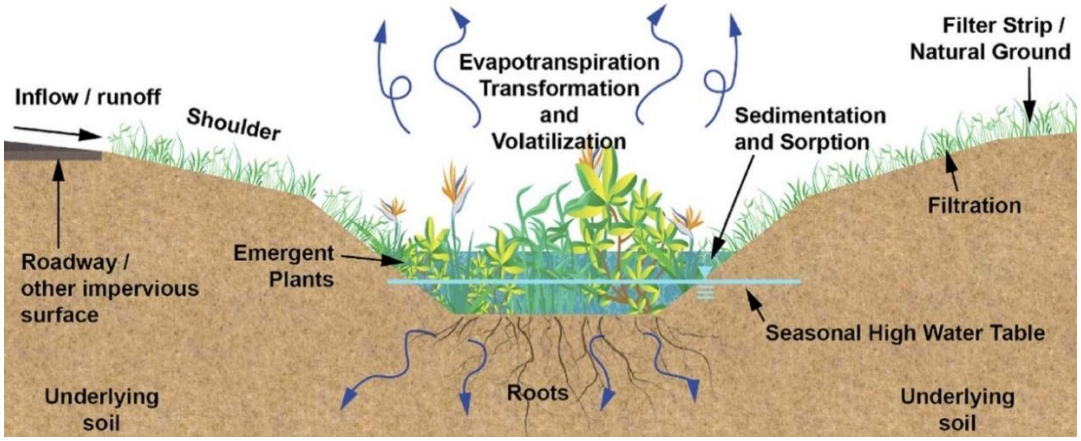

Figure 2.1: *A typical cross-section of wet swales (Ekka and Hunt 2020)*

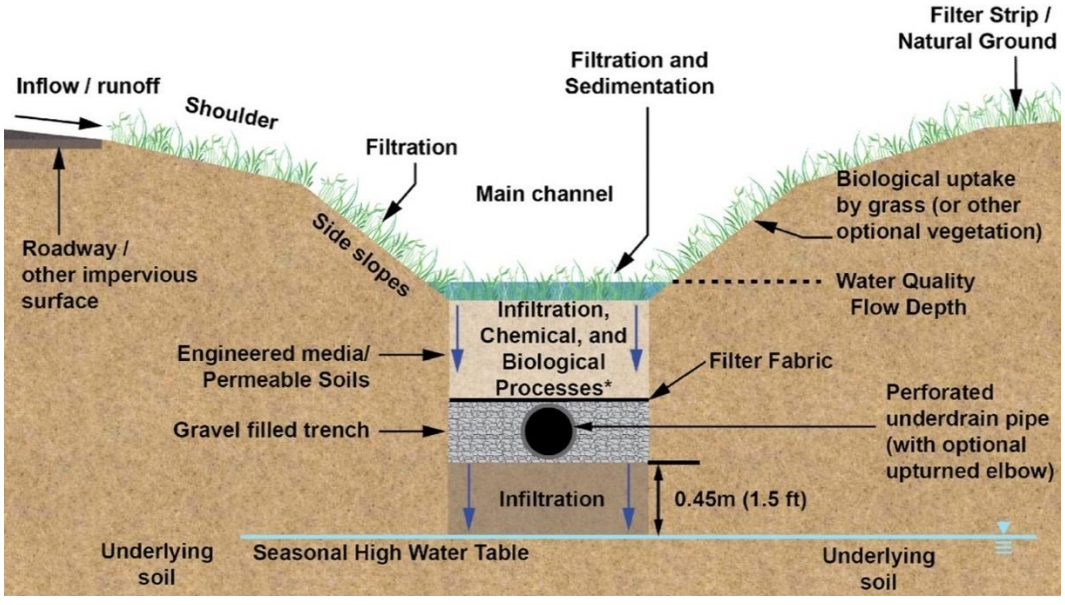

Figure 2.2: *A typical cross-section of dry swales (Ekka and Hunt 2020)*

2.14 The Efficiency of Bioswale/Bioretention Systems

Typically, infiltration in any BMPs is inter-related to soil properties of engineered, subsurface materials (native soil where the BMPs is intended to be placed), and filler materials (Minnesota Pollution Control Agency 2017). An example of each engineered media and filler materials are expanded shale, and clay/sand being mixed with an engineered media, respectively.

The efficiency of BMPs is highly related to the runoff volume reduction (Brown and Hunt 2012; Stagge et al. 2012; Wang et al. 2019) and the type of pollutants being considered. Sometimes the treatment system acts as a source of pollutants of certain kinds, such as total nitrogen (Liu et al. 2017). Irrespective of the pollutant sizes, infiltration promotes additional capturing of the pollutants in addition to settlement and sedimentation (Clark and Acomb 2008). Also, the infiltration rate of the coarser soil is higher than the finer soil particles. However, other factors affecting infiltration such as bulk density and soil layering, should also be considered for stormwater infiltration system (Minnesota Pollution Control Agency 2017).

Bioswales typically have higher efficiency in treating particulate contaminants, whereas the treatment of dissolved contaminants is less efficient. Moreover, wet swales were found to be most effective for reducing nitrogen and heavy metals from the influents (Ekka et al. 2021). Hunt et al. (2006) found that the Phosphorus index (P-index) of the soil media is inversely proportional to phosphorus removal; similarly, organic content and hydraulic conductivity were found to be influencing the total nitrogen removal efficiency. Kim et al. (2003) found evidence that 70-80% of total nitrogen removal efficiency was obtained when the engineered mix was used as a soil media in a bioretention system.

Additionally, King County (1995) conducted 39 swale surveys, out of which only 32 swales were considered for the study. The study considered swales' functionality, drainage area, and land use,

and observed that 40% of TSS and 17% of total phosphorus removal were obtained in existing good or fair conditions. The same study demonstrated that if all the swales were in good condition as they were initially designed, 83% and 33% of overall removal efficiency could be achieved for TSS and total phosphorus. More information on treatment efficiency in other studies is summarized in Table 2.3.

A comparative study on permeable pavement and bioswale conducted by Seters et al. (2006) found that bioswales were more than 50% more effective than the conventional treatment asphalt systems in reducing the common heavy metals (zinc and lead); however, the concentration of the nutrient was higher in the effluent.

Also, Fardel et al. (2019) conducted an extensive review of 59 swales-related studies and determined a correlation among TSS, total trace metals, total nitrogen, and total phosphorus. TSS and total trace metals (copper, zinc, cadmium, and lead) were highly correlated. Swales had a median reduction efficiency of 56% for TSS and 62% for the total trace metals. More than 44% reduction was seen on dissolved trace metals, and only a 30% maximum median reduction was observed for nutrients (total nitrogen and total phosphorus).

Table 2.3: *Summary of the effectiveness of different BMPs in reducing major pollutants*

Reference	Runoff Volume Reduction (%)	TSS (%)	Total Phosphorus (%)	Total Nitrogen (%)	Metals (%)	Bacteria (%)	No of observations	Remarks
(King County 1995)	-	40-83	17	-	-	-	33	Swales
(Stagge et al. 2012)	55-60	44-83	(-49.2) – 68.7	(-25.6) – 85.6	18-92.6	-	-	Dry swale (Lead, copper, zinc, and cadmium)
(Hunt et al. 2008)	96.5	60	31	32.2	31.4-59.5	69-71	23**	Bioretention Cell
(Brown and Hunt, 2011)	67	58	-10	58	-	-	161	Bioretention
(Xiao and McPherson 2011)	88.8	95	-	97	87	-	-	Bioswale
(Brown and Hunt 2012)		92	72	80	-	-	42	Bioretention
(Knight et al. 2013)	23	75	35	30	-	-	30	Bioswale
(Anderson et al. 2016)	83-97	81	-	-	81	-	-	Bioswale
(Wang et al. 2019)	-	80	67	51	90-94	-	182	Data analysis based on the previous database
(Fardel et al. 2019)	-	56	30		62	-	59	Bioswale*
(Purvis, 2018)		10	-	-	-	59-65	-	Bioswale-overflow
(Purvis, 2018)		88	-	-	-	55-75	-	Bioswale-underdrain
(EPA, 2021)		87	5-83	46-84	88-90	-	-	Grassed swale

** TN and TP studied as nutrients*

*** Number of tests or observations varies for different contaminants*

2.15 Applicability and Suitability of Bioswales

Technological, economic, and institutional considerations such as technique, costs, and area of interest should be considered while analyzing the applicability of BMPs (EPA 2016). Bioswales need to be site-specific and designed based on target pollutants (Ekka et al. 2021; Jamil and Davis 2012). The applicability of the swales can be determined based on the different goals of pollutant removal, flow control, erosion control, and groundwater recharge.

USDA (2020), under erosion and sedimentation provisions, recommends an acceptable flow rate and discharging volume based on underlying soil properties within the range of local regulations. However, if there are not any local regulatory bodies, a 2-year, 24-hour predevelopment rainfall is mandated for peak flow and runoff volume. Similarly, EPA (2021) recommends a 2-year, 24-hour storm to be considered for water quality treatment and a 10-year, 24-hour storm for flood control BMP swales.

2.16 Design of Bioswales

All the swales are project specific depending upon incoming pollutants and flow. Also, bioswales applications are watershed-specific based on drainage area configuration and desired results in addition to the area available, site slope, and the nature of inflow pollutants. Also, a combination of BMPs is occasionally used to meet the water quality requirements for treatment swales (iSWM 2014 b).

Bioswales, infiltration ditches, and vegetated land strips are typical examples of linear BMPs. As this literature review centers on the implementation of dry swales as one of the treatment practices, this section is primarily focused on exploring dry swale design principles derived from existing literature and design guidelines.

Similar to the design and implementation of any BMPs, the study by Gong et al. (2019) found that rainfall characteristics, dry period, influent loads, and imperviousness of the drainage area affect the pollutant removal efficiency of grassed swales. The site-specific constraints which can influence the selection and designing of the swale are catchment area, the slope of the terrain, imperviousness, media depths, groundwater level, land use, geometric configuration required/desired, channel depth, longitudinal slope, flow velocity, shear stress and outflow requirements for BMPs application (Ekka et al. 2021).

Flow rate is the governing factor for determining the hydraulic performance of swales (Hunt et al. 2016). In general practice, 2-year, 24-hour storm is recommended for water quality, and 20-year, 24- hour or 100-year, 24-hour storm peak flow for peak flow management is recommended in the design manual of different agencies and authorities (e.g., iSWMM 2009; King County 1995). For water quality volumes calculation, the first 1-inch of rainfall should be considered (Illinois Tollway 2018: Caltrans 2012). However, iSWM 2015 considers 1.5-inches of rainfall for water quality volume for treatment bioswales representing 85th percentile of all storm events.

The flow rate subjected to bioswales should account for 80%-95% of the stormwater runoff (Hunt et al. 2020). A wet swale can be designed to receive stormwater from a larger drainage area of 1-5 acres. A dry swale is suitable for drainage areas less than 0.5 acres and does not require any pretreatment (EPA 2021). Flow regulation also determines the maximum amount of runoff that can be subjected to bioswales design.

The infiltration rate, Manning's roughness, longitudinal slope, and flow velocity are factors affecting runoff volume and depth of the stormwater runoff. Stormwater runoff depends on abstraction, land use, and land topography within the contributing area (Zeiringer et al. 2018). Also, unless alternative flow bypassing is arranged, the maximum runoff coming from a contributing area can be considered a bioswale capacity (Caltrans 2012). The iSWM (2014a) allows the NRCS TR-55 method to be used for calculating discharge volume, whereas Caltrans (2012) suggests using the rational formula to calculate the runoff entering the bioswale.

2.16.1 Soil Properties of Underlying Media

Many studies have reported that infiltration and hydraulic conductivity greatly influence the degree of treatment capability of BMPs (Brown and Hunt 2012; Wang et al. 2019; EPA 2021). The soil should permit water infiltration, such that the swale is drained within 48 hours. The soil infiltration

can be enhanced by providing an underdrain and sometimes by increasing the depth of the standing water (Zeiringer et al. 2018). If the native soil is highly permeable, underdrain may not be necessary; however, the soil may be amended to obtain desired hydraulic conductivity and permeability (Clark and Acomb 2008). Soil can be amended with highly porous materials to promote quick drainage and enhance the infiltration rate. Likewise, soil with a coarser fraction is desired as they can hold more moisture during drought, and soils with a higher fine-particle fraction are likely to reduce infiltration by clogging the depressed surface and eventually decreasing infiltration (Ekka et al. 2021). Hence, gravel and sand-mixed gravel are used in practice, which have comparatively high hydraulic conductivity and are more likely to prevent clogging.

USDA (2020) suggests that the saturated hydraulic conductivity of the infiltrating soils should be at least 0.5 cm per hour (0.2 inch/hr), and stored water during peak events shall be drained within 72 hours. In general, if the media has an infiltration rate of at least 1.27 cm per hour (0.5 inch/hr), bioswales can be designed without an underdrain, and underdrain is optional when the infiltration rate of underlying soil is $\geq$ 0.2 inch/hr. Nevertheless, for both cases, 72 hours of drainage time should be maintained as in any infiltration system (EPA 1999a; The City of San Diego n.d.). Therefore, precautions should be taken during the construction of bioswale such that soil compaction is avoided.

Also, soil containing any amendment, irrespective of its nature (organic or inorganic), is found to increase hydraulic conductivity and retain more water, resulting in vegetation growth and hence enhancing efficiency in removing pollutants (Anderson et al. 2017; Ekka et al. 2021).

2.16.2 Swale Geometry

Channel geometry changes the hydraulic efficiency and alters the flow depth and velocity even for the same incoming flow. As a rule of thumb, it is suggested that the maximum surface area of the

swale can be as high as 1% of the drainage area (Clark and Acomb 2008; EPA 1999b). Based on the land availability and aesthetic importance, bioswales geometric design is flexible. Since recommended flow depth for water quality is capped at 6 inches or equal to the vegetation height, to have less flow depth, trapezoidal channel provide higher wetted perimeter and also they are less sensitive to the side slopes (Ekka et al. 2021). Trapezoidal channels are more often used in practice because of the clogging and construction difficulty of V-shaped and parabolic channels.

Also, the trapezoidal channel with 2 to 6 ft of bottom width and a slope of 3H:1V is suggested. Li et al. (2016) studied the pollutant removal efficiency of bioswales by keeping the surface loading rate and volume loading rate equal to study the effect of swale width. The study found a 5% to 47% increase in chemical oxygen demand removal efficiency when the width was increased by 50%. Lastly, in the case of swales with check dams, the flow depth cannot be greater than one-half of the total channel depth (Caltrans, 2012).

2.16.3 Longitudinal Slope

The slope of any channel governs the flow velocity. Milder slope ranging from 1% to 2% is desired for bioswales. In any case, the slope cannot be more than 6% or any threshold slope, that is, if present, causes bank scouring for a 10-year storm event for 6 inches of flow depth (StormwaterPA 2006). In such cases, check dams are recommended to slow down the flow velocity, promote infiltration and increase the hydraulic residence time, and eventually increase the efficiency of the purposed bioswale. Proper underdrain can be introduced in the bioswale to limit the standing water level during its operation if the slope is less than 1%. In general, a less flat swale configuration needs more length and vice versa.

2.16.4 Design Flow

BMPs are designed based on more frequent, less intense storm duration, i.e., 2-year; 24-hour storm for water quality purposes. Similarly, for peak flow conveyance, infrequent storm intensities are considered (100-year or 25-year storms). Since bioswales are to be designed both for water quality flow and for peak flow during extreme events, the depth of flow may exceed 6 inches unless bypass arrangements are provided within the swale configuration (Caltrans 2012). Increasing the depth of flow could promote infiltration that would increase efficiency, but the depth of water in swales is limited to 6 inches or vegetation height for water quality flow. If bypass arrangements are present, they can be routed to enter nearby conventional treatment systems, such as detention basins and underground storage systems (iSWMM 2009).

In addition, flow rates are limited to 5 cfs for swales (EPA 1999b). Also, based on the type of soil, the incoming velocity should not erode the channel. A velocity of 3.5 to 5 ft/s is permitted for sands, silts, or their mixture, and a higher velocity of 4.5 to 6 ft/s for clay mix soils, depending on the kind of vegetation they may have (NCDEQ 2017). Without vegetation, designers should take a maximum flow velocity of 1 ft/s for swales without vegetation for water quality purposes and 4 ft/s for highway-generated runoff (Caltrans, 2012).

Flow depth and velocity can be calculated using Manning's equation (Eq. 2.1) by considering roughness coefficient (n) value of 0.2 to 0.3 for water quality flow and 0.05 for peak events.

$$v = \frac{Q}{A} = \frac{1.49}{n} A\, R^{2/3}\, S^{0.5} \qquad (2.1)$$

where v is flow velocity (ft/s), A is cross-section area of the swale channel (ft^2), Q is flow rate (cfs), n is Manning's roughness coefficient, R is hydraulic radius of the channel (ft), and S is longitudinal slope of the channel.

In some extreme cases, when flow velocity as high as 4 ft/s must be dealt with, a geofabric may be used to cover engineered media/soil to prevent erosion of the underlying soil (Caltrans 2012).

2.16.5 Hydraulic Residence Time

Hydraulic residence time (HRT) is the average duration that the flow remains within the swale. The minimum time for water treatment design is 5 min (Caltrans 2012). It is calculated numerically by dividing the inflow volume by the flow rate.

$$HRT = \frac{V}{Q} \times 60 = \frac{L}{v} \times 60 \qquad (2.2)$$

where V is volume (ft^3), Q is flow rate (cfs), L is the swale length (ft), v is flow velocity (ft/s), and 60 is used as unit conversion to calculate *HRT* in minutes.

If an *HRT* lower than 5 min is obtained, then channel length is extended, or width can be altered, to lower the velocity. Lower velocity can also be achieved by flattening the channel slope.

Likewise, the inter-relationship formula (Eq. 2.3) must be satisfied to meet the water quality flow requirement. If not, the design procedure is repeated for different configurations (Caltrans 2012). If none of the calculations meets the following criterion, the BMP cannot be considered as a treatment BMP; however, it can be taken as a pollutant control BMP.

$$\frac{HRT \times 60}{y_{WQF} \times v_{WQF}} \geq 1300 \qquad (2.3)$$

where, *HRT* is hydraulic residence time (min), y_{WQF} is depth for water quality flow (ft), and v_{WQF} is velocity for water quality flow (ft/s), and 60 is unit conversion factor.

2.16.6 Check Dams

Check dams are small flow structures with a maximum height of 2 ft that can be constructed to hold the concentrated flow in bioswales. A check dam functions to trap sediment and heavy metal

particles, remove nutrients and chemicals, control peak flow, and enhance infiltration for stormwater runoff (Ekka et al. 2021; Stagge et al. 2012; Winston et al. 2019). Check dams may be of stones or rock structures located near the downstream end of the swale length. Check dams increase the hydraulic residence time and accelerate the processes such as absorption and nutrient uptake. Since the settlement of the particles will be more with higher hydraulic retention time, check dams promote pollutant removal. They can be installed perpendicular to the flow every 20 ft in a case when the channel slope exceeds 5% or when erosional velocity is to be avoided. The slope between any two check dams should be within 2% (The City of San Diego n.d.). However, the spacing between two check dams in case of water quality flow treatment should be at least 50 ft (iSWMM 2009; King County, 1995, EPA 1999b).

TSS removal efficiency was higher when check dams were installed perpendicular to the length of the grass swale (Deletic and Fletcher 2006). However, the study conducted by Stagge et al. (2012) on bioswales showed opposite results, which might be due to re-suspension or surface erosion of the channel during extreme events with high influent concentration. Interestingly, contrasting all the findings, Jamil and Davis (2012) concluded that addition of check dams had no impact on the TSS removal efficiency. Introducing check dams to existing swales improved runoff volume reduction by 17%; despite this, clogging and surface irregularities were reported to be higher after the construction of check dams. Hence the optimum design of check dams and maintenance was highlighted by Winston et al. (2019).

2.16.7 Shear Stress

Shear stress is the force per unit area that is exerted by water on the channel surface. The applied shear stress is a function of the flow of water, the weight of the water, as well as the slope of the bioswale. Applied shear stress can be calculated based on the following equation (Chaudhry 2022):

$$\tau = \gamma R S \quad (2.4)$$

where, τ is average shear stress (lb/ft^2), γ is specific weight of water (lb/ft^3), R is hydraulic radius of the channel (ft), and S is slope of the bioswale.

Also, the permissible shear stress is the maximum stress exerted by the flowing water without causing erosion or damage to the channel. For a stable channel, applied shear stress should always be less than permissible shear stress. Permissible shear stress is dependent on the existing vegetation and properties of the underlying soil.

2.16.8 Swale Length

The maximum possible length is desired along with the flow route (Caltrans 2012). Increasing the length of the channel increases the settling phenomenon. Length should be enough to promote settlement within the swale, and this is governed by the hydraulic residence time.

The swale length can be determined by two different approaches. One method that determines the required length of the channel based on the hydraulic residence time (*HRT*) (Eq. 2.2) which is a site-based design. The second method uses the Aberdeen equation based on the mean sediment size of the influent.

Design based on HRT (Site-based Design)

This method involves the following steps:

i) First, the design volume of stormwater needs to be evaluated for WQF or peak flow.

ii) Using Manning's equation, flow velocity is calculated for considered WQF.

iii) This velocity, along with the available swale length, is used for *HRT* calculation.

iv) The calculated *HRT* is checked with a minimum *HRT* of 5 minutes.

If the calculated *HRT* value does not satisfy the minimum required criteria, length, width, or slope are altered, and the new *HRT* is checked with the inter-relationship formula (Eq. 2.3). Sometimes, the installment of a check dam may be purposed to meet such criteria.

Design based on the Aberdeen Equation (Sediment-settling Based Design)

The approach involves the following steps:

i) The properties of the target sediment, such as mean particle size (d_s) and density of sediment particle (ρ_s) are determined.
ii) The design volume is calculated based on the application of the bioswale.
iii) Using sediment properties, settling velocity (V_s) is calculated using stokes law (Eq 2.5).

$$V_s = \frac{g}{18\,\mu}(\rho_s - \rho_w)\, d_s^2 \qquad (2.5)$$

iv) The obtained settling velocity is used to calculate the "*Fall Number"* (N_f). Available length is used in (Eq 2.6).

$$N_f = \frac{L\ V_s}{y\ v} \qquad (2.6)$$

where, L is swale length (m), V_s is settling velocity (ft/s), y is flow depth (ft), and v is flow velocity (ft/s)

v) Finally, the treatment removal efficiency by settling (Tr_s) is calculated using (Eq 2.7).

$$Tr_s(\%) = \frac{{N_f}^{0.69}}{({N_f}^{0.69}+4.95)} \times 100 \qquad (2.7)$$

The process is repeated if the target removal efficiency is not met by increasing the length of the swale. If the length is limited, then the width, slope, and incoming flow can be altered to obtain desired removal efficiency.

2.17 Limitation of Bioswale Applications

There is always a challenge in treating contaminants due to the limited space available at non-point pollution sources such as highway pavement and urbanized areas. Grassed swales are only sometimes suitable for urban landscapes since they need vast pervious areas (EPA 1999b). Grassed swales can lower the peak concentration to some degree, but they are not effective in reducing contaminants' load (StormwaterPA 2006). Also, swales were only found effective either for particles larger than 6-15 microns or sediment-bound particles and were unable to treat dissolved solids, nitrogen, and chlorine (Hunt et al. 2020). So, an effective hydraulic design is necessary for the proper functioning of the structure and purification near the source, which is challenging.

In many cases, the use of check dams in swales may retard the flow and improve the sediment removal efficiency to meet water quality flow, it decreases the hydraulic capacity of the system, and dams could make the flow turbulence downstream of the check dam (EPA 2021).

Similarly, bioswales are not suitable for landscapes with steeper slopes, and if they are constructed for larger areas exceeding 10 acres, they can only function efficiently if special provisions are implemented to increase the flow (StormwaterPA 2006).

Although bioswales may be able to meet several such water treatment requirements, the limitation of water quality flow to be within 6 inches of depth or sometimes within the vegetation height has faced area limitations in construction and implementation. This has limited the potential usage of the treatment BMPs.

The recommended removal threshold rate for TSS and phosphorus is 85%, whereas a 50% reduction is targeted for Nitrogen for water quality flow control. This removal is obtained in infiltrated runoff (StormwaterPA 2006). Hence, maximizing the infiltration within the swale is expected to increase the overall efficiency of bioswales. This expectation could be addressed by enhancing the infiltration of existing soil with materials such as sand, gravel and engineered media such as expanded shale. A study is required to explore the incorporation of expanded shale with high conductivity and transmissivity, aiming to enhance the rapid drainage of standing water and ultimately improve overall efficiency.

2.18 Expanded Shale

Expanded shale is an aggregate made from clay or shale heated (>1100 ^{o}C) in a rotary kiln until it is light and porous. It has high strength, is angular in shape, and is chemically inert with porous space, which makes it behave as a good candidate for light-weight aggregate filters (Mechleb et al. 2014).

It can be of various sizes based on particle size distribution. For example, North American rotary kiln plants commercially produce three expanded shale classes, i.e., 20-5 mm, 13-5 mm, and 10-2 mm gradations (ESCSI 2018). More details of the properties of the expanded shale are tabulated in Table 2.4.

Table 2.4: *General properties of expanded shale (ESCS) vs. Typical Granular Filter Media (ESCSI 2018)*

Aggregate Properties	Typical Values for Expanded Shale	Typical Values for Granular Filter Materials
Surface Area (ft^2/kip)	24 - 93	0.5 - 14.7
Specific Gravity	1.25 - 1.85	2.65 - 2.75
Durability Index	82-93	80 - 99
Magnesium Soundness (%)	< 6	< 6
Acid Solubility (%)	1 - 4	0.3 - 93
Caustic Solubility (%)	0 - 0.9	0 - 1
pH	6 - 10	6.5 - 11
Organic Impurities (%)	<0.5	0.5 - 10
Permeability (Constant Head) (in/hr)	50 - 1300	1 - 600
Loose Dry Density (lb/ft^3)	30 - 60	90 - 105
Loose Wet Density (lb/ft^3)	45 - 70	95 - 110
Los Angeles Abrasion (%)	20 - 40	10 - 45

Expanded shale has a remarkably high specific surface area, low density, and high durability. It offers very high drainage properties and decreases the chances of clogging like any conventional bioswales application. Expanded shale also provides 45% more surface area for microbes to colonize or get trapped on its surface, increasing treatment efficiency (ESCSI 2018). Due to these reasons, expanded shale can be used as an amendment with fine clay to improve water quality and perform as a filtering media.

Despite having a very highly draining nature, shale drainage capacity can even be enhanced by providing an underdrain in bioswale with optional geofabric depending on the soil's natural

properties. Geofabrics are often installed to hold the fine particles from entering the underdrainage system.

2.19 Experimental Studies on Expanded Shale

Expanded shale has been used in various applications, some of which are presented in the following sections.

Sloan et al. (2002) conducted a study on improving clay soil drainage by introducing expanded shale. They introduced 1-3 mm size fine shale and 3-6 mm coarse shale into the soil media. The study was based on a 50% shale-to-clay mix ratio by volume. It involved 6 inches of total media thickness with two different vegetations, namely Pansy and Scaevola. It was reported that the soil amendment promoted vegetation root growth and their survival significantly. Moreover, coarse-graded expanded shales were found more effective as an amending media than fine-graded expanded shales.

Forbes et al. (2004) analyzed dissolved phosphorus-retention in long-term use constructed wetlands. To optimize existing soil in terms of sorption and desorption capacity for phosphorus, expanded shale and masonry sand were compared with native soil using sorption isotherms and pilot scale cell experiment (Figure 2.3). They found that expanded shale was more efficient in absorbing phosphorus and simultaneously maintained high hydraulic conductivity, high surface area, and excellent sorption capacity. Also, expanded shale did not release absorbed phosphorus in desorption experiments.

In a follow-up study, Forbes et al. (2005) focused on the removal efficiency of expanded shale as a filtration media based on its capacity to remove phosphorus obtained from Forbes et al. (2004). They considered the substrate for various examinations of phosphorus forms like total phosphorus

and total inorganic phosphorus. They observed that expanded shale outperformed far better than a sand bed in phosphorus removal in constructed wetlands.

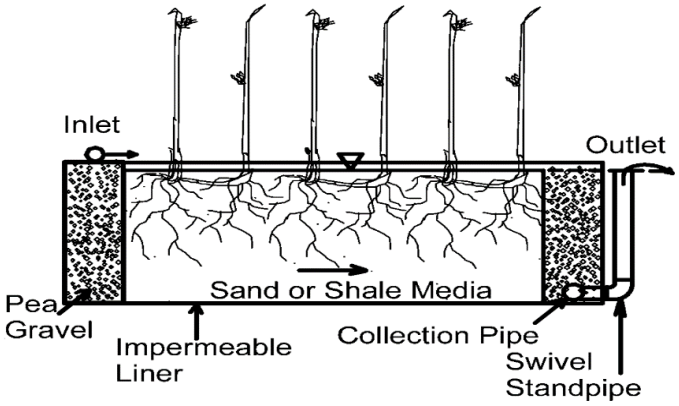

Figure 2.3: *Schematic for pilot cells (Forbes et al. 2005)*

Mateus and Pinho (2010) conducted a six-year study on phosphorus removal using lightweight expanded clay aggregate (3-8 mm size) with a specific weight of 300 kg/m^3 and 500-600 kg/m^3. A higher phosphorus removal rate was observed with vegetation than without vegetation, which was found to be an effect of nutrient uptake. Even though the life cycle for phosphorus-removal capacity was estimated to be around 1-2 years, the phosphorus removal capacity of the shale was not exhausted even until six years of operation. The study also found that phosphorus removal was directly proportional to the specific weight of lightweight aggregates. The study concluded that the higher phosphorus removal rate was obtained with media having a higher value of adsorption capacity based on isotherms parameters.

A study conducted by Sloan et al. (2010) used expanded shale (3 to 6 mm in size) to drain the water and promote aeration of the plant's roots. Organic content blended soils were used with added percentages of 0%, 15%, 30%, and 50% by volume. The three-month study found poor

vegetation growth in the expanded shale containers due to the reduced nutrient contents in the system. The result demonstrated that porosity was almost similar for high porous soils and increased porosity for low porous soil blends; however, bulk density was higher in all cases. Lastly, in terms of hydraulic conductivity of the soil, it was found that the addition of expanded shale was worthy only in soils that had poor drainage and aeration.

Later, Sloan et al. (2011) found that expanded shale could supply nutrients to vegetation by releasing adsorbed phosphorus slowly over time in a soil medium. They also noticed that expanded shale acted as an internal reservoir of water, which could be utilized by the vegetation for a prolonged period.

Laboratory research conducted by Mechleb et al. (2014) on the expanded shale involved three different soil types with varying plasticity index (PI). The different ratios of soil to expanded shale, 0% to 50%, were used for evaluation. Two different compaction methods (the standard proctor method and the reduced proctor method) were used following ASTM D2216 Standard Test Method. The laboratory tests proven that the expanded shale had greatly improved drainage quality and decreased the dry density of amened soils. Expanded shale outperformed lime-mixed clay as an engineered media despite both having the same particle size distribution (Figure 2.5). Similarly, higher hydraulic conductivity was seen for soil with a low plasticity index for the same amended soil. Lastly, the study also reported that 50% by volume of expanded shale mixed with various clay types had the same hydraulic conductivity irrespective of the test methods.

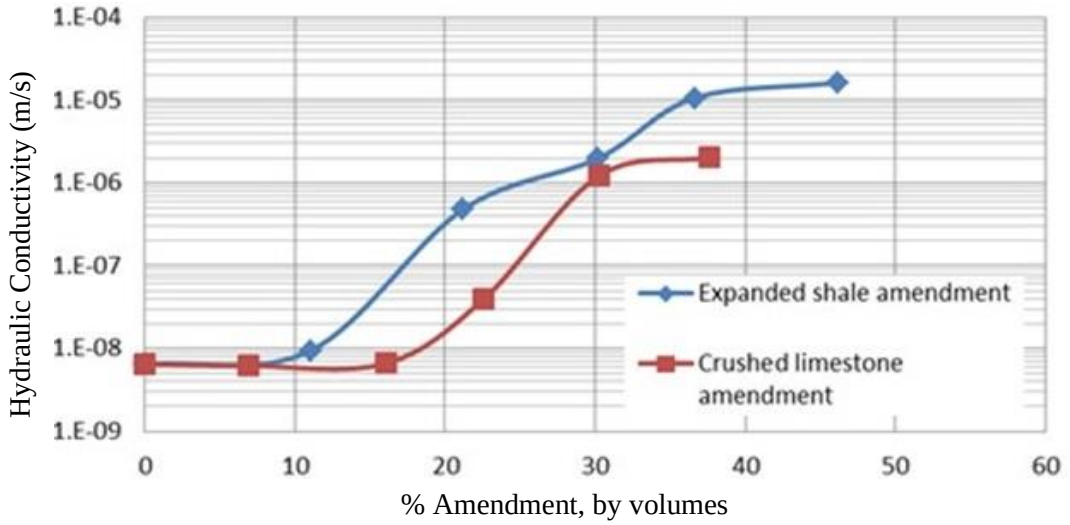

Figure 2.4: *Hydraulic conductivity for amended-soils with Expanded Shale Vs. Limestone, (Mechleb et al. 2014)*

Li et al. (2016) reported that the bioswale without vegetation had only a 7% to 49% nitrogen removal rate in low flow and almost no change in high flow conditions. The same study found that the nitrogen removal efficiency was less for inflows with higher concentration. Also, the soil-media ability of absorbing pollutants was unchanged with inflow concentration.

The California Department of Transportation (Caltrans) tested stormwater runoff in a small-scale pilot study considering different filtering media like activated aluminum, expanded shale, sand, zeolite, limestone, aluminum oxide and wollastonite, Expanded shale results were seen as remarkable in comparison to any other filter media considered. Turbidity and phosphorus removal was seen as more effective, whereas the Nitrogen result was not satisfactory as in any systems tested (Hauser et al. 2005).

CHAPTER 3
METHODOLOGY

3.1 Introduction

The performance of a swale constructed with expanded shale in removing TSS and turbidity was studied in a laboratory flume. The experimental setup was within the 'Fluid Mechanics and Hydraulics Laboratory' at the University of Texas at Arlington. Several scenarios were considered, and extensive samples were collected at various times and locations to understand the efficiency and pattern of pollutant removal. The governing factors, such as inflow rate, filter medium thickness, infiltration conditions, influent concentration, and soil properties of the expanded shale mix, were considered as variables to develop scenarios.

3.2 Experimental Setup

3.2.1 Experimental Flume

The flume in which the experiments were carried out is made of plexiglass, with a total dimension of 18 ft length, 4 ft width, and 1.5 ft depth. The inlet and outlet tanks, 2 ft in length, 3 ft in depth, and width equal to the width of the flume, are installed at the upstream and downstream ends of the flume.

The inlet tank is designed so that water enters the tank from its bottom through a 4-inch PVC pipe and a perforated horizontal spreader. Also, the inlet tank allows water to enter the flume as a uniform flow.

The flume slope can be adjusted to ± 1%; however, the slope was set to 0.3% to keep it below recommended slope (<1%) for swales with underdrains (Caltrans 2020).

Engineered media of varying thickness, comprised of 65% expanded shale and 35% sandy clay, placed in the flume with 6 inches in thickness (and 4 inches in a limited number of experiments). The flow entered via the inlet tank and left from the downstream drainage box. Figure 3.1 shows the schematic diagram of the experimental setup.

Four locations within the flume were selected to collect water samples to analyze the efficiency of the expanded shale over time and along the flume. Those four locations are upstream over the gravel, the channel's middle section, and the channels downstream outlets.

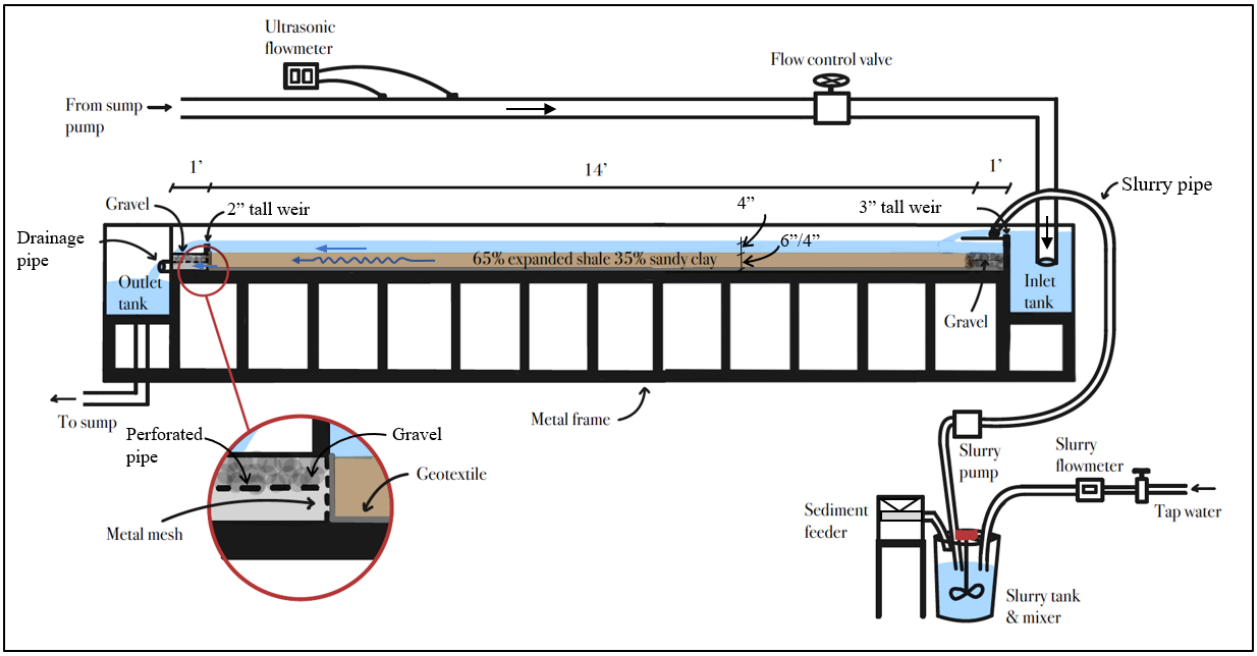

Figure 3.1: *Schematic diagram of the experimental flume (not in scale)*

3.2.2 Inlet Configuration

To promote a uniform flow distribution over the width of the flume and prevent the entry of eddies from the inlet tank, a rectangular contracted weir with a height of 3 inches was installed upstream of the flume. The crest of the weir was positioned 9 inches above the bottom of the flume.

A horizontal wood plank was installed downstream of the weir across the flume to provide a mixing area. The slurry was introduced to the flume over this area opposite the flow direction through a ½-inch perforated pipe, as shown in Figure 3.2a.

The perforated pipe used for the slurry had uniformly distributed holes with a diameter of 0.375 inches and a spacing of 2 inches between the centers of each hole. The size and number of holes were carefully designed to accommodate the targeted maximum slurry rate.

Also, a horizontal gravel bed layer was introduced at the entrance of the flume to reduce the flow velocity and avoid local erosion (Figure 3.2b).

3.2.3 Flow Source and Control

Two underground tanks were used as a source for the continuous water supply throughout the experiments. A control valve installed on the 4-inch PVC pipe controlled the water supplied to the flume from the pump installed in the underground tank. The flow was measured using a calibrated Sono-TraK ST30 ultrasonic flowmeter. More information on calibration is presented in APPENDIX A. The flowmeter was selected to be within the accepted accuracy range of ±0.5%, and the response time was up to 30 seconds. To ensure the reliability of the flowmeter, volumetric flow measurements were also conducted for each experiment using the inlet tank and a stopwatch. This allowed for accurate and consistent measurement of the flow rate during the experiments, providing reliable data for analysis and comparison.

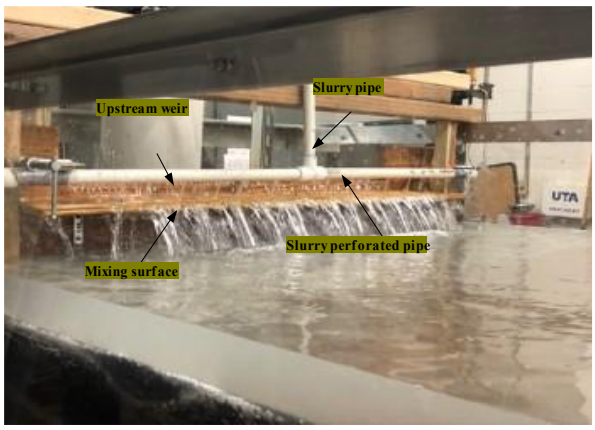

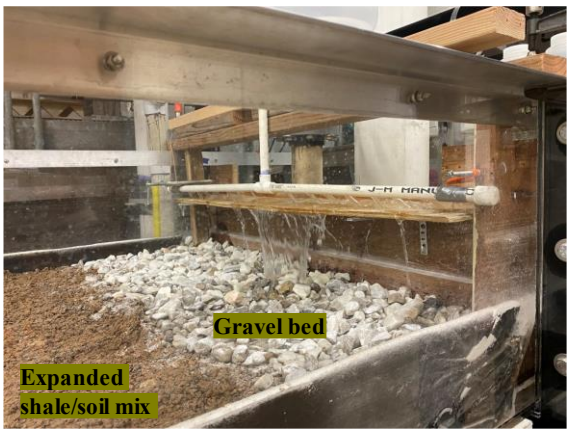

(a) *(b)*

Figure 3.2: *(a) Inlet section, (b) Expanded shale and upstream gravel bed*

3.2.4 Underdrain System

An evenly spaced horizontal network of 2-inch perforated pipes was laid on the bottom of the flume to improve infiltration (Figure 3.3). The holes were designed to be spaced such that every two holes would be within a distance equal to the diameter of the pipe used (i.e., two holes per every 2 inches). Also, the design of the drainage network was made symmetrical to both sides from the centerline of the flume.

As depicted in Figure 3.4, a ball valve was installed at the end of the main pipe. Its primary function was to regulate the flow through the underdrain system, providing the flexibility to control the drainage flow rate according to requirements. By fully closing the valve, the flow was limited to infiltration through the soil medium alone, representing the scenario without an underdrain. Conversely, when the valve was fully open, the flow passed through the soil and the underdrain pipe system, representing swales with underdrain cases.

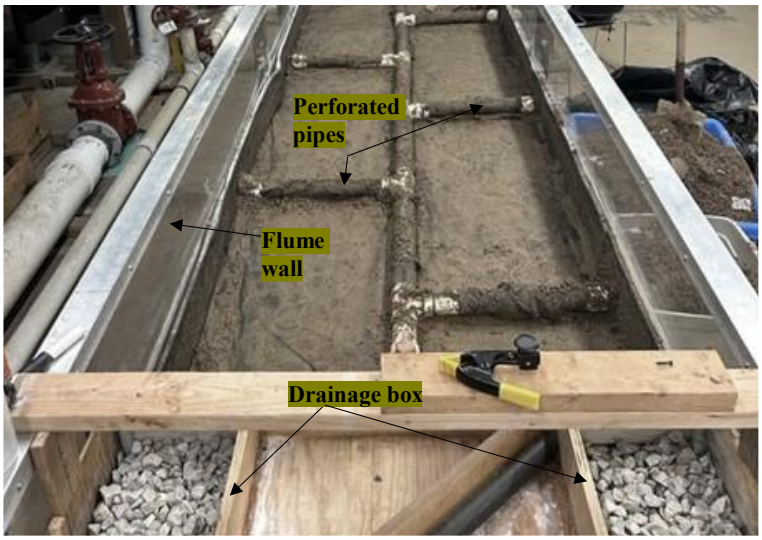

Figure 3.3: *Geotextile-wrapped perforated underdrain system*

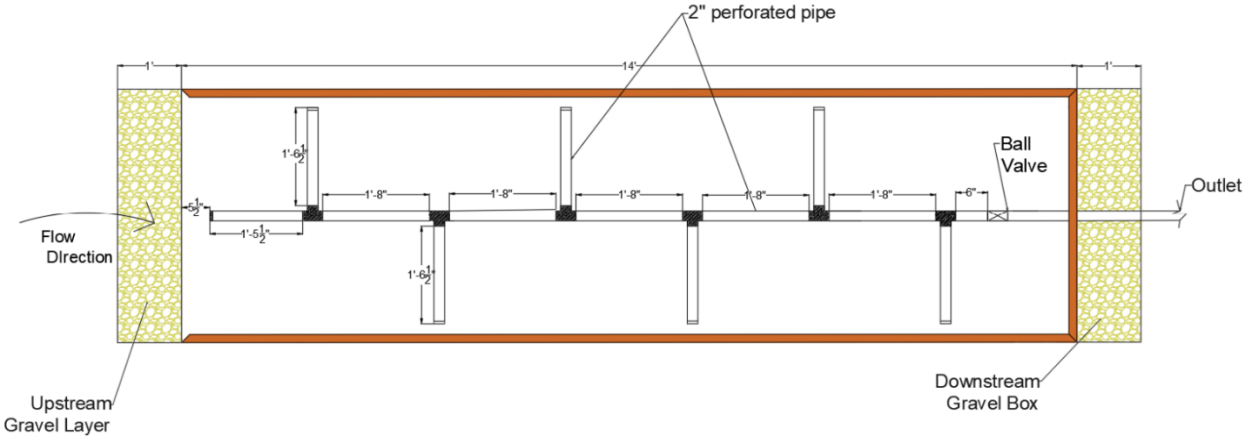

Figure 3.4: *Layout of the underdrain system in the flume (plan view)*

3.2.5 Sediment and Slurry Preparation

Silica flour #140/106u, having a median size of 0.03 mm, was used for slurry preparation. The gradation of the silica flour was tested three times in the UTA Shimadzu lab for conformity. A Shimadzu nano-particle size analyzer (Shimadzu SALD-7101), working on the principle of the laser diffraction method, was used for particle size gradation. Figure 3.5 includes the gradation curves of the silica flour provided by the manufacturers (American Graded Sand Company (AGSCO)) and those determined in this study. In this figure, prefixes UTA1, UTA2, and UTA3

stand for three individual gradation tests of silica, and UTA_AVG stands for the average values obtained for all three tests.

The gradation of silica flour from the manufacturer shows an identical gradation curve to that measured gradation in the UTA Shimadzu lab up to 0.037 mm, but the manufacturer had the lowest grading size of 0.037 mm. Hence below this size of 0.037 mm, the graph from the manufacturer is discontinuous. So, sediment gradation obtained from UTA Shimadzu lab is used for data analysis providing higher accuracy.

The silica flour used in the experiments was selected based on the requirements for sediment size as suggested by the New Jersey Department of Environmental Protection (NJDEP 2022), as shown in Table 3.1.

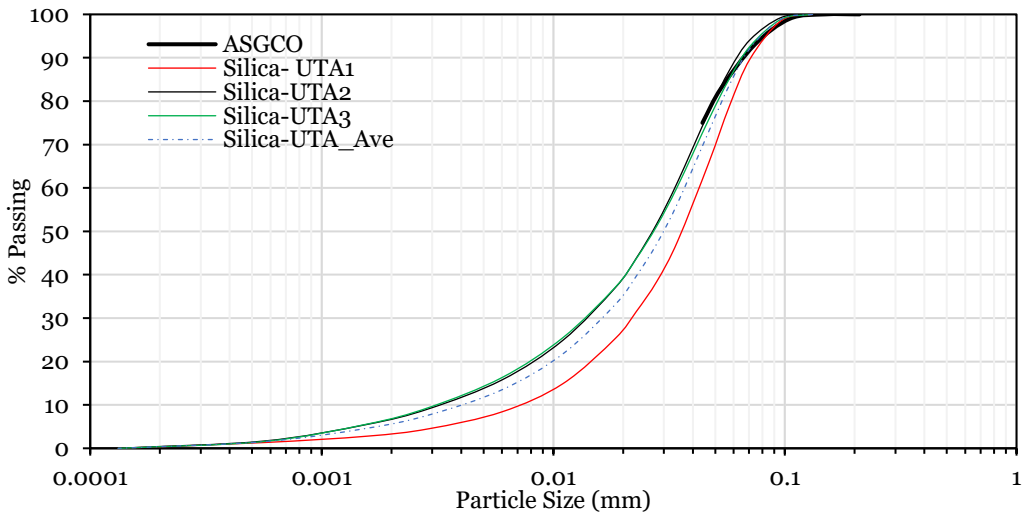

Figure 3.5: *Silica flour particle gradation size*

The silica flour was mixed with tap water at a controlled rate to prepare desired concentrations of the slurry mix. A 32-gallon cylindrical tank with a horizontal base was used for preparing the slurry mix (Figure 3.6). The tank was fitted with a floater valve that controlled the depth of the water inside the tank to a desired constant level. An in-line flowmeter was used to measure the rate

of water entering the slurry tank (Figure 3.6). Similarly, the sediment was constantly injected into the slurry tank using a volumetric feeder. The feeder was chosen because it handles dry materials and has a volumetric accuracy of 2-4% (Tecweigh n.d.). A sump pump capable of pumping sediment was used to inject the slurry at a constant rate from the slurry tank into the flume. Also, a valve was installed on the sump pump outlet pipe as shown in Figure 3.6. During each experiment, this valve was used to take samples from the slurry to check for its sediment concentration.

Table 3.1: *Test results for silica flour from UTA- Shimadzu lab vs. NJDEP sediment size requirement*

Size (µm)	**% Passing**				**NJDEP minimum passing (%)**
	Test 1	Test 2	Test 3	Average	
131.5	100	100	100	100	
100					60
96.5	98.6	99.3	98.9	98.9	
75					50
70.8	89.8	94.2	92.7	92.2	
57.6	78.9	87.13	85.2	83.7	
50					45
46.9	65.81	77.5	75.8	73.0	
34.4	47.73	61.4	60.4	56.5	
28	38.5	51.8	51.3	47.2	
22.8	31.5	43.8	43.7	39.7	
20					35
18.5	25.3	37	37.1	33.1	
11	14.9	24.9	25.5	21.8	
8					20
6	8.4	15.76	16.3	13.5	
5					10
2.9	4.5	9.12	9.4	7.7	
2					5
1.56	2.78	5.48	5.55	4.6	
0.56	1.32	1.655	1.55	1.5	
0.132	0	0	0	0.0	

A paint mixer was used to continuously mix the tap water and sediment in the tank throughout the experiments and keep the sediment in suspension (Figure 3.6). Slurry with high sediment concentration was injected into the flume over the mixing surface to be diluted with the inflow.

The concentration of diluted slurry was considered as the influent sediment concentration to calculate the swale's TSS and turbidity removal efficiency.

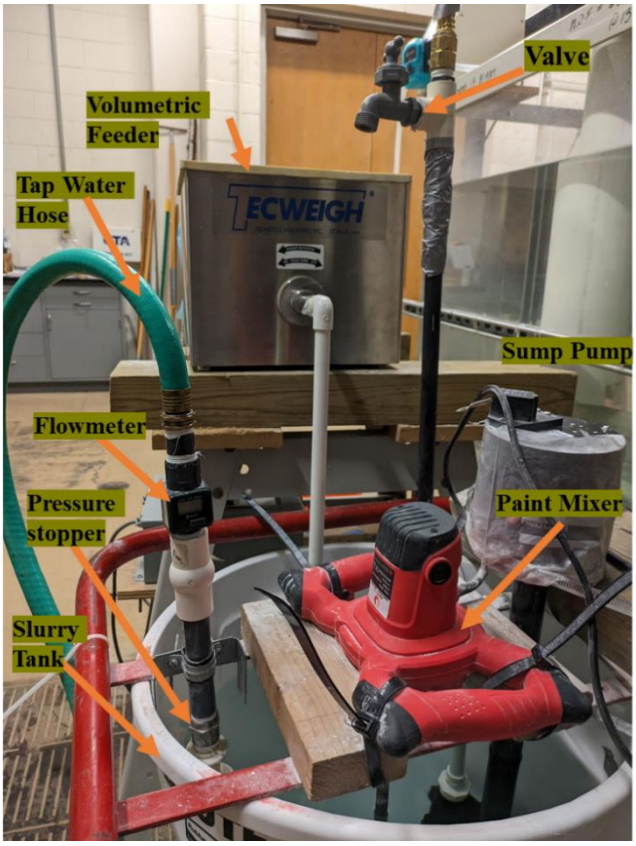

Figure 3.6: *Volumetric feeder and slurry preparation arrangement*

3.2.6 Soil Media

Two different filter media mixes were used in this study. Type 1 contained the soil mix with a coarser size of ¾" expanded shale, also called G-pile by the manufacturer. Similarly, Type 2 contained the finer expanded shale with a median size of ¼", also called J-pile by the manufacturer. Both types had the same proportion of expanded shale and sandy-clay, i.e., 65% of expanded shale and 35% of the natural sandy-clay.

Sieve analysis was performed in the UTA Geotechnical Laboratory to determine the gradation of the expanded shale types i.e., G-pile and J-pile, and the infiltration medium prepared using these

two types. The ASTM D6913 (2017) was followed for all sieve tests. The gradation curves for all G-pile, J-pile, Type-1 mix, and Type-2 mix were prepared which are discussed further in Chapter 4.1.

3.2.7 Outlet Configuration

A 1-ft long rectangular box, filled with coarse gravel, was installed on the downstream end of the flume. The box had a 6-inch tall opening space across the flume on its upstream face to allow the water to seep through the infiltration medium to this box. A mesh and a non-woven geotextile fabric were placed between the gravel and engineered medium (see Figure 3.1). This allowed the water to pass through but prevented the medium materials from washing out. The fabric had a rating of 80 sieve size, meaning particles smaller than 0.18 mm (0.007 inch) could pass through. Since the silica used in this study had a maximum size of 0.13 mm (0.005 inch) (Figure 3.5), the geotextile fabric did not hinder the soil medium's infiltration and sediment removal capacity. Also, a 2-inch perforated pipe was installed across the drainage box to collect the water infiltrating via the geotextile from the porous medium. This perforated pipe directs the flow to the outlet tank within the drainage box (Figure 3.7).

At the downstream end of the infiltration layer, on top of the drainage box, a 6-inch tall check dam was installed, causing water to pond in the flume. To enable water to overflow discharge to the outlet tank, a 1-ft wide weir was cut out in the check dam's midsection. The weir's crest elevation was chosen to ensure that the infiltration layer was always covered by at least 4-inch of water.

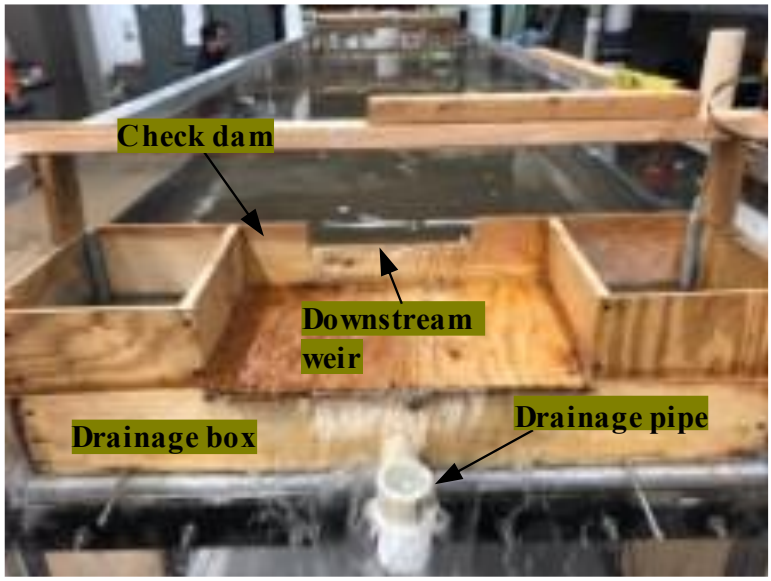

Figure 3.7: *Outlet box with underdrain pipe, check dam, and downstream weir*

3.3 Experimental Procedure

3.3.1 Selection of Inflow

For the base case scenario, the inflow rate was determined by considering a minimum 5-minute hydraulic residence time (HRT), which is a requirement in the design of bioswales according to Caltrans (2020). To calculate the maximum flow velocity, Equation 2.1 was utilized. The length of the flume, including the gravel bed, was considered 15 ft (4.6 m) in this equation, and a maximum flow velocity of 0.05 ft/s (0.015 m/s) was obtained.

The flow depth within the flume was limited to 0.33 ft (11.4 cm) due to the presence of the check dam installed downstream of the flume. Using calculated maximum flow velocity, flow depth and width, the maximum water quality flow was calculated to be 0.066 ft^3/s or 29.6 gallons per minute (gpm) (equivalent to 112 Lit/min). Considering that a portion of the inflow infiltrates through the soil, as discussed in Chapter 4.3, an inflow rate of 32 gpm (120 Lit/min) was considered for the base case scenario.

The base flow of 32 gpm (120 Lit/min) corresponds to the peak stormwater runoff generated from a drainage area of 16,145 ft² (1500 m²) when subjected to a rainfall intensity of 0.5 inches (12.7 mm/hr). This rainfall intensity is commonly used in calculations of water quality flow, as suggested by Barrett et al. (1998) and other stormwater management guidelines.

Claytor and Schueler (1996) suggested that a minimum hydraulic residence time of 10 min ensures the best filtration for water quality flow. Hence, 60 Lit/min was selected as a low flow scenario in the study. This flow gave a flow velocity of 0.026 ft/s (0.008 m/s) which is smaller than the maximum allowable velocity of 0.05 ft/s (0.015 m/s).

Since some BMPs are designed for water quality flow and peak flow reduction (Caltrans, 2020), 180 Lit/min flow was selected as the high flow scenario. Even though this flow does not satisfy the inter-relationship formula (Equation 2.2), it is still safely handled and passed through the bioswales system. The swale was modeled to function as a flow reduction/conveyance system with a flow velocity of 0.078 ft/s (0.024 m/s) that corresponds to 180 Lit/min.

3.3.2 Influent Concentrations

To represent a range of typical suspended sediment concentrations in stormwater, influent concentrations of 100 mg/L and 200 mg/L were selected based on a literature review of highway runoff effluent mean concentrations. The choice of these concentrations was made to encompass both high and low concentration scenarios, providing a comprehensive representation of the potential variability in highway runoff.

3.3.3 Testing Scenarios

Several scenarios were conducted, wherein different factors were selected and assessed. These factors included the depth of the filter media, underdrain conditions, sediment concentrations, and

the type of filter media. By altering and evaluating these variables, a comprehensive understanding of their influence on the system's performance and effectiveness could be obtained.

A total of 30 scenarios were conducted, out of which, 12 were with an active underdrain system (the underdrain system control valve was open during the experiment), whereas the remaining tests were without underdrain (underdrain system control valve was closed during the experiment). Two different influent concentrations of 100 mg/Lit and 200 mg/Lit were considered. In terms of thickness of soil media, 4-inch and 6-inch were considered in this the study. As discussed in Chapter 4.4.1, 4-inche thickness was not considered for the Type 2 soil media due to the inferior performance of the Type 1 soil mix with 4-inches thickness in reducing the TSS and turbidity. The test scenarios are summarized in Table 3.2.

There were two different testing scenarios regarding the drainage condition: Case-1 and Case-2. In Case 1, the objective was to simulate the implementation of a bioswale in a native soil environment with limited infiltration capacity (Figure 2.1). To achieve this, the underdrain system's outlet valve was closed, allowing for infiltration solely through the soil medium. Additionally, to control the water level within the soil medium, a 2-inch diameter 90-degree PVC elbow was installed at the end of the outlet pipe after it exited the drainage box (Figure 3.8 (a)). The elevation of the exit point of the elbow was set to align with the top of the soil medium, effectively regulating the water level within the bioswale. This configuration of the upturned elbow was in consistent with the experimental study performed by Brown and Hunt (2011).

In Case 2, the focus was on simulating swales with an underdrain system that is connected to a downstream stormwater system (Figure 2.2). Throughout the experiment, the outlet valve was kept open, facilitating the promotion of infiltration. In this setup, the elbow that was present in Case 1 was removed, allowing the drained water to flow freely into the outlet tank (Figure 3.8 (b)). This

configuration enabled the measurement and analysis of the drainage flow and its impact on the overall performance of the swales.

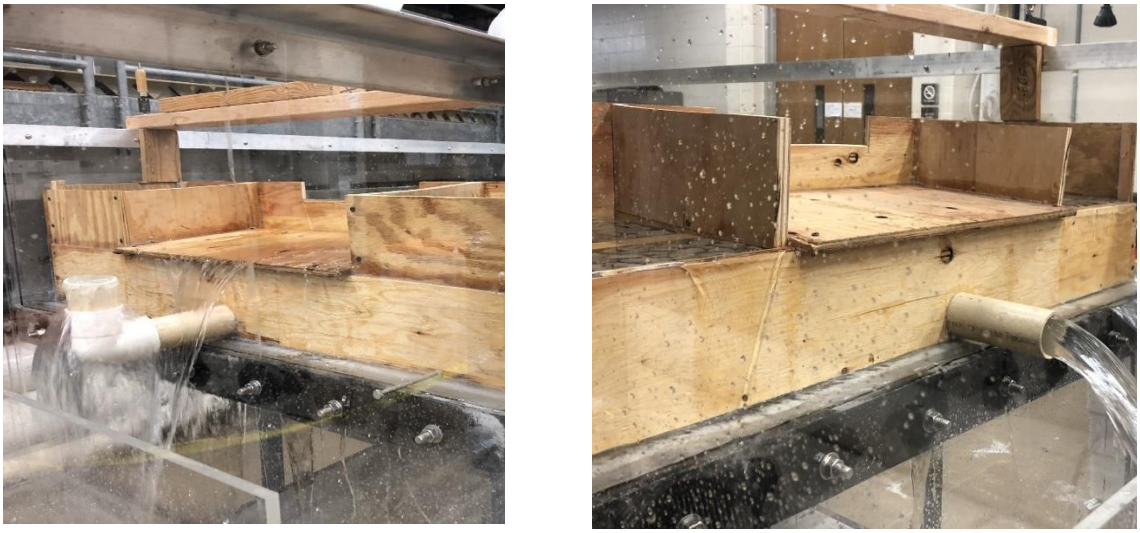

(a) (b)

Figure 3.8: *Outlet configurations for a), Without underdrain system, and b) With underdrain system*

Water samples were collected for TSS and turbidity analysis from various parts of the flume. Initially, sampling locations were chosen from the slurry tank, upstream weir at the inlet, upstream of soil media over the gravel, the middle section of the flume, water exiting the underdrain, and water flowing over the downstream weir (if any). After a few preliminary tests, the results showed more uniform mixing over the gravel bed; hence, sampling from upstream weir location was discontinued. All the time, the sampling was only started after the 4-inch water depth was established over the soil, and for the low flow when there was no substantial change in flow depth over time.

Samples were collected by a single 'grab sample' as defined by USGS (2006). Every time a clean 1-liter bottle, washed with distilled water, was used to take a sample using a swift horizontal motion to represent the middle 2/3rd portion of the flume width to avoid the walls' effects. Every experiment was run for 40 minutes representing the rainfall duration and in reference to the

requirements set by NJDEP for filtration treatment device tests mandating more than 30 minutes test duration (NJDEP 2022). Similarly, a 10 min sampling interval was selected based on one resident time requirement. For this study, the maximum resident time was calculated as 8 minutes for the low flow condition.

Table 3.2: *Summary of all testing scenarios for TSS and Turbidity*

Experiment No.	Infiltration Media	Media Thickness (inch)	Drainage Condition	Inflow (Lit/min)	Influent Sediment Concentrations (mg/Lit)
1	Coarse media (G-Pile)	6	With underdrain	60	100
2				120	
3				180	
4				60	200
5				120	
6				180	
7			Without underdrain	60	100
8				120	
9				180	
10				60	200
11				120	
12				180	
13		4 *	Without underdrain	60	100
14				120	
15				180	
16				60	200
17				120	
18				180	
19	Finer media (J- Pile)	6	With underdrain	60	100
20				120	
21				180	
22				60	200
23				120	
24				180	
25			Without underdrain	60	100
26				120	
27				180	
28				60	200
29				120	
30				180	

** 4 inch thickness were not considered for turbidity testing*

All collected samples were tested on the same day for TSS and turbidity. On some occasions, samples were stored at room temperature and tested within 24 hours to avoid any change in sample

composition or decaying of sediments by any undesirable means, such as decomposition of sediments or microbial activities (if any). The samples were swirled and vigorously shaken before being tested. The TSS test was repeated when values were not within ±20% of overall mean values to ensure reliability.

All the samples considered for the TSS tests were also tested for turbidity (except for samples from the slurry tank). Samples from scenarios 1 to 3 were not tested for turbidity. Additionally, some of the samples were selected for particle size gradation test.

3.3.4 Infiltration Measurement Procedure

Samples from infiltrated water for both underdrain valve conditions (open and close conditions) were collected using the 'Bucket and Stopwatch' method (EPA 2023c). Every infiltration volume measurement was taken for at least 10 sec following the criteria set by EPA 2023c. All such manual flow measurements were repeated at least three times for reliability.

3.3.5 Testing Procedures for TSS

All the samples taken from the flume were considered for TSS tests. The protocol followed for the TSS test was EPA method 160, 2 (EPA 2017c). The sub-sampling was done from the 1-Lit standard sample at each location for TSS measurement. A sub-sampling volume of 25 ml was taken for slurry concentrate and 250 ml for the rest of the sampling locations. Regardless of the location, all samples were subjected to vigorous shaking before sub-sampling. Filters used for the TSS test were 1.5 μm pore size glass fiber of diameter 4.7 cm that was either 934-AH grade or Whatman grade pre-rinsed and dried filters. An aluminum weighing dish of 42 ml capacity was used to contain the filters before and after the filtration for weighing purposes.

Weighing was done using a Mettler Toledo-XS105, an automatic weighing balance with the least count of 0.00001 grams (Figure 3.9 (a)). This enabled an accuracy of 0.01 mg/Lit on every 250 ml sample considered.

Samples were kept in the oven after filtration for at least one hour and kept in a desiccator to avoid errors due to moisture before weighing. Two desiccators were used simultaneously to place all the samples inside the desiccators (Figure 3.9 (b)). Also, all reading from the weighing balance was only recorded, when the reasding in the scale was stable.

(a) (b)

Figure 3.9: *(a) Weighing balance, (b) Desiccators used for TSS measurement*

3.3.6 Testing Procedures for Turbidity

All the turbidity tests were conducted using a portable turbidimeter at the UTA Environmental Laboratory. A Hach 2100Q turbidimeter was calibrated using standards sample of 20, 100, and 800 NTU. After calibration, the 10 NTU standard was used to verify the calibration of the turbidimeter as suggested by EPA Field Turbidity Measurement (EPA, 2023c). Only after the verification of the calibration process was accepted, all the turbidity measurements were carried out. For each turbidity test, a closed-capped sub-sampling cell having a volume of 15 ml was utilized. Before each measurement, the cells were wiped with a clean cloth.

3.3.7 Laser Diffraction Method

A SALD-7101 nano-particle size analyzer was used to determine particle size distribution. The procedure was followed thoroughly to maintain the accuracy of the UV laser-equipped analyzer. Distilled water, obtained from reverse-osmosis, was used to wash the sampling bottles and to dilute the sample when necessary. Samples taken from the flume were in liquid state, but the silica flour in its dry form was diluted for the test with distilled water. The laser diffraction method works on the principle of optical deflection when laid upon the particles. The overall working principle of SALD-7101 is illustrated in Figure 3.10.

Each sample was evaluated three times for consistency. Samples from the high flow condition (180 Lit/min) and the low flow condition (60 Lit/min) were evaluated for particle size distribution. Samples from both types of expanded shale media experiments and high and low concentrations were tested. Samples for each condition were taken and tested at four sampling locations every 10 minutes.

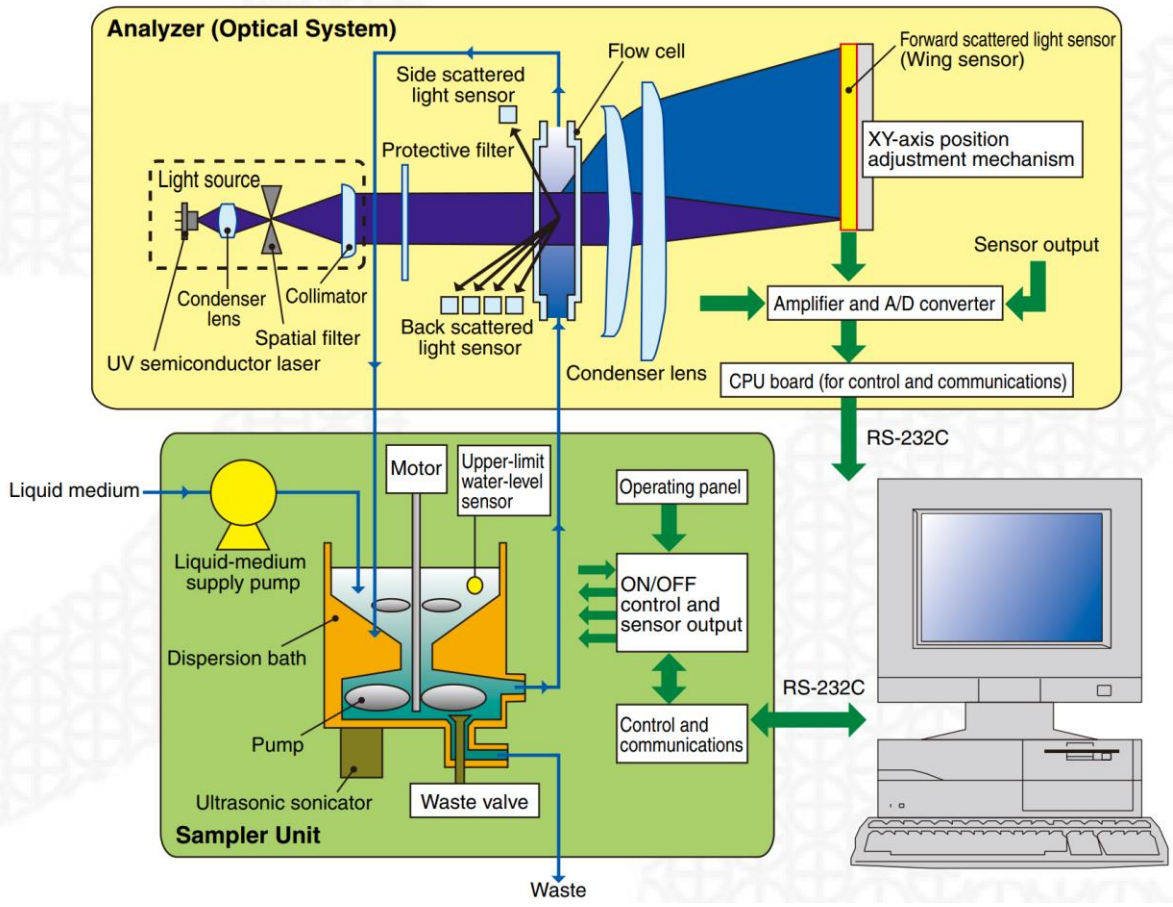

Figure 3.10: *Configuration of the SALD-7101 Laser Diffractor (Prophelab n.d.)*

CHAPTER 4
RESULTS AND DISCUSSION

4.1 Introduction

The analysis of data collected during laboratory experiments performed on the expanded shale soil media is presented in this chapter, and the findings of this study are discussed. The primary evaluation in this study revolves around the performance of the expanded shale media in removing TSS and turbidity from stormwater. Furthermore, the results of particle gradation tests on water samples, expanded shale, and filter media are presented and discussed.

4.2 Sieve Analysis on Infiltration Media:

Sieve tests were conducted on two types of expanded shale materials (G-pile and J-pile) and the two types of soil mix media (Type 1 and Type 2) at the UTA Geotechnical Laboratory. The ASTM D6913 standard was followed for sieve analysis.

The median diameters (d_{50}) of the coarse (G-pile) and fine (J-pile) expanded shale material was found to be approximately 5.5 mm (0.22 in) and 2.45 mm (0.09 in), respectively (Figure 4.1).

The Type 1 and Type 2 soil mix media were prepared by mixing expanded shale with natural soil with a ratio of 3:1 (65% expanded shale, 35% soil). The gradation of soil mix Type 1 and Type 2 are presented in Figure 4.2. The d_{50} of Type 1 and Type 2 are found to be approximately 2.25 mm (0.09 in) and 1.5 mm (0.06 in), respectively. More details of the calculations on the sieve analysis are presented in APPENDIX B.

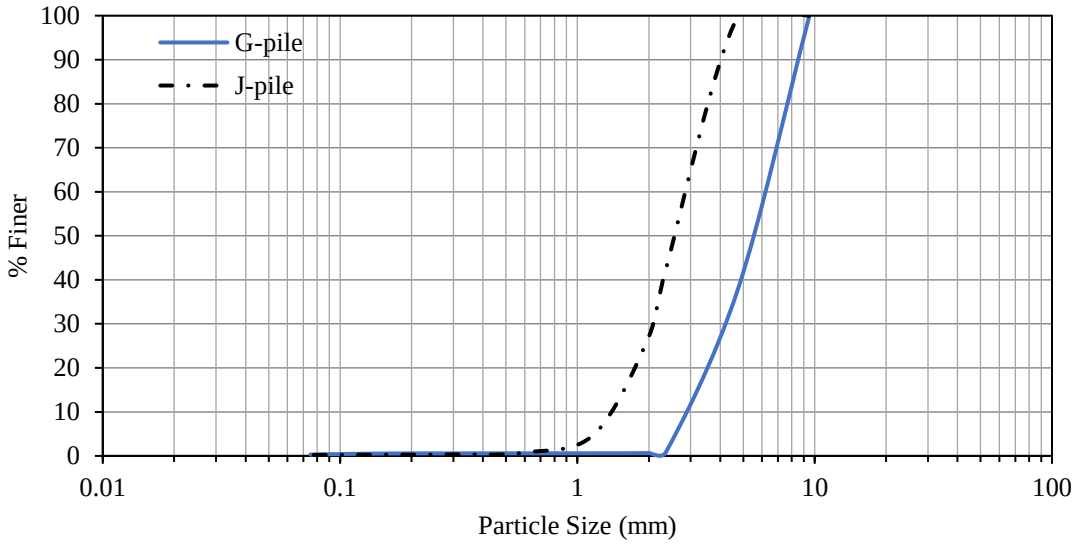

Figure 4.1: *Particle size gradation of coarse (G-pile) and fine (J-pile) expanded shale*

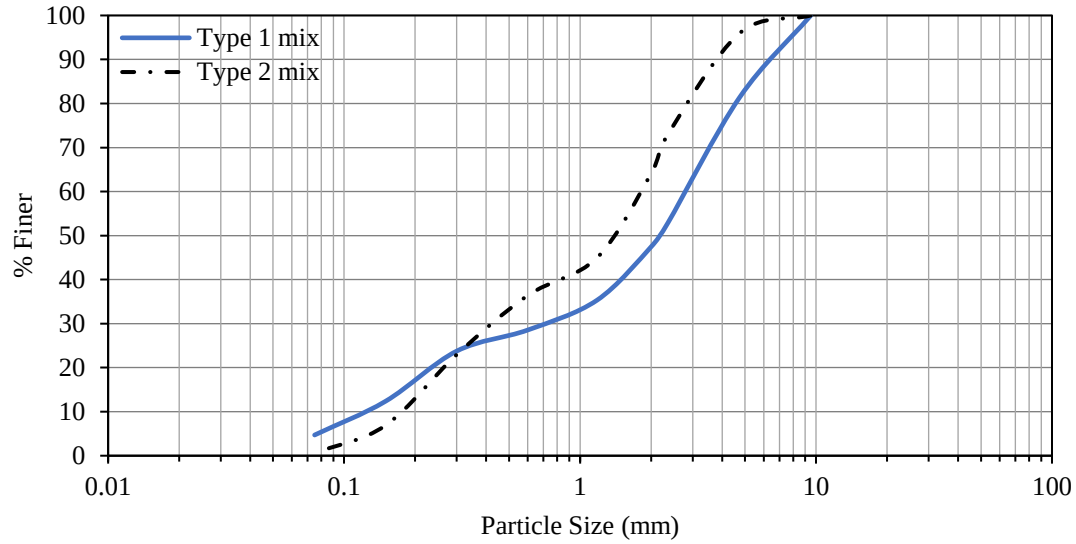

Figure 4.2: *Particle size gradation of Type-1 and Type-2 soil mix*

4.3 Drainage Capacity Experiments

The drainage capacity of Type 1 and Type 2 soil media was determined before conducting flume experiments. The flow rate over the downstream weir (overflow) and through the outlet pipe (infiltrated water) was measured with 60, 120, and 180 Lit/min as inflow. Additionally, the drainage rate was measured at the zero-overflow condition. For this purpose, the inflow rate was

gradually increased until a 4-inch water depth was observed in the flume without water flowing over the downstream weir. Both types of expanded shale media were tested. The water depth just before the downstream weir was also recorded during each experiment with overflow.

Type 1 Media:

When the underdrain was not provided, the drainage capacity of Type 1 was obtained at 46.2 Lit/min at zero overflow conditions. This value increased to 55.2 Lit/min for the 180 Lit/min inflow. The same media had an infiltration rate of 66.5 Lit/min at zero-overflow conditions when the underdrain system was active. The drainage capacity was up to 72 Lit/min when the flow was maintained at 180 Lit/min. The results of the experiments are summarized in the Table 4.1.

Type 2 Media:

Drainage capacity measurements were performed for Type 2 for 60, 120, and 180 Lit/min inflow and zero-overflow. During the inactive underdrain system, a zero-overflow rate of 41.2 Lit/min was recorded, and up to 48 Lit/min was obtained for 180 Lit/min inflow. When the underdrain was active, a maximum of 60.7 and 72.6 Lit/min was seen for the zero-overflow condition and 180 Lit/min inflow, respectively. The results of the experiments for Type 2 soil media are summarized in the Table 4. **2**.

Results showed that when underdrain was provided, both media had similar infiltration rates. However, during the inactive underdrain system, Type 1 had a higher infiltration rate at zero-overflow condition. This higher infiltration rate for Type 1 media agrees with the (Minnesota Pollution Control Agency 2017) that indicates soil properties affect the infiltration rate i.e., coarser soil has higher infiltration.

Table 4.1: *Drainage capacity experiment results for Type 1 soil medium (6-inch)*

Experiment Number	Target Flow (Lit/min)	Actual flow (Lit/min)	Infiltration Capacity (Lit/min)	Overflow (Lit/min)	Water Depth * (cm)	Remarks
1	-	46.2	46.2	-	10.2	Without underdrain
2	60	59.5	48	11.5	10.3	
3	120	120.2	53.4	66.8	11.1	
4	180	182.2	55.2	127	11.9	
5	60	60.7	60.7	-	-	With underdrain
6	-	66.5	66.5	-	10.2	
7	120	120.2	68.4	51.8	10.8	
8	180	182.2	72	110.2	11.6	

Table 4. 2: *Drainage capacity experiment results for Type 2 soil medium (6-inch)*

Experiment Number	Target Flow (Lit/min)	Actual flow (Lit/min)	Infiltration Capacity (Lit/min)	Overflow (Lit/min)	Water Depth * (cm)	Remarks
1	-	41.2	41.2	-	10.2	Without underdrain
2	60	62.1	42	20.1	10.3	
3	120	120.2	43.8	76.4	11.4	
4	180	182.2	48	134.2	12.1	
5	60	60.7	60.7	-	-	With underdrain
6	-	70.6	65.4	5.2	10.2	
7	120	120.2	71.4	48.8	10.8	
8	180	185.2	72.6	112.6	11.7	

* depth measured from the top of the soil media to the water surface level

4.4 Suspended Sediment Removal Efficiency

A total of 30 experiments were conducted to evaluate the efficiency of the soil media in reducing TSS concentration. Water samples were collected from the slurry tank, upstream of the flume (inlet), the middle section of the flume, outflow (infiltrated water through the soli media), and flow over the downstream weir (overflow). Each experiment was conducted for 40 min duration, and samples were collected at 10 min intervals. The TSS concentrations were calculated using Equation 4.1.

$$\text{TSS concentration (mg/Lit)} = \frac{w_2 - w_1}{V} \times 1000 \qquad (4.1)$$

where, w_1 is the weight of the aluminum dish and filter before filtration in grams (g), w_2 is the weight of the aluminum dish and filter after filtration in grams (g), and V is the volume of the sample (ml).

Also, the overall efficiency of each soil type was compared using the weighted average TSS reduction. The flow rate and TSS reduction at overflow and outflow were considered to calculate the weighted average TSS reduction using Equation 4.2.

$$\text{Weighted Average TSS Reduction (\%)} = \left(\frac{\text{Underdrain flow rate} \times \text{Underdrain TSS} + \text{Overflow rate} \times \text{Overflow TSS}}{\text{Total Inflow rate} \times \text{Influent TSS}} \right) \times 100 \qquad (4.2)$$

Although every attempt was made to achieve the target TSS at the inlet, due to the minor unavoidable non-linearity of the sediment feeder and pumping system, it was not possible to achieve the target TSS in all cases. Hence the obtained inlet concentration values were adjusted to 100 mg/Lit and 200 mg/Lit. Therefore, all the TSS and turbidity values measured at different locations and time were adjusted accordingly. See Appendix C for more details.

4.4.1 Effect of Media Thickness on TSS Removal Efficiency

Only Type 1 soil media was considered for determining the effect of media thickness on treatment efficiency. Twelve experiments were performed, comprising six experiments with 4-inch and six experiments with 6-inch thicknesses. The percentage reduction in TSS obtained for each experiment is plotted in Figure 4.3 and Figure 4.4.

Plotted data shows a 65% to 79% TSS reduction in the underdrain flow for the 6-inch soil, whereas only a 53% to 67% reduction was obtained for the 4-inch medium. Similarly, overflowing water had a TSS reduction of 32% to 64% for 6-inch medium, whereas only a 29% to 59% TSS reduction was obtained for the 4-inch medium.

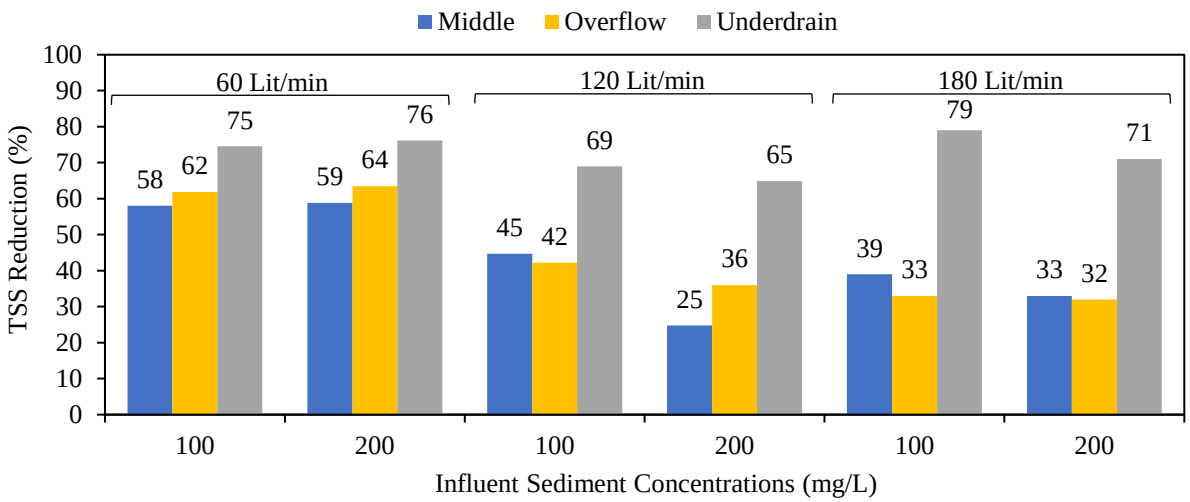

Figure 4.3: *Effect of soil media thickness on TSS removal efficiency (Type 1: 6-inch media (without underdrain)*

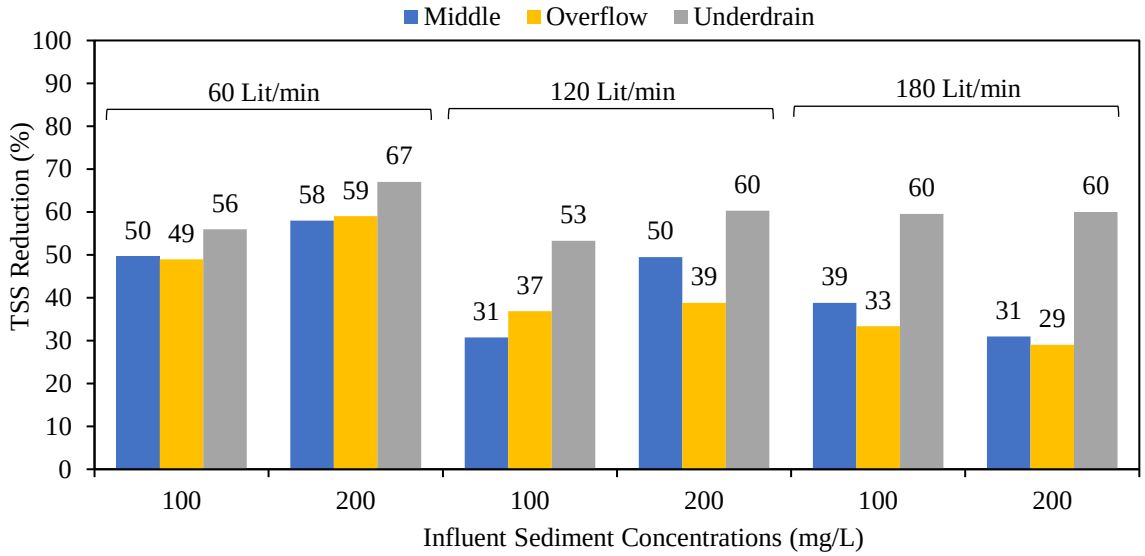

Figure 4.4: *Effect of soil media thickness on TSS removal efficiency (Type 1: 4-inch media (without underdrain)*

The results are summarized in Table 4.3. The weighted average TSS reductions for the same experiment conditions were grouped and calculated. The mean value of weighted average TSS removal efficiency was then calculated and compared. Since the obtained mean of weighted average TSS removal efficiencies of the 4-inch medium were also smaller than those of the 6-inch

medium without underdrain, i.e., 43% vs. 48%, the 4-inch experiments were discontinued for further testing and not considered for in other scenarios.

Table 4.3: *Mean of weighted average TSS removal for 4 inches and 6 inch soil media*

	Inflow (Lit/min)			Overall weighted average TSS removal
Description	**60**	**120**	**180**	
4"soil media without underdrain	56%	40%	33%	43%
6" soil media without underdrain	66%	42%	36%	48%

A previous study by Brown and Hunt (2012) found that the inflow volume reduction due to infiltration was more in media with higher thickness. The same study confirmed that the volume reduction and pollutant removal were seen mutually associated. A similar study by Li et al. (2009) also concluded that the media depth, as a primary factor for volume reduction by infiltration, change the hydrologic performance of bioretention facilities especially the BMPs incorporating infiltration media. These studies agree with the performance of the current laboratory experiments on expanded shale, demonstrating that the higher thickness of 6-inch is more effective in removing TSS.

4.4.2 Effect of Underdrain System on TSS Removal Efficiency

The influence of promoting infiltration of the soil media was evaluated, and each experiment with the same conditions but with and without the underdrain system were compared. Figure 4.5 and

Figure *4.6* show the effect of the underdrain system on TSS removal efficiency over Type 1 and Type 2 soil media, respectively. In both Type 1 and Type 2 soil media, it is seen that in almost all cases, tests with the underdrain system outperformed those without underdrain.

Table 4.4 summarizes the performance of swales with or without the underdrain. Considering the results from all experiments, an overall average removal efficiency of 56% was obtained when the

underdrain was active, whereas only a 47% overall average removal efficiency was observed when the underdrain system was inactive. This results show that with the underdrain, the removal efficiency was improved. This result aligns with the existing literature findings (e.g., Clark and Acomb 2008; Stagge 2012), which indicate that the pollutant removal efficiency is directly related to the degree of infiltration.

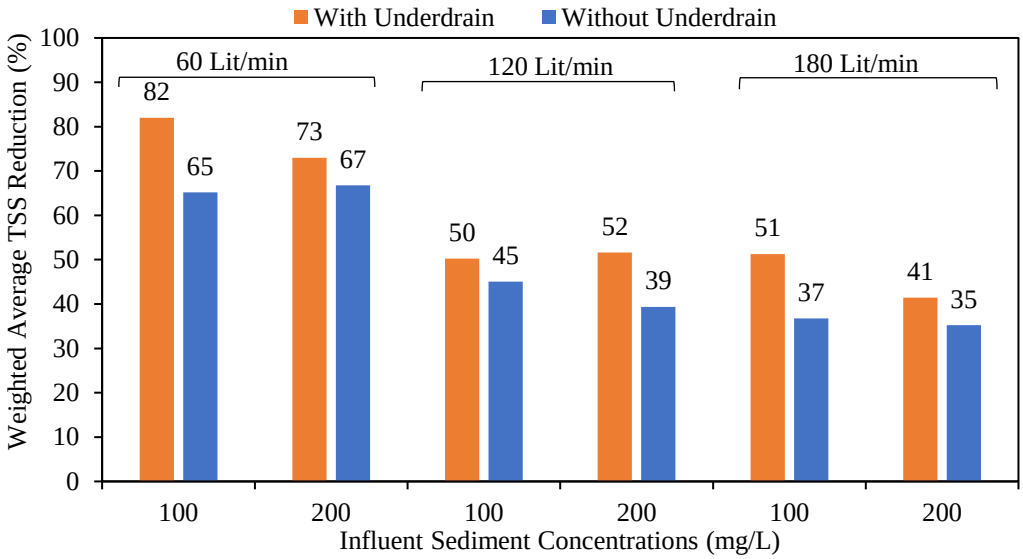

Figure 4.5: *Effect of underdrain system on TSS removal (Type 1 media, 6-inch)*

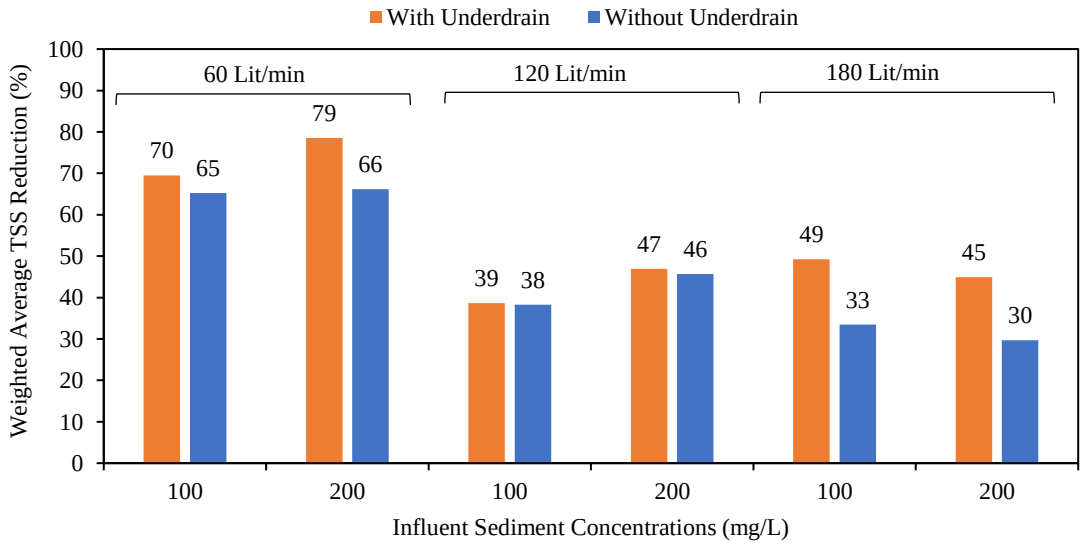

Figure 4.6: *Effect of underdrain system on TSS removal (Type 2 media, 6-inch)*

Table 4.4: *Overall mean and range of weighted average TSS removal for 6-inch media with and without underdrain*

Condition	Mean of Weighted Average TSS Removal Efficiency (%)	Range of Weighted Average TSS Removal Efficiency (%)
With Underdrain	56	39 - 82
Without Underdrain	47	30 - 67

4.4.3 Effect of Expanded Shale Type on Removal Efficiency

Two different expanded shales, Type 1 and Type 2, were tested. Individual experiments' TSS reductions were compared based on type of media, keeping all other factors same.

Figure 4.7 and Figure 4.8 show the performance comparison chart for Type 1 and Type 2 expanded shales classifying with and without underdrain, respectively. The charts show that for almost all comparisons, Type 1 had better performance than Type 2 soil media. In nine out of twelve experiments, Type 1 had a higher weighted average TSS reduction than Type 2.

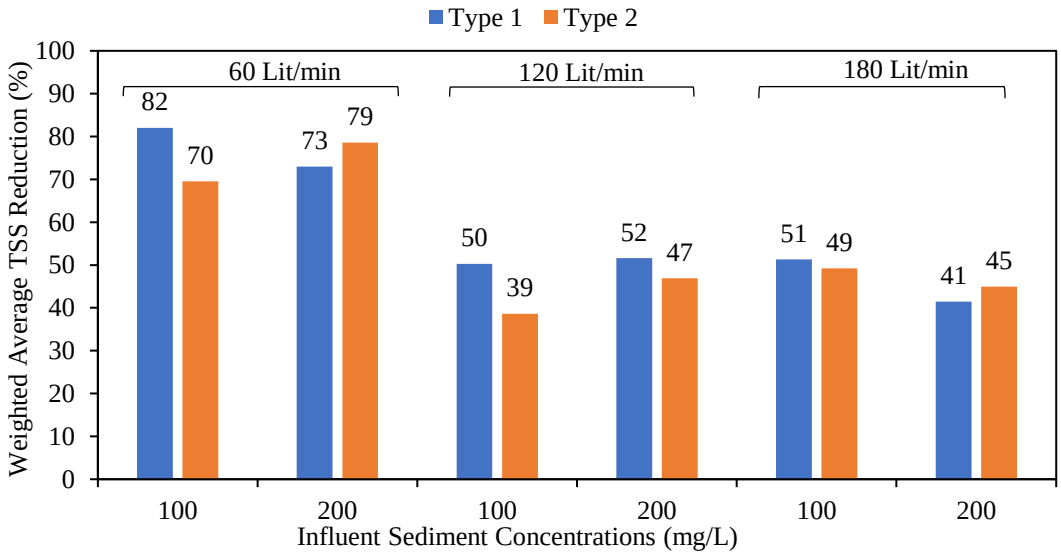

Figure 4.7: *Effect of type of soil media in TSS removal efficiency (with underdrain, 6-inch)*

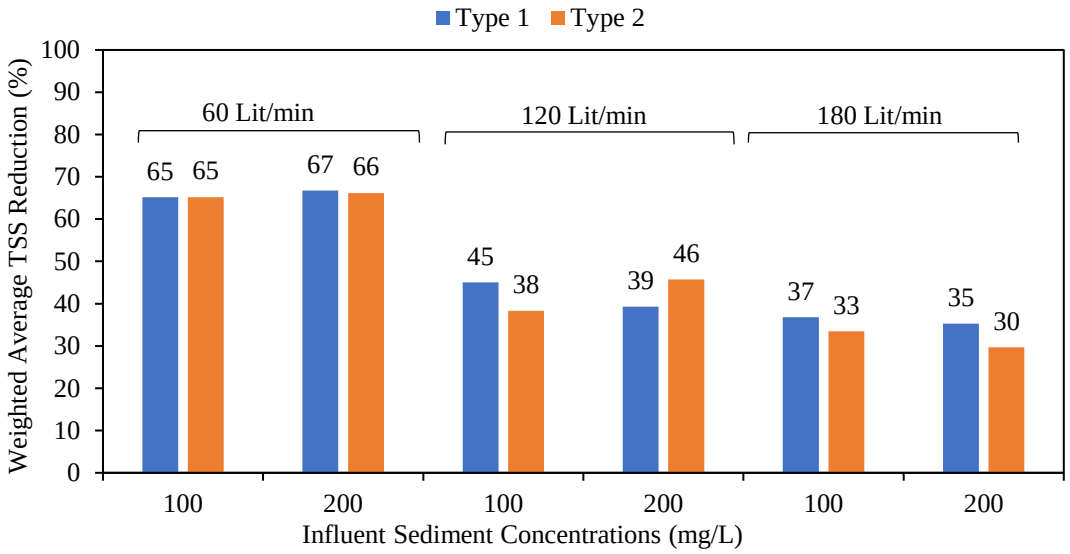

Figure 4.8: *Effect of type of soil media in TSS removal efficiency (without underdrain, 6-inch)*

Table 4.5 presents the overall removal efficiency of all 6-inch media experiments, which were grouped based on the type of expanded shale. Noticeably, the mean of weighted average TSS removal efficiency was higher for Type 1 than Type 2, although they performed equally at 60 Lit/min when the inflow was below drainage capacity and under-drain was provided.

In the other cases, when inflow was higher than drainage capacity, Type 1 media being coarser and with higher or equal drainage capacity (cases with or without underdrain), higher portion of the water passes through the outlet (infiltrating water) than in Type 2 media. This allowed Type 1 soil media to get in contact with a higher volume of water than Type 2 when the drainage capacity was exceeded. Thus, it is supposed that the reason of Type 1 media resulting in higher TSS removal efficiency is higher volume of water infiltrating through the media than Type 2.

Table 4.5: *Overall mean and range of weighted average TSS removal for 6-inch media*

Condition	Mean of Weighted Average TSS Removal Efficiency (%)	Range of Weighted Average TSS Removal Efficiency (%)
Type 1	53	35 - 82
Type 2	51	30 - 79

4.4.4 Effect of Inflow Rate on TSS Removal Efficiency

The results from experiments with the same conditions but varying inflow are compared. Figure 4.9 and Figure 4.10 illustrate the comparison of removal efficiency of expanded shale corresponding to the three different inflow rates tested, i.e., 60, 120, and 180 Lit/min. These figures clearly distinguish between the efficiencies of different inflow rates. They show that the soil medium under low flow (60 Lit/min) had higher efficiency in all case, since a larger proportion of inflow water passed through the filter media.

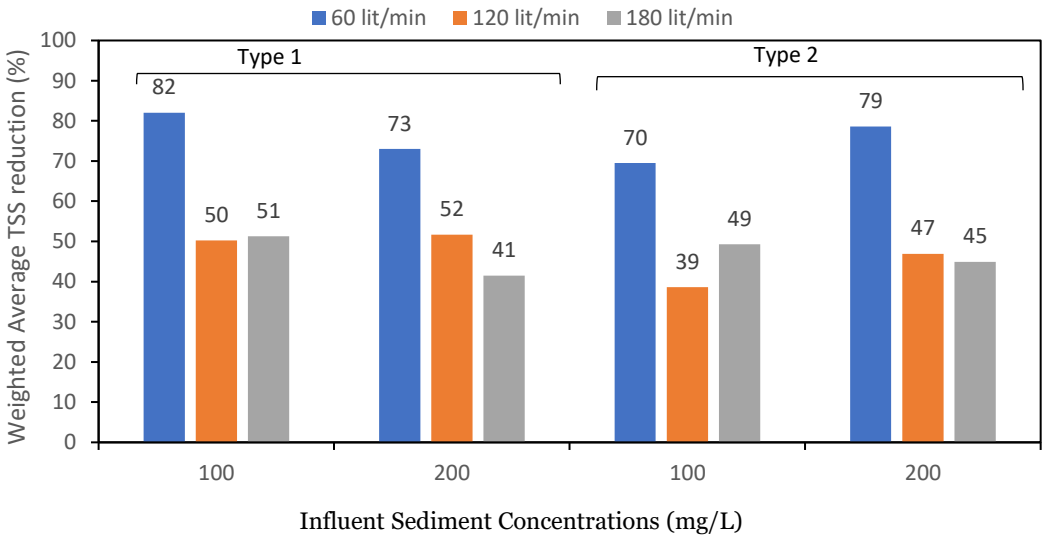

Figure 4.9: *Effect of inflow rate on TSS removal efficiency (with underdrain, 6-inch)*

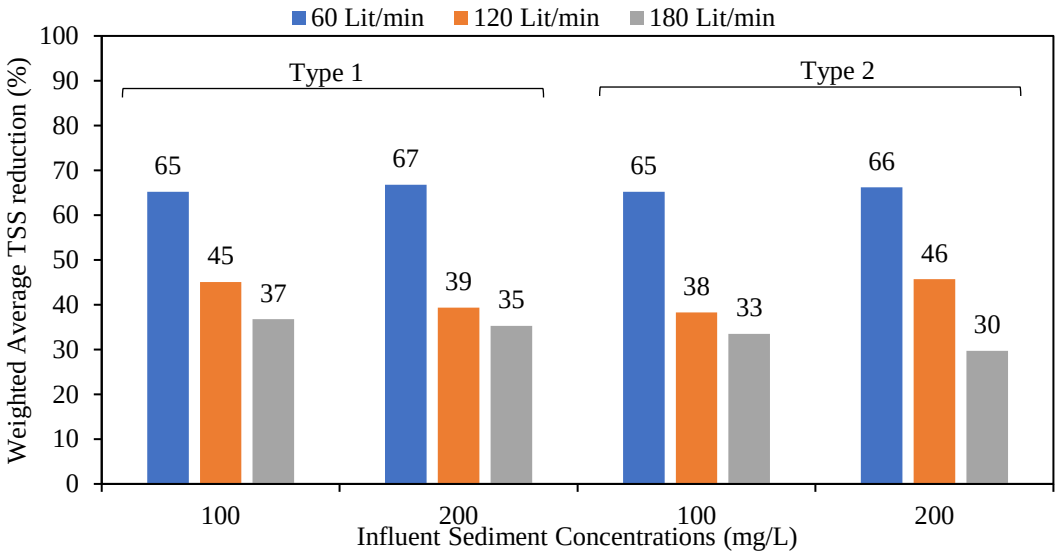

Figure 4.10: *Effect of inflow rate on TSS removal efficiency (without underdrain, 6-inch)*

Table 4.6 summarizes the weighted average for all three flow rates considered. It is observed that the overall removal efficiency decreased with an increase in inflow rate from 71% being the highest for 60 Lit/min and 40% for 180 Lit/min. This findings agrees with work of Brown and Hunt (2012) and Stagge et al. (2012) that reported the volume reduction through the infiltration enhances the removal efficiency. This outcome of our study also indicates that when infiltration is constrained by drainage capacity, increased inflow rates lead to a greater fraction of overflow volume. Consequently, resulting in a reduced TSS removal efficiency since volume reduction (infiltration) in higher flow is smaller fraction of total inflow. This caused the weighted average TSS removal efficiency to decrease with increase in inflow (See Table 4.6). Also, higher efficiency for lower inflow and decreasing trend of efficiency with increasing inflow is comparable to that reported for TSS removal in bioswales (Groves et al. 1999).

Table 4.6: *Overall mean and range of weighted average TSS removal for 6-inch media for different inflows*

Flow rate (Lit/min)	Mean of Weighted Average TSS Removal Efficiency (%)	Range of Weighted Average TSS Removal Efficiency (%)
60	71	65 - 82
120	44	38 - 52
180	40	30 - 51

4.4.5 Effect of Influent Concentration on TSS Removal Efficiency

Figure 4.11 shows the effect of influent concentration on treatment removal efficiency of the 6-inch media with an underdrain. With the underdrain system, the TSS removal efficiency varied between 39% and 82% in all cases. Likewise, Figure 4.12 shows the effect of influent concentration on treatment removal efficiency for without underdrain cases. Without the underdrain system, the TSS removal efficiency varied from 30% to 67%. The TSS reduction was more during low flow for any influent concentration when underdrainage was provided which is consistent with previous findings in Section 4.4.2.

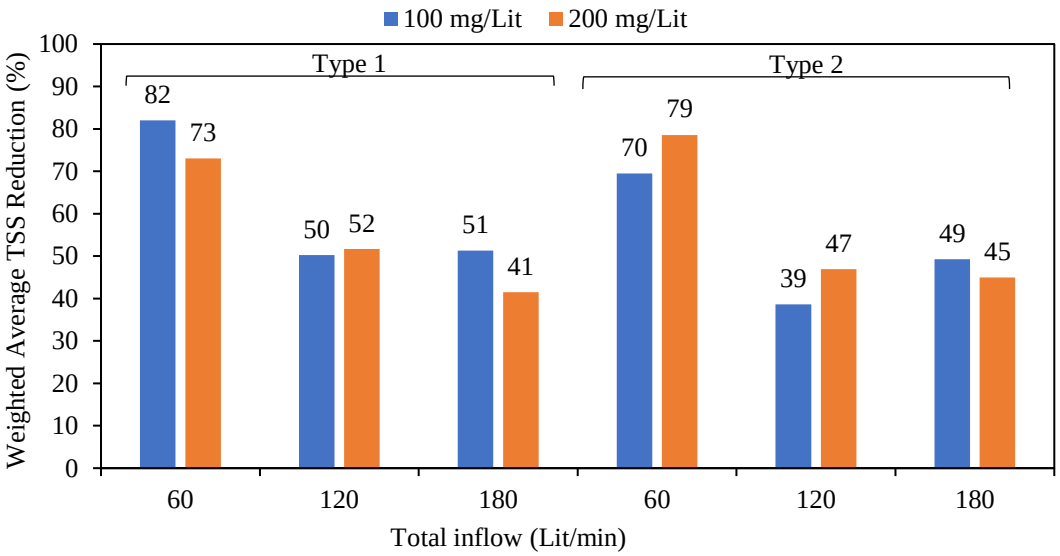

Figure 4.11: *Effect of influent concentration on TSS removal efficiency (6-inch with underdrain)*

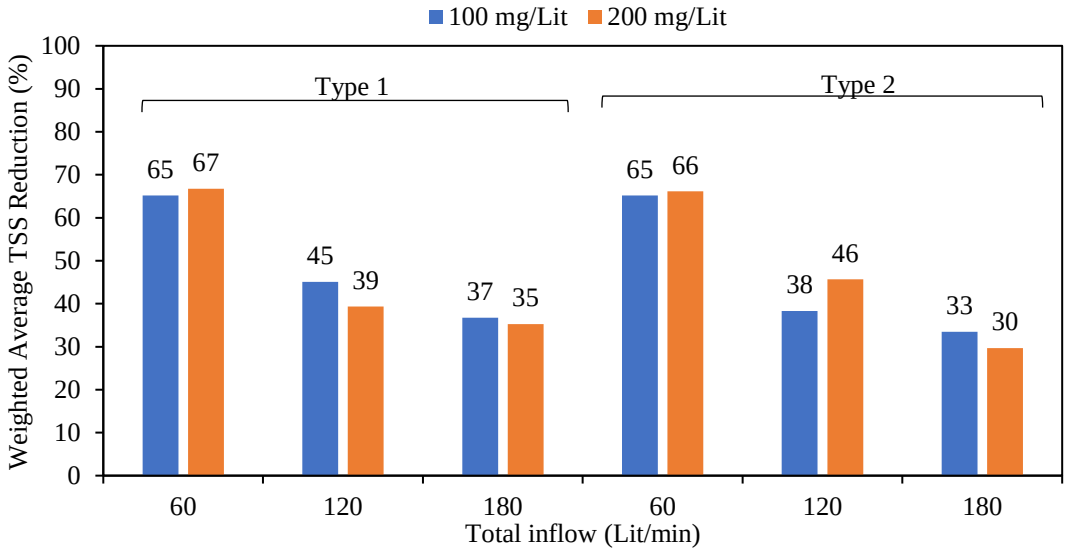

Figure 4.12: *Effect of influent concentration on TSS removal efficiency (6-inch without underdrain)*

Among the 24 experiments conducted, both low and high concentrations were observed to outperform the others an equal number of times. A clear trend was not observed regarding removal efficiency due to concentration differences of the individual experiments. However, The upper-bound of the range for TSS removal efficiency was slightly higher in experiments with lower influent concentration, an equal mean value of 52% was obtained for weighted average TSS removal for both cases. The mean of weighted average TSS removal of experiments with 100 and 200 mg/Lit influent concentrations is calculated and are presented in Table 4.7.

Although, the overall efficiency of both influent concentrations were equal at 52%, the individual experiments had differences in TSS removal at the outflow (infiltrated water). For an influent concentration of 100 mg/Lit, a range of 18-47 mg/Lit was observed, whereas a range of 38 - 90 mg/Lit was observed for an influent with 200 mg/Lit sediment concentration irrespective of the inflow rate. In other words, when the influent concentration was doubled, the effluent concentration range was also approximately doubled. This observation agrees to the Barrett (2005). Barret (2005) concluded that efficiency of the bioswales is dependent on the influent

concentration i.e., effluent concentration is a constant function of influent concentration in bioswales.

Table 4.7: *Overall mean and range of weighted average TSS removal for 100 mg/Lit and 200 mg/Lit in 6 inch media*

Flow rate (Lit/min)	**Mean of Weighted Average Removal Efficiency (%)**	**Range of Weighted Average Removal Efficiency (%)**
100 mg/Lit	52	33 - 82
200 mg/Lit	52	30 - 79

4.5 TSS Removal Efficiency at Sampling Locations

The overall TSS removal efficiency was calculated when all the tests performed were grouped only based on the location, irrespective of the other considerations. The percentage of TSS removal at the middle section, overflow, and outflow were compared. The overall removal efficiency was determined as the means of all calculated TSS removal efficiency for individual sampling locations. Table 4.8 illustrates the overall efficiency observed for different sampling locations.

It is seen that, on average, 42% of sediment reduction was observed in the samples taken in the middle section of the flume and 43% in the overflowing water, and 68% in the infiltrating water (at the outflow). The range of TSS removal for each location is 20% to 75%, 19% to 75%, and 55% to 82%, respectively. This confirms that the average TSS was decreasing along the flume, and the overflow had slightly smaller suspended solids than the middle section but significantly higher than the infiltrated water. This is in line with the previous studies which suggest that TSS concentration reduces exponentially along the flow (e.g., Deletic 2005; Lucke et al. 2014).

Table 4.8: *Overall and range of TSS removal efficiency at different sampling locations*

Location	Overall TSS Removal Efficiency (%)	Range of TSS Removal Efficiency (%)
Middle	42	20 - 75
Overflow*	43	19 - 75
Outflow	68	55 - 82
Average**	52%	30 - 82

*Not all experiments had overflow
** Including all the experiments

4.5.1 Effect on TSS removal efficiency due to Underdrain and Flow at Sampling Locations

Lastly, the overall effect of the underdrain system and inflow rate were classified and grouped to determine the overall TSS removal efficiency of the soil media. Table 4.9 shows the average TSS removal efficiency calculated for different inflow rates for the soil medium classified as with and without the underdrain system. Figure 4.13 shows the mean of weighted average efficiency of TSS reduction of the soil medium with and without the underdrain system under different inflow rates. A mean of weighted average efficiency is calculated as the average of all TSS percentage reduction for each sampling location using Equation 4.2, irrespective of its soil type.

Initially, it was observed that at the low inflow rate of 60 Lit/min, the average TSS reduction percentage was higher in any location when underdrain was active. It is also observed that except for low flow (60 Lit/min), the middle and outflow's average TSS reduction were almost similar with or without underdrain. But still, the overall weighted average TSS removal efficiency was consistently higher for underdrain-active cases because of the difference in the outflow rate. Although in both cases the outflow had the highest TSS removal than the other two locations, the outflow rate was significantly higher in cases where underdrain was active. This has resulted in higher overall removal efficiency for cases with underdrain. Internal water storage (IWS) integration was seen as one potential design modification to incorporate into the system to reduce

the overflow and promote overall removal efficiency. Kim et al. (2003) found that nutrient removal efficiency was enhanced when IWS was incorporated into the bioretention system. Hence, it could be concluded that bioswale pollutant removal would be higher in cases when infiltration is promoted.

A 20% to 75% average TSS reduction was observed in all cases for the middle section, 55% to 82% for outflow (infiltrated water), and 19% to 75% TSS reduction for overflowing water. Overall, 41% to 76% was observed as an overall weighted average efficiency when all the experiments were considered. Regardless of any conditions, a weighted average TSS removal of 52% was obtained. Although, the expanded shale media's removal efficiency in bioswales has not been documented, the obtained results are found to be comparable with the average TSS removal in BMP applications as reported in different studies. Yu et al. (1994), Kings County (1995), Hunt et al. (2008), Brown and Hunt (2012), and Fardel et al. (2019) obtained overall TSS removal of 50%, 40%, 59.5%, 58%, and 56% respectively. Similarly, an experimental study from Stagge and Davis (2006) obtained 65% to 71% mean sediment reduction when grass swale efficiency was evaluated.

However, the results were not consistent with findings from other studies such as Xiao and McPherson (2011) reporting 95% efficiency which may be because it was obtained in a large-scale field experiment in a parking lot, nearly 34 ft long, 7.8 ft wide and 3 ft deep of engineered soil (almost 26 times larger by volume and five times larger by surface area than the current study).

Similarly, in terms of underdrained water, a study conducted by Purvis et al. (2018) had 88% removal efficiency for underdrained water, which is significantly higher than the finding of this study (66%). Also, Purvis et al. (2018) considered significantly large-scale field experiments as compared to the scale of the laboratory set up in this study having limited filter media thickness. Purvis et al. (2018) performed their experiments in a 137 ft long, 4 ft wide and 2.25 ft average

depth triangular media, which was significantly higher in terms of volume and depth than the current study. In other words, it was approximately 44 times larger by volume and ten times longer by length than the current study.

Since the target TSS removal for the onsite bioswale practices is 80% (iSWM 2015; iSWMM 2006; EPA 2016), these results of this study at the current scale did not meet such target. In addition to the size of the experimental setup, the current laboratory study represents the TSS removal efficiency without the presence of vegetation. Having said that, undersized BMPs are reported to perform less efficiently (Maryland Stormwater Design Manual 2000).

This is further supported by the finding by Groves et al. (1999) that the TSS removal increased 46% to 54% (for lower rainfall intensity) and from 25% to 30% (for higher storm intensity) upon increasing the area of bioswale by 2.4 times Therefore, a large scale experimental setup is required to determine the actual efficiency of expanded shale in the field. Overall, this study showed that the expanded shale media have a competitive TSS removal performance as compared to other type of filter media.

Table 4.9: *Average TSS removal efficiency for all scenarios (6 inches media)*

Descriptions	**Inflow rate (Lit/min)**	**Average TSS removal efficiency**			**Overall Weighted Average Efficiency (%)**
		Middle section (%)	Outflow (%)	Overflow (%)	
With underdrain	60	66	79	67	76
	120	36	62	32	47
	180	27	64	38	47
Without underdrain	60	60	75	62	66
	120	34	63	38	42
	180	31	66	30	34

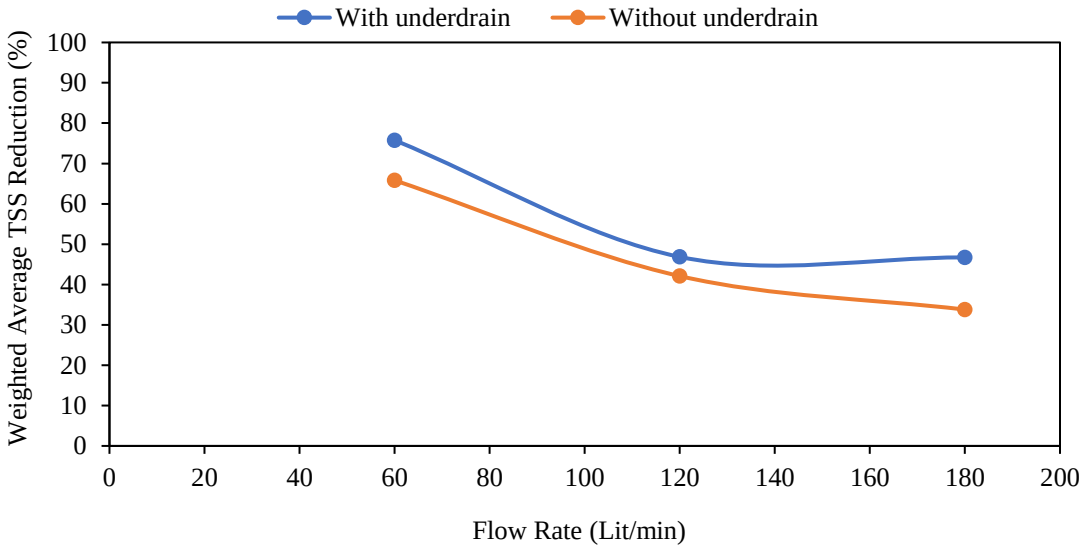

Figure 4.13: *Weighted average TSS removal under with and without underdrain conditions*

4.6 Turbidity Removal Efficiency

Water samples from twenty four experiments were tested for turbidity. This includes 12 experiments with the underdrain system (valve in underdrain system was open) and 12 experiments without underdrain (valve in underdrain system was closed). All the experiments were conducted with filter media of 6-inch thickness. Removal efficiency was calculated based on the influent turbidity and the turbidity at the sampling locations. Turbidity at three sampling locations was compared.

4.6.1 Effect on Turbidity Removal Efficiency due to Underdrain, Influent Concentration, and Inflow Rate

The effects of the underdrain system, inflow rate, and influent sediment concentration were analyzed for the obtained data in terms of turbidity removal efficiency. The turbidity removal percentage was always found to be higher for low flow conditions, and it gradually decreased and remained almost constant at higher flows. Groves et al. (1999) observed a similar result in

bioswales study. As previously discussed, this is due to the higher hydraulic residence time available for low flow and this trend is also consistent with TSS removal.

Upon looking into the effect of underdrain on turbidity removal efficiency, in all cases, experiments with underdrain had significantly higher mean of weighted average removal efficiency than experiments without underdrain (Figure 4.14). This is also consistent with the TSS removal findings as discussed previously.

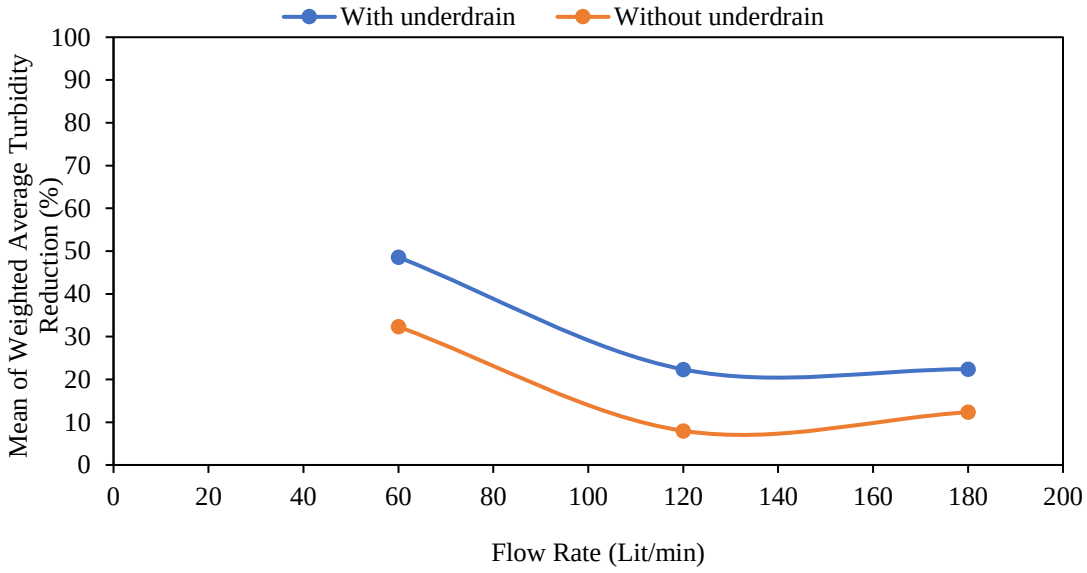

Figure 4.14: *Weighted average turbidity removal under with and without underdrain conditions*

Furthermore, Table 4.10 shows the results of turbidity removal calculated based on drainage condition and influent concentration. For each considered comparison, none other factors were considered. After comparing the results, irrespective of any other factors, experiments with underdrain always had higher overall weighted average efficiency removal than experiments without underdrain with limited infiltration.

Although the turbidity was found to be significantly lower for the outflow, overflow always had a lower average turbidity reduction than that of the outflow and the middle section. Outflow has the lower turbidity as the media removes the particles by filtration whereas the overflowing water does

not undergo filtration process. Comparing overflow concentration with the samples taken at the middle section of the flume does not hold for the general assumption that the turbidity would be decreasing along the length. Results associated with the lower reduction in overflow turbidity compared to that in the middle section could be attributed to the resuspension of the sediment on the downstream due to the presence of the check dam. Also, observed higher turbidity in overflow than outflow was documented in the bioswales by Purvis et al. (2018).

Table 4.10: *Average turbidity removal efficiency at different sampling locations*

Description	**Average Turbidity Removal Efficiency (%)**			**Mean Weighted Average Turbidity Removal (%)**
	Middle section	Outflow	Overflow	
With underdrain	18	43	17	31
Without underdrain	15	38	14	18
100 mg/Lit	16	39	12	22
200 mg/Lit	18	41	18	26

4.6.2 Turbidity Removal Efficiency at Sampling Locations

The efficiency of the expanded shale media at sampling location was determined by calculating the overall average turbidity removal. All the turbidity removal efficiency obtained for individual experiments were averaged to obtain the overall average turbidity removal percentage. An average reduction in turbidity of 17 % was obtained within the half length of the flume with a range of -4% to 43% varying within different experiments. The water infiltrating through filter media (the outflow) had an average reduction of 40% while the range was 22% to 61% reduction. The water that overflowed through the downstream weir had 15% turbidity removal, with a range of -7% to 49% (see Table 4.11). In all cases, the turbidity was seen to have a mean weighted average reduction of 24% irrespective of test conditions. The negative weighted average reduction could

be due to those experiments in which the turbidity at different sampling locations were higher than the inlet turbidity.

Results in this study with mean turbidity removal of 40% at underdrain and 15% at overflow are relatable to the 36% and 4% turbidity removal in the study of Purvis et al. (2018).

Table 4.11: Overall and range of turbidity removal efficiency at different sampling locations (6-inch)

Location	Overall Turbidity Removal Efficiency (%)	Range of Turbidity Removal Efficiency (%)
Middle	17	(-4) - 43
Overflow*	15	(-7) - 49
Outflow	40	22 - 61
Average**	24%	(-3) - 56

*Not all experiments had overflow
** Including all the experiments

As observed, the overflow's average turbidity reduction was slightly lower than that of the middle section, but the overflow's average TSS reduction was almost similar (i.e., weighted average) to those at the middle and overflow section. Since, Bright et al. (2020) studied the specific turbidity which is a measure of degree of scattering of the light by the sediment. As reported, presence of finer particles increases along the flow and, the finer particles are known to scatter more light causing higher turbidity. This resulted in the speculations that whether the coarser particles are settling down along the way as reported by Bright et al. (2020) or if it is due to the increased turbidity at the overflow section.

4.7 Change in Sediment Particle Gradation

Five experiments were selected to perform the particle size gradation of the suspended sediment. Samples taken in five experiments were tested by the laser diffraction method for gradation. The experiments that were considered for the suspended sediment particle size gradation are tabulated in Table 4.12.

Table 4.12: *Experiments considered for sediment gradation size test (6-inch media with underdrain)*

Type of Medium	Flow (Lit/min)	Influent Concentration (mg/Lit)
Type 1	60	100
	180	200
Type 2	60	200
	180	100
	180	200

4.7.1 Sediment Size Variation Along the Length of the Flume

The gradation test results were compared based on two different types of expanded shale used. First, the average value was taken for all three repeated tests. Subsequently, the average values were calculated for various time intervals—specifically, 10 minutes, 20 minutes, 30 minutes, and 40 minutes—based on the obtained average value. Ultimately, the graphs were generated using the average values for different sampling stations under consideration. The results are illustrated in Figure **4.15** and Figure 4.16.

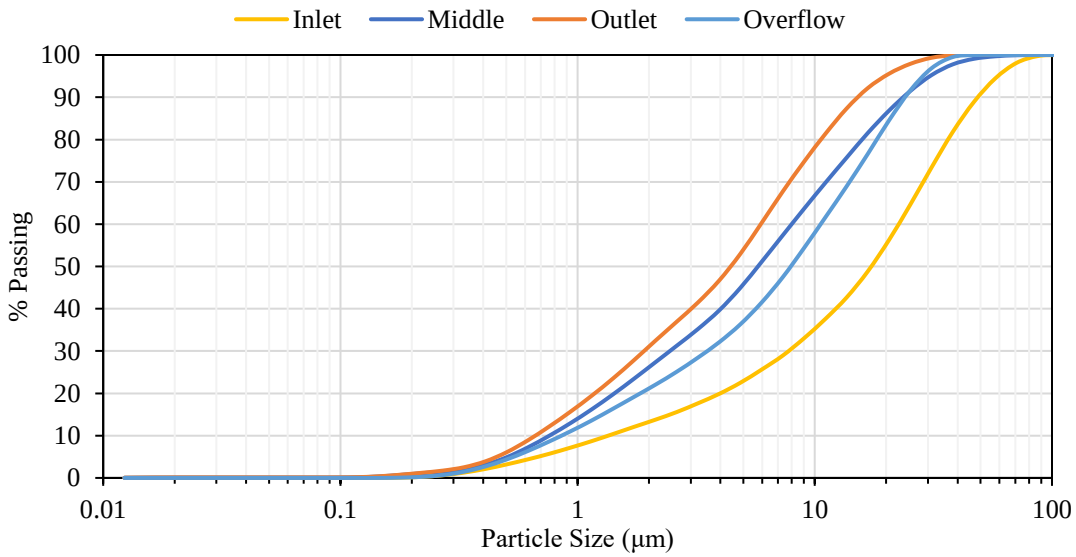

Figure 4.15: Sediment size variation along the length (Type 1 media, 6 inch)

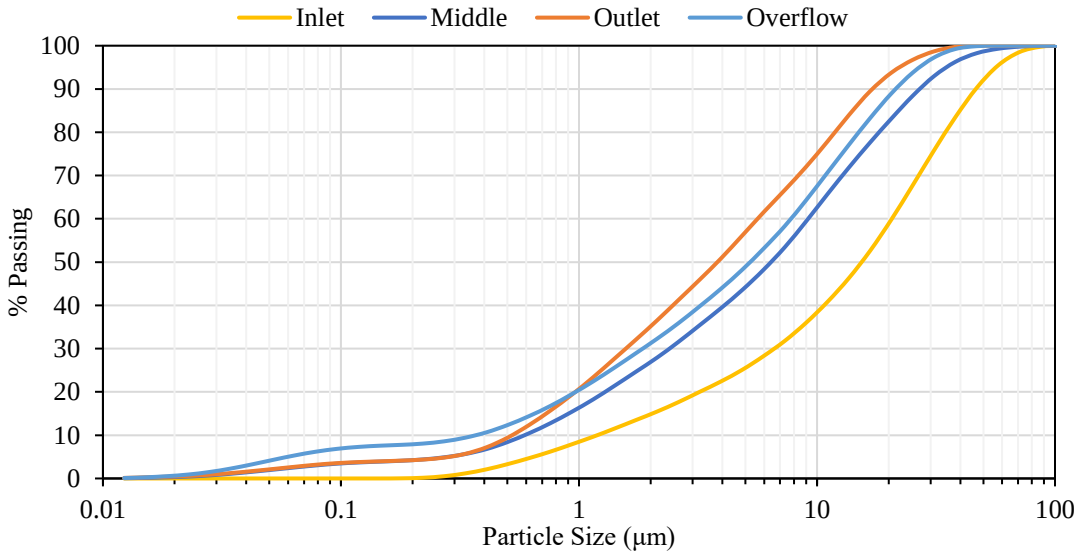

Figure 4.16: *Sediment size variation along the length (Type 2 bed layer, 6 inch)*

The results showed a distinctive sediment size variation along the flume. In both media types, the sediment lost the coarser particles as moving along the flow direction, as shown in

Figure **4.15** and Figure 4.16. Moreover, we see a similar gradation change in outflow sediment regardless of the soil media type. Nevertheless, an atypical pattern in overflow gradation was observed, displaying divergence, prompting a need for additional investigation. For that, all the observed sediment variation is re-analyzed for this investigation concerning the incoming flow rate. The results based on flow categorization as high flow (180 Lit/min) and low flow (60 Lit/min) are shown in

Figure 4.17 and Figure 4.18.

Low Flow

The drastic change in particle size was observed during low flow conditions where the mean particle diameter from drops 15 µm to 3 µm within half the length of the flume (Figure 4.17). Apart from this, the particle size was similar for outflow and the middle section. But the mean size of particles in overflowing water was finer (2 µm) than the particles in the outflow/middle (3 µm),

possibly because of higher hydraulic residence time for low flow. Due to the higher hydraulic residence time for low flow, the particles had enough time to drop off coarser particles. The findings of this study regarding low-flow scenarios align with the observations made in earlier research by Deletic (2005) and Lucke et al. (2014), where exponential variations in sediment size along the length were also noted.

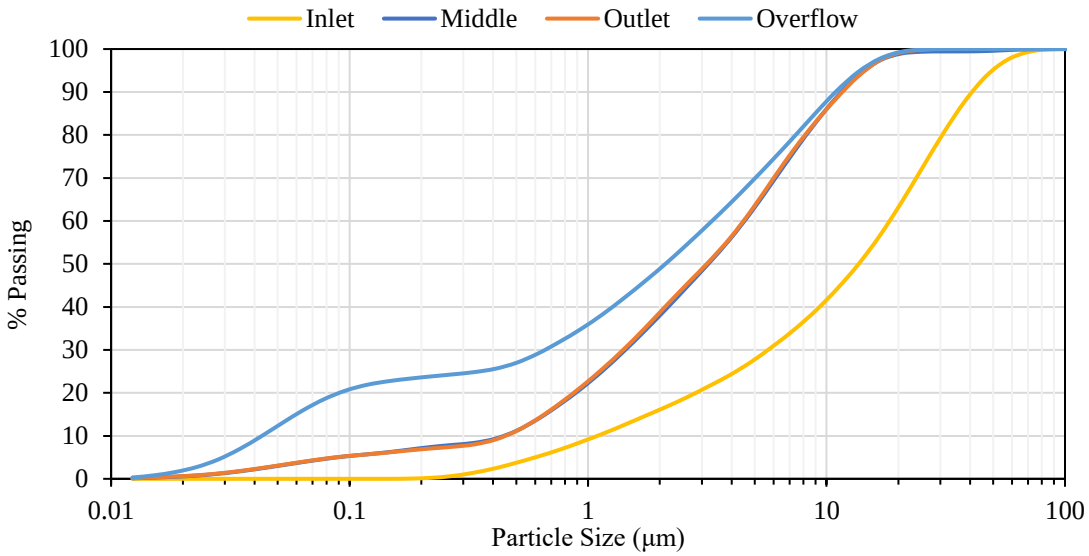

Figure 4.17: *Sediment size variation along the length during low flow (60 Lit/min)*

High Flow:

During high flow, particles in outlet flow had the smallest median diameter of any other sampling locations (Figure 4.18). Also, sediments in overflow were finer than at the middle section. The size of 15 µm median size particles introduced at the inlet reduces to 10 µm in size when it travels half of the length of the flume. This shows that the sediment did not have enough time to settle out the coarser particles during higher flow. This is due to shorter hydraulic residence time available and sediment traveling at higher velocities. Unlike during low flow, where particles were found to be finer than those in the middle section, high flow conditions resulted in the observation of coarser particles in the overflow due to the reduced hydraulic residence time.

Similarly, the outflow water had the smallest sediment size (5 µm) than at any other locations. Overflow water had a slightly higher mean size of 8 µm, and the middle section had a mean size of 10 µm. This shows that the drastic change in particle size was not observed during high flow experiments as observed during low flow cases. This is also due to the low hydraulic residence time available at higher flow.

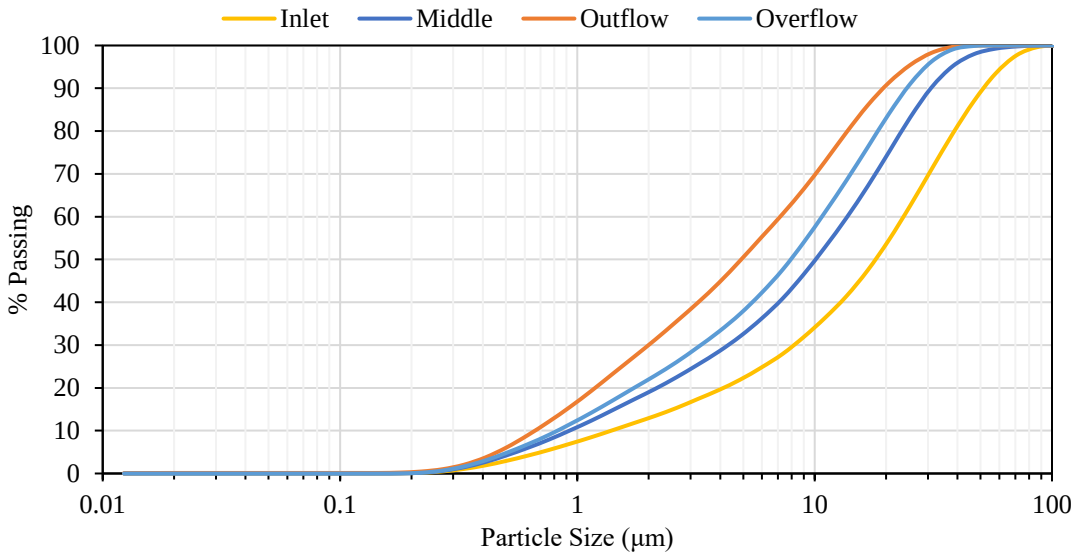

Figure 4.18: *Sediment size variation along the length during high flow (180 Lit/min)*

4.7.2 Sediment Gradation Change over Time

A pattern of change in sediment gradation was analyzed for sampling locations with respect to time of sampling during each experiment. Samples were collected after 10, 20, 30, and 40 min after the experiment was started. Samples collected from the middle section, overflow, and outflow were analyzed to determine the change in gradation with time.

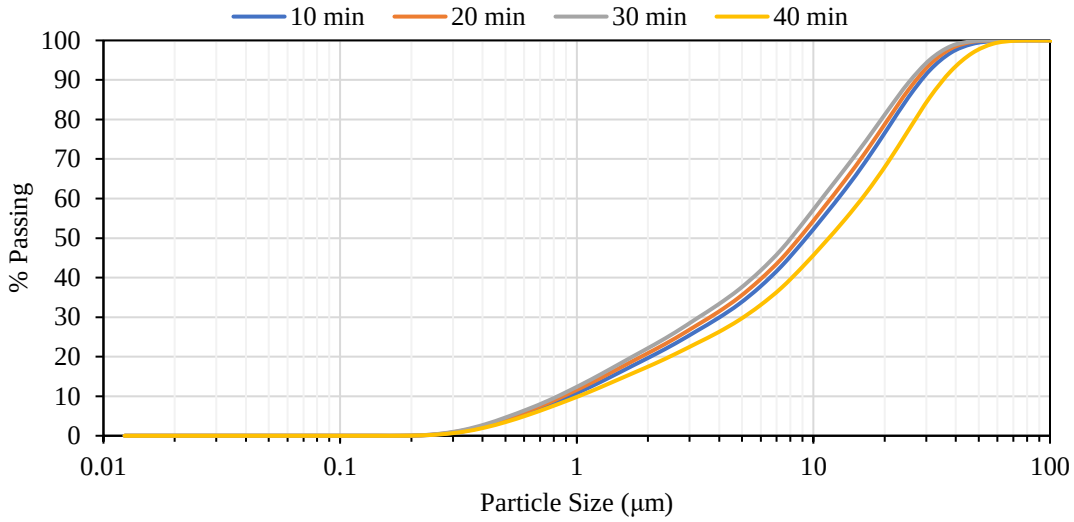

Figure 4.19: *Change in suspended sediment gradation with time at middle section of the flume*

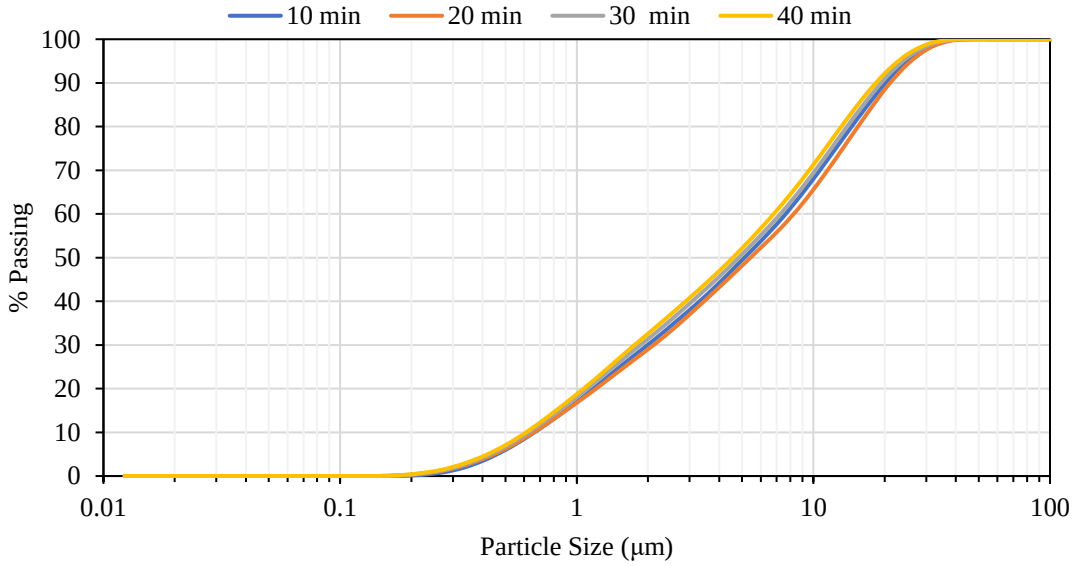

Figure 4.20: *Change in suspended sediment gradation with time at outflow*

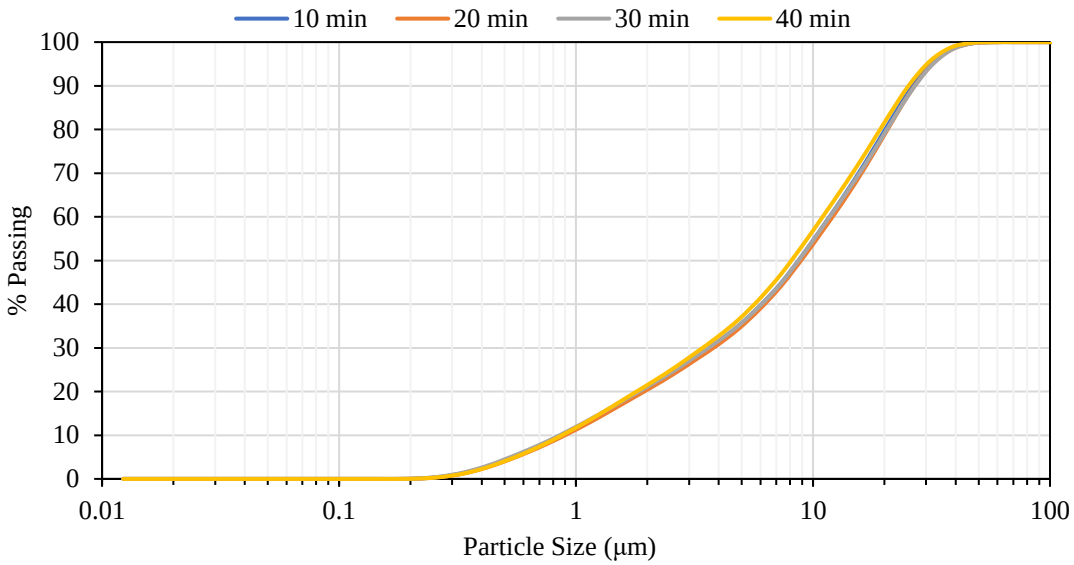

Figure 4.21: *Change in suspended sediment gradation with time at overflow*

Except for minor changes in gradation of suspended sediment in samples taken from the middle section of the flume, all sediment gradation curves at other sampling locations were the same throughout the experiment. This observation suggests that the flow was steady and the bioswale did not become clogged during the experiments. If there was any reduction in performance, the sediment gradation should have changed with time during the experiments. However, a long-term performance of the expanded shale regarding clogging was not included in this study.

4.8 Calculation of Trapping Efficiency

The Aberdeen equation was used to assess the trapping efficiency due to the sedimentation-only process. For dry swales, settling is the dominant process compared to biological uptake and adsorption, Aberdeen equation gives the expected efficiency of the swale (Hunt et al. 2020). Hence for the this study, the efficiency obtained is compared with the expected efficiency using Aberdeen Equation. Since, the Aberdeen equation is only applicable in laminar viscous flows (Hunt et al. 2020), only the 60 Lit/min inflow was used for the comparative study.

A particle size distribution (PSD) was considered to calculate the weighted average trapping efficiency for the sediment used in the experiment. The efficiency obtained based on the PSD was compared with the efficiency calculated based on the median diameter (d_{50}) of the sediment gradation at the inlet.

Table 4.13 shows the information on experiment with a total of 60 Lit/min inflow and the overflow at the rate of 44 Lit/min (passing through downstream weir). The rest of the water was passing through the underdrain. Therefore, the underdrain rate was deducted from the total flow for the calculation of trap efficiency using the Aberdeen equation. For the flume with net length of 14 ft, the maintained flow depth of 4 inches and a 4 feet flow width, the trap efficiency was calculated.

Firstly, for 14 ft of full-length using Aberdeen equation trapping efficiency of 19.6 % using median diameter (~0.014 mm) and 21.5% based on PSD were obtained. In an actual a 75% reduction of suspended sediment concentration was observed in the lab for this scenario.

Similarly, a trap efficiency of 13.1% (using the median diameter) and 15.7% (using the PSD) was calculated for the middle section of the flume. From the laboratory experiment, the sediment reduction of 71% was obtained for the middle portion of the flume for this scenario. The differences between the calculated trap efficiencies using d_{50} and PSD is similar to observed results in previous studies (e.g., Deletic 2005; Hunt et al. 2020). A summary of the trap efficiency calculations based on both median size and PSD is presented in Table 4.13.

The theoretical required length to achieve 80% sediment reduction solely due to settlement was determined using Aberdeen equation. For this purpose, the trapping efficiency was calculated for different hypothetical flume lengths.

Table 4.13: *Summary of Calculated and Measured Trapping Efficiency*

Actual Overflow (Lit/min)	**Flume Width (m)**	**Velocity (m/s)**	**HRT (min)**	**Method of Calculation**	**Calculated Trap Efficiency (%)**		**Observed Trap Efficiency (%)**	
					Full length	Half length	Full length	Half length
44	1.22	0.006	8.81	based on d_{50}	19.6	13.1	71	75
				based on PSD	21.5	15.7		

The trap efficiency vs. the flume length in plotted in Figure 4.22. According to this figure, the length required to achieve 80% sediment removal efficiency is 250 m.

The observed efficiencies for the half and full length of the flume are also plotted in Figure 4.22. An exponential relationship was used to draw a best fit curve. The exponential relationship was selected since the Aberdeen equation is also developed based on an exponential relationship between reduction in sediment concentration with the length. Using the relationship for best fit curve, a flume length of 22 ft (6.8 m) was calculated to achieve an 80% reduction in sediment load.

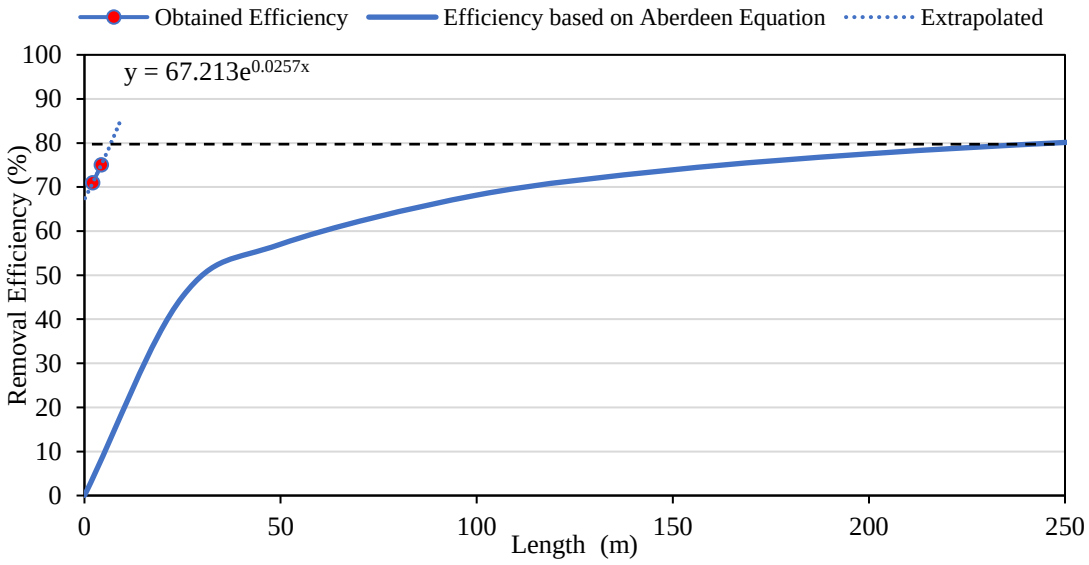

Figure 4.22: *Trapping Efficiency vs Required Length using Aberdeen Equation*

CHAPTER 5
CONCLUSIONS

5.1 Summary and Conclusion

Bioswales, commonly employed as Best Management Practices (BMPs), are designed to serve as water quality flow treatments and reduce peak flows during extreme events. The efficiency of BMPs is assessed based on their overall capacity to reduce pollutants. To achieve optimal efficiency in bioswales, a thorough understanding of the removal mechanisms is essential.

The main objective of this study was to determine the treatment effectiveness of expanded shale when used as an infiltration medium. To achieve this, the study first investigated the influence of infiltrating media thickness on the overall efficiency of sediment removal. Subsequently, the selected thickness of the expanded shale media underwent testing under various conditions to evaluate its effectiveness in removing TSS and turbidity. Testing conditions included variables such as soil media properties, inflow rate, influent concentrations, and drainage conditions. Furthermore, tests were conducted to examine the variation of sediment particles along the channel length.

The following are the significant conclusions drawn from the study:

- Expanded shale with a 6-inch thickness consistently outperformed the 4-inch thickness in terms of TSS reduction along the entire channel length, regardless of the scenarios tested.

- The presence of an underdrain system significantly improved pollutant removal efficiency compared to systems without an underdrain. Enhanced drainage allowed increased exposure of water to the expanded shale media, enhancing sediment adsorption.
- Coarser expanded shale mix generally performed better than finer mix when the underdrain was active, but they showed similar performance under inactive underdrain conditions.
- In reference to the previously reported studies, the incorporation of expanded shale into soil alongside vegetation is anticipated to improve treatment effectiveness. Additionally, use of expanded shale in low porous soils is likely to foster increased vegetation growth.
- Overall removal efficiency decreased with the increasing flow rate.
- While TSS and turbidity showed similar reduction patterns in most scenarios, turbidity in overflowing water was higher than at the middle section of the flume due to changes in sediment particle gradation and resuspension caused by the check dam.
- The maximum TSS and turbidity reduction achieved for water infiltrated through the expanded shale media were 82% and 61%, respectively, while for overflowing water, it was up to 75% for TSS and 49% for turbidity. Maximum efficiency was observed at a water quality flow rate of 60 Lit/min. The weighted average TSS reduction was 52%, and turbidity reduction was 24%.
- The particle size gradation indicated that coarser particles settled along the flow, resulting in 42% TSS reduction and 17% turbidity removal within half of the flume's total length.
- The particle gradation change along the flume length remained constant over time, but the gradation in the middle and overflow sections varied with the flow rate.

- To achieve an 80% treatment goal for water quality flow, a length of 22 feet was expected, but with an underdrain, this goal was achieved within 14 feet, reducing the required length by 1.6 times.

In conclusion, higher thickness of coarser expanded shale with enhanced infiltration under low flow conditions significantly improved water quality. Increasing the infiltration rate through soil amendment or reducing the flow rate resulted in higher treatment efficiency. In cases without an underdrain system, the presence of finer particles in the infiltrating media significantly impacted the infiltration rate.

5.2 Recommendations for Future Research

Based on the findings of this study, the following recommendations are proposed for future research:

- Investigate the impact of clogging on expanded shale media over an extended period. Since clogging was evident in experiments with varying conditions, a more detailed analysis is needed to understand its long-term effects on pollutant removal efficiency.
- Address the effects of inflow patterns by conducting studies that incorporate lateral flows. The current experimental facilities were limited in this regard, and exploring different inflow patterns could provide valuable insights into system performance.
- Examine the influence of vegetation on expanded shale media. In real-world scenarios, natural vegetation growth can affect flow dynamics and pollutant removal efficiency. Studying the combined effect of vegetation and expanded shale would be valuable for practical stormwater management.

- Explore the treatment efficiency of expanded shale beyond TSS and turbidity, including its effects on nutrients and metals such as Phosphorus, Nitrate-Nitrogen, and Zinc. A broader assessment of its pollutant removal capabilities would be valuable.
- Conduct a cost-benefit analysis comparing expanded shale as a filter media with existing filter media. This comparative study would provide insights into the economic feasibility of utilizing expanded shale in stormwater management.
- Conduct a comprehensive field experiment to assess the actual efficiency of expanded shale by incorporating volume reduction through the bottom and sides. The current study was limited to a glass flume with restricted infiltration, which may not fully represent the potential treatment efficiency of expanded shale.

By addressing these aspects, future research can contribute to a more comprehensive understanding of the potential and limitations of expanded shale as a stormwater management solution.

REFERENCES

1. Akan, A. O., and R. J. Houghtalen. 2003. Urban Hydrology, Hydraulics, and Stormwater Quality: Engineering Applications and Computer Modeling. John Wiley & Sons.
2. Anderson, B. S., B. M. Phillips, J. P. Voorhees, K. Siegler, and R. Tjeerdema. 2016. "Bioswales reduce contaminants associated with toxicity in urban stormwater." Environmental Toxicology and Chemistry, 35 (12): 3124–3134. https://doi.org/10.1002/etc.3472.
3. Anderson, C., J. Klett, J. Bousselot, and K. Barbarick. 2017. "Expanded shale as a soil amendment for the Rocky Mountain region." Text. Colorado State University. https://www.proquest.com/openview/83adea18df9ebbd8ebfc432346b5f003/1?pq-origsite=gscholar&cbl=18750
4. ASTM International. 2017. "Standard test methods for Particle-Size Distribution (Gradation) of soils using Sieve analysis." ASTM D6913-04. https://doi.org/10.1520/D6913-04.
5. Barrett, M. E., L. B. Irish, J. F. Malina, and R. J. Charbeneau. 1998. "Characterization of Highway Runoff in Austin, Texas, Area." J. Environmental Engineering, 124 (2): 131–137. American Society of Civil Engineers. https://doi.org/10.1061/(ASCE)0733-9372(1998)124:2(131).
6. Bertrand-Krajewski, J.-L. 2021. "Integrated urban stormwater management: Evolution and multidisciplinary perspective." J. Hydro-Environment Research, Sustainable Urban Drainage, 38: 72–83. https://doi.org/10.1016/j.jher.2020.11.003.
7. Björklund, K., M. Bondelind, A. Karlsson, D. Karlsson, and E. Sokolova. 2018. "Hydrodynamic modelling of the influence of stormwater and combined sewer overflows on receiving water quality: Benzo(a)pyrene and copper risks to recreational water." J. Environ. Manage., 207: 32–42. https://doi.org/10.1016/j.jenvman.2017.11.014.
8. Brander, K. E., K. E. Owen, and K. W. Potter. 2004. "Modeled Impacts of Development Type on Runoff Volume and Infiltration Performance1." JAWRA Journal of the American Water Resources Association, 40 (4): 961–969. https://doi.org/10.1111/j.1752-1688.2004.tb01059.x.
9. Brinkmann, W. L. F. 1985. "Urban stormwater pollutants: Sources and loadings." GeoJournal, 11 (3): 277–283. https://doi.org/10.1007/BF00186341.
10. Bright, C., S. Mager, and S. Horton. 2020. "Response of nephelometric turbidity to hydrodynamic particle size of fine suspended sediment." Int. J. Sediment Res., 35 (5): 444–454. https://doi.org/10.1016/j.ijsrc.2020.03.006.
11. Brown, R. A., and W. F. Hunt. 2012. "Bioretention Performance in the Upper Coastal Plain of North Carolina." 1–10. American Society of Civil Engineers. https://doi.org/10.1061/41009(333)95.
12. Caltrans (California Department of Transportation) 2020. Biofiltration Swale Design Guidance, Caltrans Division of Design, Office of Hydraulics and Stormwater Design, Sacramento, CA. https://dot.ca.gov/-/media/dot-media/programs/design/documents/2_dg-biofiltration_swale_ada.pdf
13. City of San Diego (n.d.) "Bioswale", Clairemont Boys and Girls Club Accessed 7/4/2023 https://www.sandiego.gov/sites/default/files/legacy/thinkblue/pdf/bioswalelidcard.pdf
14. Chaudhry, M. H. 2022. "Channel Design." Open-Channel Flow, M. H. Chaudhry, ed., 283–303. Cham: Springer International Publishing.
15. Clar, M. L., B. J. Barfield, and T. P. Connor. 2004. "Stormwater Best Management Practices Design Guide Volume 2 - Vegetative Biofilters." US Environmental Protection Agency, 2.
16. Clark, M., and Acomb, G. 2008. Bioswales/Vegetated Swales. Retrieved July 19, 2023, from https://buildgreen.ifas.ufl.edu/fact_sheet_bioswales_vegetated_swales.pdf

17. Claytor, R. A. 1996. Design of stormwater filtering systems. Solomons, MD (P.O. Box 1280, Solomons 20688), Silver Spring, MD (8737 Colesville Rd., Silver Spring 20910): Chesapeake Research Consortium.

18. Dang, D. P. T., L. Jean-Soro, and B. Bechet. 2023. "Pollutant characteristics and size distribution of trace elements during stormwater runoff events." Environmental Challenges, 11: 100682. https://doi.org/10.1016/j.envc.2023.100682.

19. Deletic, A. 2005. "Sediment transport in urban runoff over grassed areas." J. Hydrol., 301 (1): 108–122. https://doi.org/10.1016/j.jhydrol.2004.06.023.

20. Deletic, A., and T. D. Fletcher. 2006. "Performance of grass filters used for stormwater treatment—a field and modeling study." Journal of Hydrology., 317 (3): 261–275. https://doi.org/10.1016/j.jhydrol.2005.05.021.

21. Eckart, K., Z. McPhee, and T. Bolisetti. 2017. "Performance and implementation of low impact development – A review." Science of The Total Environment, 607–608: 413–432. https://doi.org/10.1016/j.scitotenv.2017.06.254.

22. Eckenfelder, W. W. 1970. Water quality engineering for practicing engineers. New York: Barnes & Noble. https://archive.org/details/waterqualityengi0000ecke

23. EPA 1999a. "Preliminary Data Summary of Urban Storm Water Best Management Practices." Office of Water. Accessed July 18, 2023. https://www.epa.gov/sites/default/files/2015-11/documents/urban-stormwater-bmps_preliminary-study_1999.pdf

24. EPA 1999b. "Storm Water Technology Fact Sheet Vegetated Swales." Office of Water. Accessed July 29, 2023. https://nepis.epa.gov/Exe/ZyPDF.cgi/200044A8.PDF?Dockey=200044A8.PDF

25. EPA 2012. "Green Infrastructure, Western Ecology Division." Office of Research and Development. Accessed July 25, 2023. https://nepis.epa.gov/Exe/ZyPURL.cgi?Dockey=P100Z2P1.txt

26. EP 2014. "Best Management Practices (BMPs) Siting Tool." Overviews and Factsheets. Accessed June 16, 2023. https://www.epa.gov/water-research/best-management-practices-bmps-siting-tool.

27. EPA 2021. "Stormwater Best Management Practice, Grassed Swales." NPDES. Accessed July 29, 2023. https://www.epa.gov/system/files/documents/2021-11/bmp-grassed-swales.pdf

28. EPA 2016. "Summary of State Post Construction Stormwater Standards." Office of Water. Accessed July 21, 2023. https://www.epa.gov/sites/default/files/2016-08/documents/swstdsummary_7-13-16_508.pdf

29. EPA 2017a. "2017 National Water Quality Inventory Report to Congress." Reports and Assessments. Accessed June 16, 2023. https://www.epa.gov/waterdata/2017-national-water-quality-inventory-report-congress.

30. EPA 2017b. "NPDES, Storm Water Preliminary Data Summary." Accessed July 29, 2023. https://www.epa.gov/sites/default/files/2015-10/documents/usw_b.pdf

31. EPA 2017c. "Total Suspended Solids, EPA Method 160.2 (Gravimetric)." https://19january2017snapshot.epa.gov/sites/production/files/2015-06/documents/160_2.pdf

32. EPA 2021. "Stormwater Best Management Practice, Grassed Swales." NPDES. Accessed July 29, 2023, https://www.epa.gov/system/files/documents/2021-11/bmp-grassed-swales.pdf

33. EPA 2022. " NPDES, National Menu of Best Management Practices (BMPs) for Stormwater" Accessed July 29, 2023. https://www.epa.gov/npdes/national-menu-best-management-practices-bmps-stormwater

34. EPA 2023a. "What is Green Infrastructure ?" Green Infrastructure. Accessed July 29, 2023. https://www.epa.gov/green-infrastructure/what-green-infrastructure

35. EPA 2023b. "Problems with Stormwater Pollution" NPDES stormwater program. Accessed July 29, 2023. https://www.epa.gov/npdes/npdes-stormwater-program

36. EPA 2023c. " Operating Procedure: Wastewater Flow Measurement." Assessed on July 25, 2023

https://www.epa.gov/sites/default/files/2015-10/documents/wastewater_flow_measurement109_af.r4.pdf

37. Ekka, S. A., H. Rujner, G. Leonhardt, G.-T. Blecken, M. Viklander, and W. F. Hunt. 2021. "Next generation swale design for stormwater runoff treatment: A comprehensive approach." J. Environmental Management, 279: 111756. https://doi.org/10.1016/j.jenvman.2020.111756.

38. Ekka, S. and Hunt, B. (2020). Swale Terminology for Urban Stormwater Treatment, Urban Waterway Series, NC State Extension, North Carolina State University. Retrieved from: https://content.ces.ncsu.edu/swale-terminology-for-urban-stormwater-treatment (Assessed June 14, 2023)

39. ESCSI (Expanded Shale, Clay and Slate Institute). (2018).Expanded Shale, Clay and Slate in Water Filtration, Publication #8676 02-2018. Chicago, IL. Accessed July 29, 2023. www.escsi.org/wp-content/uploads/2018/03/ESCSI-Water-Treatment-Brochure-1.9-FINAL.pdf

40. Fardel, A., P.-E. Peyneau, B. Bechet, A. Lakel, and F. Rodriguez. 2019. "Analysis of swale factors implicated in pollutant removal efficiency using a swale database." Environmental Science and Pollution Research, 26 (2): 1287–1302. https://doi.org/10.1007/s11356-018-3522-9.

41. Fletcher, T. D., W. Shuster, W. F. Hunt, R. Ashley, D. Butler, S. Arthur, S. Trowsdale, S. Barraud, A. Semadeni-Davies, J. L. Bertrand-Krajewski, P. S. Mikkelsen, G. Rivard, M. Uhl, D. Dagenais, and M. Viklander. 2015. "SUDS, LID, BMPs, WSUD and more - The evolution and application of terminology surrounding urban drainage." Urban Water Journal, 12 (7): 3–20. https://doi.org/10.1080/1573062X.2014.916314.

42. Forbes, M., K. Dickson, T. Golden, P. Hudak, and R. Doyle. 2004. "Dissolved Phosphorus Retention of Light-Weight Expanded Shale and Masonry Sand Used in Subsurface Flow Treatment Wetlands." Environmental Science and Technology, 38: 892–8. https://doi.org/10.1021/es034341z.

43. Forbes, M. G., K. L. Dickson, F. Saleh, W. T. Waller, R. D. Doyle, and P. Hudak. 2005. "Recovery and Fractionation of Phosphorus Retained by Lightweight Expanded Shale and Masonry Sand Used as Media in Subsurface Flow Treatment Wetlands." Environmental Science and Technology, 39 (12): 4621–4627. American Chemical Society. https://doi.org/10.1021/es048149o.

44. Gong, Y., D. Yin, C. Liu, J. Li, H. Shi, and X. Fang. 2019. "The influence of external conditions on runoff quality control of grass swale in Beijing and Shenzhen, China." Water Practice and Technology, 14 (2): 482–494. https://doi.org/10.2166/wpt.2019.031.

45. Grooves W. G. W.,P. E. Hammer, K. L. Knutsen, S. M. Ryan, and R. A. Schlipf, " Analysis of Bioswale efficiency for Treating Surface Runoff", University of California, Santa Barbara https://bren.ucsb.edu/projects/analysis-bioswale-efficiency-treating-surface-runoff

46. Hauser, J., J. Curtis, J. Johnston, D. Patel, and M. Keisler. 2005. "Small-Scale Pilot Testing of Stormwater Treatment Systems To Meet Numerical Effluent Limits in the Lake Tahoe Basin." Proceedings of Water Environment Federation Technical Exhibition and Conference, 3051–3081. http://dx.doi.org/10.2175/193864705783865271

47. Hunt, W. F., E. A. Fassman-Beck, S. A. Ekka, K. C. Shaneyfelt, and A. Deletic. 2020. "Designing Dry Swales for Stormwater Quality Improvement Using the Aberdeen Equation." Journal of Sustainable Water in the Built Environment, 6 (1): 05019004. American Society of Civil Engineers. https://doi.org/10.1061/JSWBAY.0000886.

48. Hunt, W. F., A. R. Jarrett, J. T. Smith, and L. J. Sharkey. 2006. "Evaluating Bioretention Hydrology and Nutrient Removal at Three Field Sites in North Carolina." Journal of Irrigation and Drainage Engineering, 132 (6): 600–608. American Society of Civil Engineers. https://doi.org/10.1061/(ASCE)0733-9437(2006)132:6(600).

49. Hunt, W. F., J. T. Smith, S. J. Jadlocki, J. M. Hathaway, and P. R. Eubanks. 2008. "Pollutant Removal and Peak Flow Mitigation by a Bioretention Cell in Urban Charlotte, N.C." Journal of Environmental Engineering, 134 (5): 403–408. American Society of Civil Engineers. https://doi.org/10.1061/(ASCE)0733-9372(2008)134:5(403).

50. Illinois State Toll Highway Authority. March 2020 "Drainage Design Manual". Assessed on 7/4/2023 https://www.illinoistollway.com/documents/20184/238191/Drainage+Design+Manual_Mar2020.pdf/498191e4-6457-43a5-b4b3-5c601d4c2478?version=1.4

51. iSWM (Integrated Stormwater Management) 2014 a. “iSWM Technical Manual, Water Quality” Accessed July 3, 2023. https://iswm.nctcog.org/Documents/technical_manual/Water%20Quality_9-2014.pdf

52. iSWM (Integrated Stormwater Management) 2014 b. “iSWM Criteria Manual, Site Development Controls” Accessed July 3, 2023. https://iswm.nctcog.org/Documents/technical_manual/Site_Development_Controls_9-2014.pdf

53. iSWM (Integrated Stormwater Management) 2015. “iSWM Criteria Manual for Site Development and Construction” Accessed July 3, 2023. https://iswm.nctcog.org/Documents/iSWM_Criteria_Manual_01142015.pdf

54. King County 1995. “ Evaluation of Water Quality Ponds and Swales in the Issaquah/East Lake Sammamish Basins” Accessed July 4, 2023. https://your.kingcounty.gov/dnrp/library/1995/kcr853.pdf.

55. Kim, H., E. A. Seagren, and A. P. Davis. 2003. “Engineered bioretention for removal of nitrate from stormwater runoff.” Water Environment Research, Publication: Water Environment Federation, 75 (4): 355–367. https://doi.org/10.2175/106143003x141169.

56. Knight, E. M. P., W. F. Hunt, and R. J. Winston. 2013. “Side-by-side evaluation of four level spreader–vegetated filter strips and a swale in eastern North Carolina.” Journal of Soil Water Conservation, 68 (1): 60–72. Soil and Water Conservation Society. https://doi.org/10.2489/jswc.68.1.60.

57. Lee, H., X. Swamikannu, D. Radulescu, S. Kim, and M. K. Stenstrom. 2007. “Design of stormwater monitoring programs.” Water Research, 41 (18): 4186–4196. https://doi.org/10.1016/j.watres.2007.05.016.

58. Lee, J. H., K. W. Bang, L. H. Ketchum, J. S. Choe, and M. J. Yu. 2002. “First flush analysis of urban storm runoff.” Sci. Total Environ., 293 (1): 163–175. https://doi.org/10.1016/S0048-9697(02)00006-2.

59. Lee, J. Y., H. Kim, Y. Kim, and M. Y. Han. 2011. “Characteristics of the event mean concentration (EMC) from rainfall-runoff on an urban highway.” Environmental Pollution, 159 (4): 884–888. https://doi.org/10.1016/j.envpol.2010.12.022.

60. LeFevre, G. H., K. H. Paus, P. Natarajan, J. S. Gulliver, P. J. Novak, and R. M. Hozalski. 2015. “Review of Dissolved Pollutants in Urban Storm Water and Their Removal and Fate in Bioretention Cells.” Journal of Environmental Engineering, 141 (1): 04014050. American Society of Civil Engineers. https://doi.org/10.1061/(ASCE)EE.1943-7870.0000876.

61. L-H, K., J. S-M, and K. S-O. 2007. “Determination of first flush criteria using dynamic EMCs (event mean concentrations) on highway stormwater runoff.” Water Science and Technology, 55 (3): 71–77. London, United Kingdom: IWA Publishing. https://doi.org/10.2166/wst.2007.074.

62. Li, H., L. J. Sharkey, W. F. Hunt, and A. P. Davis. 2009. “Mitigation of Impervious Surface Hydrology Using Bioretention in North Carolina and Maryland.” Journal of Hydrologic Engineering, 14 (4): 407–415. American Society of Civil Engineers. https://doi.org/10.1061/(ASCE)1084-0699(2009)14:4(407).

63. Li, J., C. Jiang, T. Lei, and Y. Li. 2016. “Experimental study and simulation of water quality purification of urban surface runoff using non-vegetated bioswales.” Ecol. Eng., 95: 706–713. Elsevier. https://doi.org/10.1016/j.ecoleng.2016.06.060.

64. Liu, Y., B. A. Engel, D. C. Flanagan, M. W. Gitau, S. K. McMillan, and I. Chaubey. 2017. “A review on effectiveness of best management practices in improving hydrology and water quality: Needs and opportunities.” Science of Total Environment, 601–602: 580–593. https://doi.org/10.1016/j.scitotenv.2017.05.212.

65. Lucke, T., Kachchu Mohamed, M. A., and Tindale, N. (2014). Pollutant removal and hydraulic reduction performance of field grassed swales during runoff simulation experiments.Water,6(7), 1887-1904. http://dx.doi.org/10.3390/w6071887

66. Maniquiz-Redillas, M., M. E. Robles, G. Cruz, N. J. Reyes, and L.-H. Kim. 2022. “First Flush Stormwater Runoff in Urban Catchments: A Bibliometric and Comprehensive Review.” Hydrology, 9 (4): 63. Multidisciplinary Digital Publishing Institute. https://doi.org/10.3390/hydrology9040063.

67. Maryland Stormwater Design Manual 2000. "BMP Pollutant Removal Documentation" Appendix D.5. Accessed on July 21, 2023. https://mde.maryland.gov/programs/water/StormwaterManagementProgram/Documents/www.mde.state.md.us/assets/document/sedimentstormwater/Appnd_D5.pdf

68. Mateus, D. M. R., and H. J. O. Pinho. 2010. "Phosphorus Removal by Expanded Clay—Six Years of Pilot-Scale Constructed Wetlands Experience." Water Environment Research, 82 (2): 128–137. Water Environment Federation. https://doi.org/10.2175/106143009X447894

69. McGrane, S. J. 2016. "Impacts of urbanisation on hydrological and water quality dynamics, and urban water management: a review." Hydrological Science Journal, 61 (13): 2295–2311. Taylor & Francis. https://doi.org/10.1080/02626667.2015.1128084.

70. Mechleb, G., R. Gilbert, M. Christman, R. Gupta, and B. Gross. 2014. Use of Expanded Shale Amendment to Enhance Drainage Properties of Clays. 3454. https://doi.org/10.1061/9780784413272.334

71. Minnesota Pollution Control Agency. 2017. Overview of stormwater infiltration https://stormwater.pca.state.mn.us/index.php?title=Overview_of_stormwater_infiltration

72. Mustaffa, N., N. A. Ahmad, and M. A. M. Razi. 2016. "Variations of Roughness Coefficients with Flow Depth of Grassed Swale." IOP Conference Series: Material Science and Engineering, 136 (1): 012082. IOP Publishing. https://doi.org/10.1088/1757-899X/136/1/012082.

73. NRCS (Natural Resources Conservation Service) 2005. "Bioswales" Accessed July 28 2023 https://mostcenter.umd.edu/sites/default/files/2020-04/NRCS_Bioswale_Fact_Sheet.pdf

74. NCDOT (North Carolina Department of Transportation) 2014 "Stormwater Best Management Practices Toolbox." n.d. Accessed July 28, 2023. https://connect.ncdot.gov/resources/hydro/HSPDocuments/2014_BMP_Toolbox.pdf

75. NCDEQ (North Carolina Department of Environmental Quality). 2017. "Stormwater BMP manual" Assessed July 4,2023. https://files.nc.gov/ncdeq/Energy%20Mineral%20and%20Land%20Resources/Stormwater/BMP%20Manual/C-11_Treatment_Swale.pdf

76. NCDEQ (North Carolina Department of Environmental Quality). 2020. "Stormwater Design Manual" Accessed July 3, 2023. https://www.deq.nc.gov/about/divisions/energy-mineral-and-land-resources/stormwater/stormwater-program/stormwater-design-manual.

77. NJDEP (New Jersey Department of Environmental Protection) 01/14/2022. "Laboratory Protocol to Access TSS Removal by a Filtration Manufactured Treatment Method" Assessed on 7/19/2023 https://dep.nj.gov/wp-content/uploads/stormwater/filter-protocol-final-2022-0114.pdf

78. Nuamah, L. A., Y. Li, Y. Pu, A. S. Nwankwegu, Z. Haikuo, E. Norgbey, P. Banahene, and R. Bofah-Buoh. 2020. "Constructed wetlands, status, progress, and challenges. The need for critical operational reassessment for a cleaner productive ecosystem." Journal of Cleaner Production, 269: 122340. https://doi.org/10.1016/j.jclepro.2020.122340.

79. Osouli, A., A. A. Bloorchian, M. Grinter, A. Alborzi, S. L. Marlow, L. Ahiablame, and J. Zhou. 2017. "Performance and Cost Perspective in Selecting BMPs for Linear Projects." Water, 9 (5): 302. Multidisciplinary Digital Publishing Institute. https://doi.org/10.3390/w9050302.

80. Pringle, C. M. 2000. "Managing riverine connectivity in complex landscapes to protect 'remnant natural areas.'" SIL Proc. 1922-2010, 27 (3): 1149–1164. Taylor & Francis. https://doi.org/10.1080/03680770.1998.11901419.

81. Purvis, R. A. n.d. "Bioswale Design Optimization for Enhanced Application and Pollutant Removal." Ph.D. United States -- North Carolina: North Carolina State University.

82. Riverside County 2020. "LID BMP Handbook." Watershed Protection, Accessed May 7, 2023. https://rcwatershed.org/permittees/riverside-county-lid-bmp-handbook/.

83. Seters, T., D. Smith, and G. MacMillan. 2006. “Performance Evaluation Of Permeable Pavement and a Bioretention Swale.” http://www.sept.org/techpapers/1304.pdf

84. Sloan, J. J., R. I. Cabrera, P. A. Y. Ampim, S. A. George, and W. A. Mackay. 2010. “Performance of Ornamental Plants in Alternative Organic Growing Media Amended with Increasing Rates of Expanded Shale.” HortTechnology, 20 (3): 594–602. American Society for Horticultural Science. https://doi.org/10.21273/HORTTECH.20.3.594.

85. Stagge, J. H., A. P. Davis, E. Jamil, and H. Kim. 2012. “Performance of grass swales for improving water quality from highway runoff.” Water Res., 46 (20): 6731–6742. https://doi.org/10.1016/j.watres.2012.02.037.

86. StormwaterPA (Pennsylvania Stormwater) 2006. “Best Management Practices Manual- Chapter 6.”. Accessed June 16, 2023. https://www.stormwaterpa.org/bmp-manual-chapter-6.html.

87. Sun, N., Limburg, K. E., & Hong, B. 2019. The Urban Hydrological System. In Understanding Urban Ecology. https://doi.org/10.1007/978-3-030-11259-2_6

88. Thorpe, A., and R. M. Harrison. 2008. “Sources and properties of non-exhaust particulate matter from road traffic: A review.” Science of Total Environment, 400 (1): 270–282. https://doi.org/10.1016/j.scitotenv.2008.06.007.

89. USDA (U.S. Department of Agriculture). 2020. “Stormwater Runoff Control (Ac.) (570) Conservation Practice Standard, Natural Resources Conservation Service.” Accessed July 28, 2023. https://www.nrcs.usda.gov/sites/default/files/2022-10/Stormwater_Runoff_Control_570_CPS_9_2020.pdf

90. USGS (U.S. Geological Survey) 2006 “National Field Manual for the Collection of Water-Quality Data.” Accessed July 25, 2023. https://www.usgs.gov/centers/new-england-water-science-center/science/quality-stormwater-runoff-discharged-connecticut.

91. USGS (U.S. Geological Survey) 2023 “Quality of Stormwater Runoff Discharged from Connecticut Highways.” Accessed June 16, 2023. https://www.usgs.gov/centers/new-england-water-science-center/science/quality-stormwater-runoff-discharged-connecticut.

92. Tecweigh (n.d.) “Volumetric Feeders/Auger Feeders.” Accessed July 19, 2023. https://www.tecweigh.com/products/volumetric-feeders/

93. Walsh, C. J., A. H. Roy, J. W. Feminella, P. D. Cottingham, P. M. Groffman, and R. P. Morgan. 2005. “The urban stream syndrome: current knowledge and the search for a cure.” Journal of the North American Benthological Society, 24 (3): 706–723. The University of Chicago Press. https://doi.org/10.1899/04-028.1.

94. Wang, R., X. Zhang, and M.-H. Li. 2019. “Predicting bioretention pollutant removal efficiency with design features: A data-driven approach.” Journal of Environmental Management, 242: 403–414. https://doi.org/10.1016/j.jenvman.2019.04.064.

95. Wang, Y., H. Yin, Z. Liu, and X. Wang. 2022. “A Systematic Review of the Scientific Literature on Pollutant Removal from Stormwater Runoff from Vacant Urban Lands.” Sustainability, 14 (19): 12906. https://doi.org/10.3390/su141912906.

96. Winston, R. J., J. T. Powell, and W. F. Hunt. 2019. “Retrofitting a grass swale with rock check dams: hydrologic impacts.” Urban Water Journal, 16 (6): 404–411. Taylor & Francis. https://doi.org/10.1080/1573062X.2018.1455881.

97. Xiao, Q., and G. McPherson. 2011. “Performance of engineered soil and trees in a parking lot bioswale.” Urban Water Journal 84 241-253, 8 (4): 241–253. https://doi.org/10.1080/1573062X.2011.596213.

98. Yang, D., Y. Yang, and J. Xia. 2021. “Hydrological cycle and water resources in a changing world: A review.” Geography and Sustainability, 2 (2): 115–122. https://doi.org/10.1016/j.geosus.2021.05.003.

99. Yu, S., S. Barnes and V. Gerde. 1993. Testing of Best Management Practices for Controlling Highway Runoff, Phase II. Virginia Transportation Research Council. FHWA/VA-94-R21.

100. Zeiringer, B., C. Seliger, F. Greimel, and S. Schmutz. 2018. “River Hydrology, Flow Alteration, and Environmental Flow.” Riverine Ecosystem Management, Aquatic Ecology Series, S. Schmutz and J. Sendzimir, eds., 67–89. Cham: Springer International Publishing.

101. Zhang, W., J. Li, H. Sun, and W. Che. 2021. “Pollutant first flush identification and its implications for urban runoff pollution control: a roof and road runoff case study in Beijing, China.” Water Science and Technology, 83 (11): 2829–2840. https://doi.org/10.2166/wst.2021.157.

APPENDIX A

FLOW CALIBRATION

Table A.1: *Flow Calibration Table*

S.N.	Manual Flow Measurement (lit/min)					Flow (sensor) (Lit/min)
	Initial Time (t1)	Final Time (t2)	Avg time taken (t)	Volume (Lit)	Actual Flow (Lit/min)	
1	29	30	29.5	96	195.25	175
2	90	92	91	48	31.64	26
3	82.5	80	81.25	96	70.89	64.5
4	57	55	56	96	102.85	100
5	33	32	32.5	96	177.23	155
6	25	26.5	25.75	96	223.68	200
7	20.85	21.57	21.21	96	271.57	251

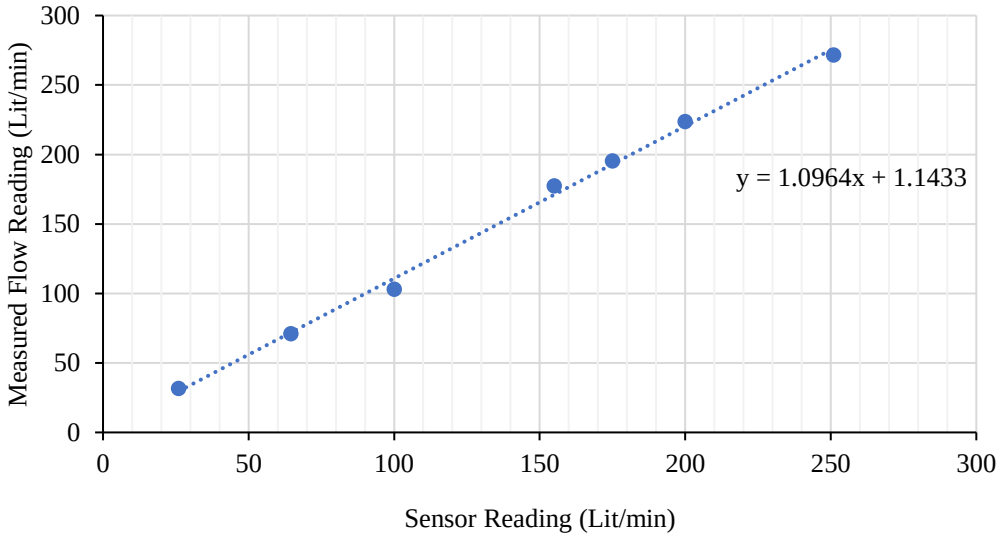

Figure A. 1: *Sensor Reading vs. Actual Flow*

APPENDIX B

SIEVE ANALYSIS

Sample Sieve Analysis

Sample: G-pile

Sample weight: 700 grams

Table B.1: *Sample Sieve Analysis Calculation Table (G-pile)*

Sieve Number	Sieve Size (mm)	Mass of Sieve, (g) (M1)	Mass of each Sieve + Soil Retained, (g) M2	Mass of soil retained (g), (M2-M1)	Percent Retained on Sieve, %	Cumulative % Retained on Sieve	Percent Finer, %
3/8 inch	9.5	544.6	544.6	0	0	0	**100**
4	4.75	514.9	949.6	434.7	62.11	62.11	**37.89**
8	2.36	431.4	690.8	259.4	37.06	99.17	**0.83**
10	2	620.7	622	1.3	0.19	99.36	**0.64**
16	1.18	644.2	644.5	0.3	0.04	99.40	**0.60**
30	0.6	574	574.1	0.1	0.01	99.41	**0.59**
50	0.3	550.2	550.3	0.1	0.01	99.43	**0.57**
100	0.15	514.3	514.5	0.2	0.03	99.46	**0.54**
200	0.075	520.7	522.4	1.7	0.24	99.70	**0.30**
Receiving Pan	-	499.9	502	2.2	0.30	100.00	**0**
			Total	700	grams		

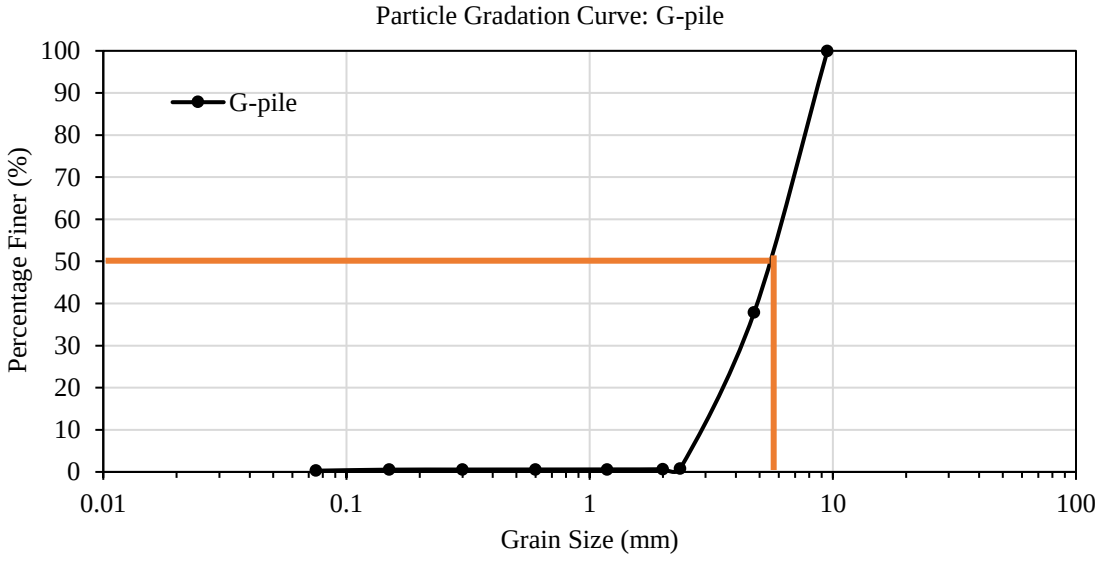

Figure B.1: *Sample Gradation Curve showing the d_{50} size.*

d_{50} of G-pile = 5.5 mm

APPENDIX C

SAMPLE CALCULATION FOR TSS ADJUSTMENT

Experiment number: 19 (b)

Date: April 19, 2023

Total Target Flow: 120 Lit/min

Target Concentration: 200 mg/Lit

Table C.1: *Sample TSS Adjustment Sheet*

S.N.	Location	Time (min)	Measured TSS (mg/Lit)	Adjusted TSS (mg/Lit)	Average Measured TSS (mg/Lit)	Average Adjusted TSS (mg/Lit)
1	Slurry Tank	10	4672		4419	
2		20	4378			
3		30	4617.2			
4		40	4008			
5	Inlet	10	219.4	202	217	200
6		20	222.4	205		
7		30	221.3	204		
8		40	204.6	189		
9	Middle	10	146.6	135	170	157
10		20	172.8	159		
11		30	171.4	158		
12		40	165.7	153		
13	Outlet (drainage)	10	83.5	77	91	84
14		20	88.2	81		
15		30	99.9	92		
16		40	86.1	79		
17	Outlet (overflow)	10	107.2	99	125	115
18		20	119.0	110		
19		30	130.8	121		
20		40	124.9	115		

Table C.2: *Illustration of Actual vs. Adjusted Percent Reduction (TSS)*

Sampling Location	Actual TSS (mg/Lit)	Actual Percent Reduction (%)	Average Adjusted TSS (mg/Lit)	Adjusted Percent Reduction (%)
Inlet	217		200	
Middle section	170	22	157	22
Outlet	91	58	84	58
Overflow	125	42	115	42